Effect of watershed management practices on hydrological response and soil erosion in the semiarid highlands of northern Ethiopia

[北エチオピア半乾燥高地における
水文応答と土壌侵食に対する流域管理の効果について]

Fenta Ayele Almaw

The United Graduate School of Agricultural Sciences

Tottori University, Japan

2018

Effect of watershed management practices on hydrological response and soil erosion in the semiarid highlands of northern Ethiopia

[北エチオピア半乾燥高地における
水文応答と土壌侵食に対する流域管理の効果について]

Fenta Ayele Almaw

Submitted to the United Graduate School of Agricultural Sciences, Tottori University in partial fulfillment of the requirements for the degree of Doctor of Philosophy in Global Arid Land Science

Major Supervisor:

Hiroshi Yasuda (Assoc. Prof.)

Co–supervisors:

Katsuyuki Shimizu (Assoc. Prof.)

Yasuomi Ibaraki (Prof.)

DEDICATION

This thesis is dedicated to the memories of my late families who wanted to see my dream come true, but left early!!!

Acknowledgements

Foremost, I would like to thank the Almighty God for his mercy and showers of blessings all the way throughout my life. I praise God for giving me good health, strength, knowledge and wisdom to successfully complete my PhD study.

I am deeply indebted to the Government of Japan for providing this study opportunity and financial support through the Ministry of Education, Culture, Sports, Science, and Technology (MEXT) scholarship and Mekelle University of Ethiopia for granting me study leave.

This research would not have been possible without the very helpful individuals around me. It is a great pleasure for me to acknowlde those who contributed to the success of my PhD study.

First, I would like to express my deep and sincere gratitude to my major supervisor Dr. Hiroshi Yasuda for his great support, invaluable and constructive advice, and guidance to make this PhD study come to fruition. I also thank my co-supervisors Dr. Katsuyuki Shimizu and Prof. Yasuomi Ibaraki for their helpful comments and suggestions. My sincere thanks with high appreciation go to Dr. Nigussie Haregeweyn who provided myriad useful comments and encouragement during the course of my PhD study. I would also like to extend my thanks to Dr. Kifle Woldearegay and Dr. Aklilu Negussie for their useful contributions in my study.

I'm also grateful to all members of the division of Environmental Conservation - Hydrology subdivision, especially Dr. Takayuki Kawai and Ms. Atsuko Yonehara for their unreserved support. I also thank all administrative staff members of Tottori University who have always been willing to provide support and administrative information.

Most importantly, I would like to forward my special thanks to my lovely wife Bayush Yimer (Ba) for her never ending concern, unwavering support and encouragement. Ba, had it not been for your accompany and support, life in Japan would have been difficult. I am also grateful to my family and friends back home for their gracious support and prayers throughout the years.

I offer my warmest thanks to friends in Tottori (Dagnenet Sultan, Kindiye Ebabu, Fantahun Aklog, Zerihun Nigussie, Misganaw Teshager, Sisay Dinku, Mesenbet Yibeltal, Fekiremariam Asargew, Mulat Liyew, Birhanu Kebede, Shigdaf Mekuriaw, Gashaw Tena, Getu Abebe, and others) for the interesting discussion we often had on both academic and non-academic matters. Last but not least, I extend my heartily appreciation to the whole Ethiopian community in Tottori for making me feel home away from home, especially during Ethiopian Holidays.

Table of Contents

List of Figures

List of Tables

List of Abbreviations

ASTER	Advanced Space-borne Thermal Emission and Reflection Radiometer
CGIAR	Consultative Group for International Agriculture Research
CSI	Consortium for Spatial Information
CV	Coefficients of Variation
DEM	Digital Elevation Model
DKUR	Density Kurtosis
DSK	Density Skewness
ETM+	Enhanced Thematic Mapper plus
EUROSEM	European Soil Erosion Model
FAO	Food and Agriculture Organization
GIS	Geographic Information Systems
GPS	Global Position System
HC	Hypsometric Curve
HTS	Hunting Technical Services
ITCZ	Intertropical Convergence Zone
KUR	Hypsometric Kurtosis
LULC	Land Use/Land Cover
MK	Mann-Kendall
MKS	Mann-Kendall-Sneyers
ML	Maximum Likelihood
MoARD	Ministry of Agriculture and Rural Development
MoFED	Ministry of Finance and Economic development
MoWIE	Ministry of Water, Irrigation and Energy
NMA	National Mapping Agency

NMA	National Meteorology Agency
PET	Potential Evapotranspiration
RUSLE	Revised Universal Soil Loss Equation
SK	Hypsometric Skewness
SRTM	Shuttle Radar Topography Mission
SWC	Soil and Water Conservation
TM	Thematic Mapper
UNESCO	United Nations Educational, Scientific, and Cultural Organization
USGS	United States Geological Survey
USLE	Universal Soil Loss Equation
UTM	Universal Transverse Mercator
WEPP	Water Erosion Prediction Project
WFP	World Food Program

Chapter 1

General Introduction

1.1. Background

1.1.1. Topography and river basins of Ethiopia

With an area of about 1.1 million km^2, Ethiopia is among the largest countries of Africa characterized by a wide variety of landscapes, with marked contrasts in elevation ranging from about 125 m below sea level of Assale Lake, in the Danakil depression, to about 4,620 m above sea level at Ras Dejen. The Great Rift Valley of the eastern Africa divides the country into two plateaus (western and southeastern highlands) and stretches from northeast to southwest creating more terrain complexity to the country (Figure 1.1). To the west of the rift system are the massive western highlands which include high altitude mountain ranges separated by the deep, steep sided valleys of the major rivers. To the eastern flank of the rift system are the southeastern highlands of Sidamo, Bale, Arsi, and Harerge. The lowlands are to the west of the western highlands, and to the east and south of the southeastern highlands which have isolated hills scattered over the well developed plains. Ethiopia is endowed with a substantial amount of water resources but with very high hydrological variability. Most of the major river basins of the country originate from the high altitude mountain ranges and accelerate across steep valley systems. The country possesses twelve basins (Figure 1.1), eight of which are river basins, one lake basin, and remaining three are dry basins, with no or insignificant flow out of the drainage system. These river basins form three major drainage systems (FAO 2016):

- The Nile basin (including Abbay or Blue Nile, Baro-Akobo, Tekeze and Mereb which together contribute about 85% of the river year-round flow: Abtew and Melesse (2014)) covers 33% of the country and drains the northern and central parts westwards;

- The Rift Valley basin (including Awash, Danakil, Omo-Gibe and Central Lakes) covers 28% of the country and consists of a group of independent interior basins extending from Djibouti in the north to the United Republic of Tanzania in the south, with nearly half of its total area being located in Ethiopia;
- The South-East basin (including Wabi-Shebelle, Genale-Dawa and Ogaden) covers 39% of the country and drains the southeastern mountains towards the Republic of Somalia and the Indian Ocean.

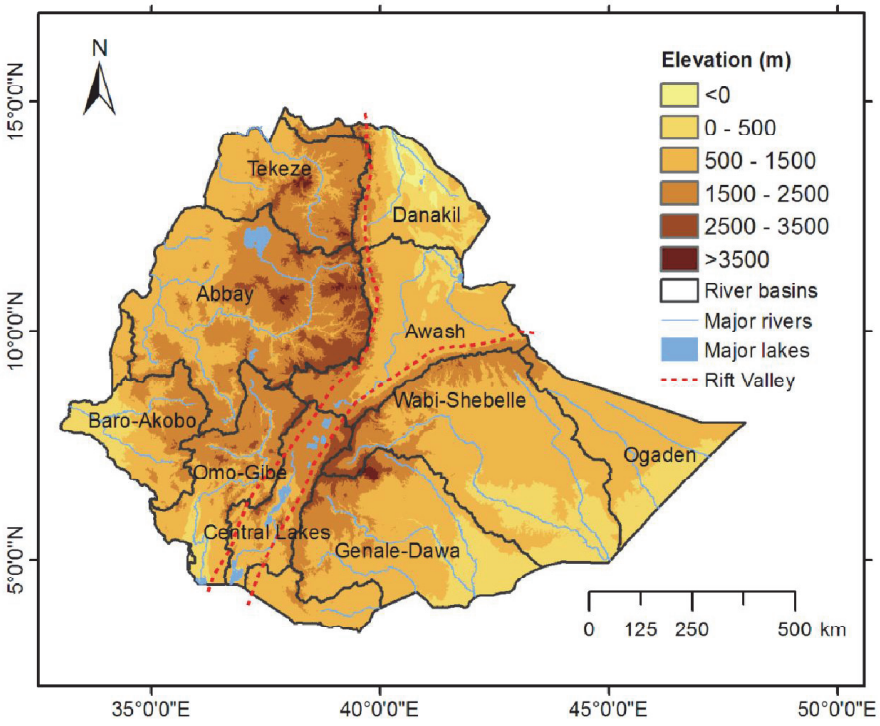

Figure 1.1 Topography and major river basins of Ethiopia extracted from 90 m resolution Shuttle Radar Topography Mission (SRTM) Digital Elevation Model (DEM).

Basins drained by rivers originating from the mountains west of the Rift Valley flow toward the west into the Nile River basin system, and those originating from the eastern highlands flow towards the east into the Republic of Somalia. Rivers draining in the Rift Valley originate from

the adjoining highlands and flow north and south of the uplift in the center of the Ethiopian Rift Valley. The potential of annual surface water from 12 river basins is estimated to be around 120 billion m^3 (FAO 2016). Since most of the surface water originate from the highlands and high rainfall areas and is lost as runoff to the neighboring countries (nearly 80% of flow: FAO 2016), Ethiopia is considered to be the water tower of the Horn of Africa. Ethiopia's groundwater resources potential is low when compared with surface water resources. Moreover, the groundwater potential is not known with certainity but the potential is estimated to be about 2.6 billion m^3 per year (Awlachew 2010). With existing water resources, Ethiopia could irrigation over 5 million ha (Awlachew 2010), whereas the country's hydropower potential is estimated at 45,000MW (MoFED 2010). Nevertheless, these huge potentials of development are not fully utilized because of many factors including limited financial resources, technical challenges, and lack of good governance (Berhanu et al. 2014). Consequently, the country has not been able to meet the increased demand for food, water supply, and energy for the increasing population as well as for the rapid expansion of urbanization and economic activity.

1.1.2. Climate of Ethiopia

Given the high topographic variability and Ethiopia's geographic position close to the equator and the Indian Ocean, Ethiopia is subjected to large spatial variations in temperature and precipitation (Fazini et al. 2015). The climate of Ethiopia is therefore mainly controlled by the seasonal migration of the Intertropical Convergence Zone (ITCZ) and associated atmospheric circulations (Beltrando and Camberlin 1993), but also influenced by the complex topography and the marked contrast in elevation among large areas of the country (Berhanu et al. 2014; Fenta et al. 2017a). The proximity of the Asiatic continent has to be considered as well (Fazini et al.

2015). In winter, in fact, the contrast between the thermal anticyclone of western Asia and Egypt and the equatorial low pressures determines the presence of trade winds blowing from northeast to southwest. These winds relatively cool but rather dry, control the dry period (locally called *Bega*). In spring, the influence of southwestern winds, coming from the Congo basin, determines the season of 'little rains' (locally called *Belg*) that can bring relatively abundant precipitation in the southern part of the country. In summer, the Guinean monsoon, consisting of equatorial warm and humid winds, results in bountiful rains (locally called *Kiremt*) which are also substantially influenced by the orographic variations. Such a complex meteorological dynamics is reflected by the high spatial variability of annual rainfall, where in the Danakil depression it is constantly less than 250 mm but can be as low as 50 mm; by contrast, on the highlands, 2,000 mm can be locally exceeded. The temperature in Ethiopia is greatly influenced by changing altitude (Fazini et al. 2015). Extremes in temperatures range from the mean annual temperature of about 35°c in the Danakil depression at 155 m below sea level to mountain slopes of over 4000 m above sea level where minimum temperatures fall below zero (UNESCO 2004). Landscapes with contrasting characteristics in terms of topography, such as the highlands and the lowlands, experience a variety of climates from arid to humid typical of equatorial mountains, with further differentiation at local scale. Even though climate conditions are classified into generalized areas of specific types of climate, there are significant microclimatic variations over relatively small areas due to micro-relief variations. To have a clear picture of the extent of aridity in Ethiopia, the aridity index (ratio of the mean annual precipitation to the mean annual potential evapotranspiration) map (Figure 1.2) was generated using data available from Global-Aridity Geo-Database (Trabucco and Zomer 2009). This geo-database is constructed based on WorldClim Global Climate Data (Hijmans et al. 2005) which is a high-resolution global geo-

database (30 arc seconds or about 1 km) of monthly average data (1950–2000) of precipitation, mean, minimum and maximum temperature. The classification of the different climatic zones was adopted from the United Nations Environmental Program (Barrow 1992). The aridity index map (Figure 1.2) shows that the main climatic regions of Ethiopia constitute: arid (27%), semiarid (34%), dry subhumid (13%) and humid (26%).

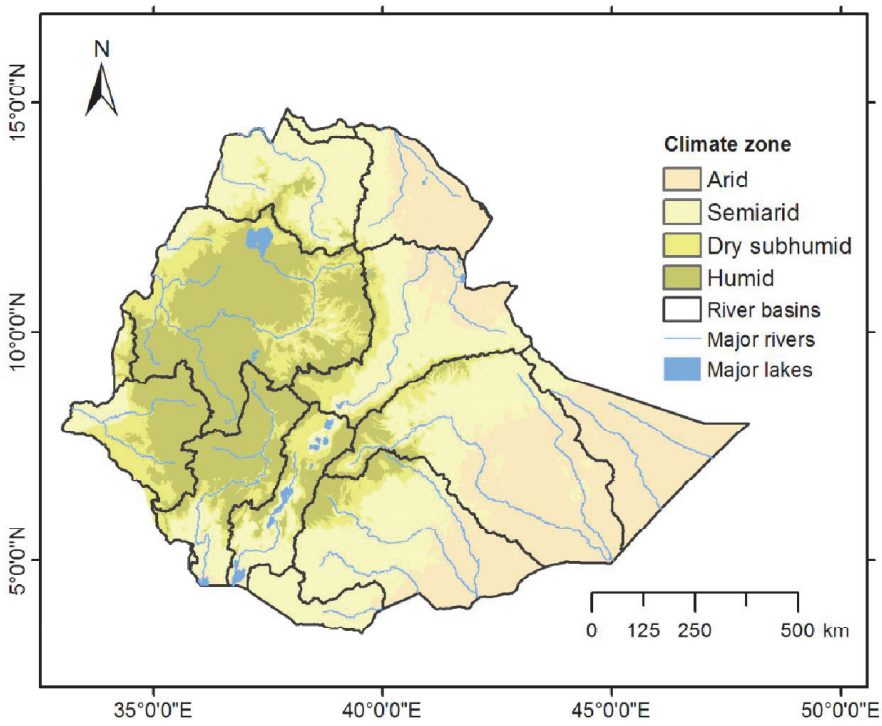

Figure 1.2 Climate classification of Ethiopia based on the Global Aridity Index dataset provided by the Consultative Group for International Agriculture Research–Consortium for Spatial Information (CGIAR-CSI) via CGIAR-CSI GeoPortal (http://www.csi.cgiar.org).

1.1.3. Land degradation in the Ethiopian highlands

Agricultural development in Ethiopia is hampered by many factors; a major one among these is land degradation (Berry 2003; Taddese 2001). Land degradation can be defined as the loss of land productivity, quantitatively or qualitatively through various processes such as soil erosion,

salinization, waterlogging, and depletion of soil nutrients and soil contaminants (Tadesse 2001). Among all forms of land degradation processes in Ethiopia, soil erosion by water is the most severe threat to food security, environmental sustainability and prospects for rural development (Berry 2003). Although no region is immune, soil erosion is more severely affecting developing countries like Ethiopia mainly attributed to lack of proper methodologies to assess the risks and appropriate technologies to reduce soil erosion (Haregeweyn et al. 2015). Land degradation by soil erosion is most severe in the highlands (elevation >1500 m and covering about 45% of total area) of Ethiopia where roughly 88% of the population lives and 95% of the regularly cultivated lands are found (Bekele 2003). Severe soil erosion in the highlands of Ethiopia is mainly the result of mismanagement, overpopulation, and historical dynamics of the political-ecological system and regional land policies (Lanckriet et al. 2016). This is further exacerbated by high rainfall intensity, large volume rainstorms and steep topography (Meshesha et al. 2014; Nyssen et al. 2005). Based on a national level study carried out by the mid-1980s, it was estimated that annually Ethiopia loses over 1.5 billion tons of topsoil from the highlands by erosion (Hurni 1988). This could have added about 1–1.5 million tons of grain to the country's harvest. The same study estimated that around 45% of the total annual soil loss occurred on cropland, with an average soil loss rate of 42 t ha^{-1} from cropland. This soil loss rate is higher than the soil formation rate for Ethiopia which is less than 2 to 27.5 t ha^{-1} yr^{-1} (Hurni 1983a) and much higher than the tolerable soil loss (2–18 t ha^{-1} yr^{-1}), defined as the maximum level of soil erosion that can occur without significant reduction in crop crop productivity (Hurni 1983b). According to Sonneveld and Keyzer (2003), the annual cost of soil erosion to the national economy is around US$ 1.0 billion. This clearly shows the extent to which soil erosion is a contributory factor to the country's food insecurity problem. Another study by Haregeweyn et al. (2008) reported that land

degradation by soil erosion results in loss of fertile topsoil that can lead to substantial socio-economic and ecological problems that impair agricultural productivity. Soil erosion also negatively affects the natural water-storage capacity of catchments, design-life of man-made reservoirs and dams, quality of surface water resources, aesthetic landscape beauty and ecological balance in general (Haregeweyn et al. 2006; Lanckriet et al. 2016; Tamene et al. 2011). Furthermore, the fact that soil is almost a non-renewable natural resource over the human time-scale makes soil erosion a critical problem. The multitude impacts of soil erosion in agricultural productivity and status of natural resources suggest that concerted efforts that integrate resources conservation and development measures are critically needed in Ethiopia.

1.1.4. Watershed management in the Ethiopian highlands

Land degradation problem has had serious consequences in Ethiopia including occurrence of persistent food insecurity, economic losses and various environmental hazards such as recurrent drought (Shiferaw and Holden 1999). Despite the severe consequences of land degradation problem, investment in soil conservation was largely neglected in Ethiopia prior to 1970s. In the 1970s, countrywide large-scale resource conservation efforts were initiated subsequent to the devastating famine of the time (Hurni 1993; Shiferaw and Holden 1999) for which the farmers were mobilized for campaign works. These conservation efforts were supported by various international donor organizations by supplying food grains and edible oil that were used as food-for-work payments for the participating farmers. The emphasis of the conservation efforts has been on implementation of both physical and biological soil and water conservation (SWC) measures. The major physical conservation measures include construction of soil or stone bunds, check dams, micro-basins and hillside terraces. The biological measures include establishment of

exclosures in which natural vegetation is protected from humans and livestock, tree seedling production, planting of tree seedlings on farmlands (agro-forestry), afforestation, and tree plantations around the homesteads and tree plantation in exclosures as enrichment to the natural regeneration (Bewket 2007; Hurni 1993; Mekuria et al. 2012; Yayneshet et al. 2009). The main objective was to reduce soil erosion, restore soil fertility, rehabilitate degraded lands, improve micro-climate, improve agricultural production and productivity and restore environmental condition (Bewket 20097; Mekuria et al. 2007). Initially, however, the practice was not participatory and farmers did not appreciate most of the soil conservation works as they thought that physical structures might take extra land from their small land holdings, and shelter rodents (Tadesse 2001). As a result, farmers were reluctant to maintain the SWC measures and some farmers have even ploughed away the terraces and earth embankments and destroyed vegetated exclosures on severely degraded lands (Tadesse 2001). Although the acceptance of SWC measures by local farmers was initially low, SWC efforts are continuing in Ethiopia.

Since the beginning of the 1990s, participatory watershed management approaches that integrate SWC, intensified natural resource use, and livelihood objectives have been implemented as part of agricultural extension programs of the current government (Haregeweyn et al. 2012, 2015). According to German et al. (2007), the concept of participatory integrated watershed management can be qualified through two aims: first the process must be participatory in terms of the particular issues to be worked on; and second the approach is to emphasize the integration of disciplines (technical, social and institutional dimensions) and/or objectives (conservation, food security, income generation). In 2005 the Ethiopian Ministry of Agriculture and Rural Development (MoARD), in collaboration with several international development organizations, published guidelines for the first time, for ‘Community Based Participatory

Watershed Development' (MoARD 2005). Besides summarizing technical details of SWC measures, the guidelines emphasized the integration of land users in the SWC design and implementation process. Despite all these efforts, Haregeweyn et al. (2015) noted that most of the previous SWC efforts focused primarily in drought-prone areas and until recently land management had been given little policy attention in the northwestern and southwestern parts of the country, where drought risks are low and the productivity of soils is relatively high.

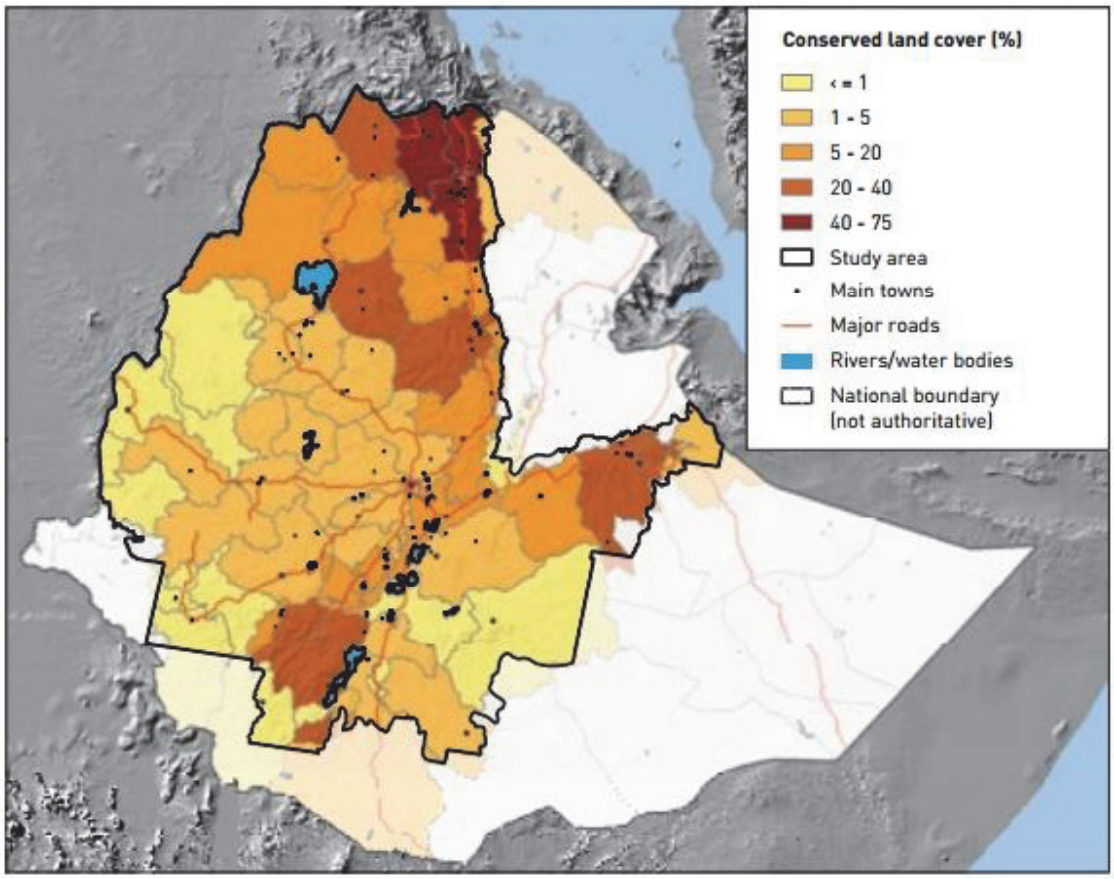

Figure 1.3 The share of the existing conservation structures by land cover classes (For most of the regions the structures only occur on croplands wheras in central Tigray, eastern Tigray, south Tigray, north Wello and south Wello, structures exist on cropland, bushland, grassland, and degraded hills) (Source: Hurni et al. 2015).

Since 2010, the government of Ethiopia has embarked on a massive SWC campaign using mass mobilization at watershed level. Concurrently, a conservation-based, agricultural development-led industrialization development strategy is focusing on promoting conservation of natural resources and improvement of agricultural productivity (MoFED 2010). Despite Ethiopia's huge investment in SWC practices, the quantities of SWC measures implemented in the country are generally poorly recorded. Recently, Hurni et al. (2015) attempted to quantify the current distribution of existing conservation structures in the Ethiopian highlands using an expert-based approach and a combination of spatial proxies (land cover, slope and village accessibility) to model the locations where the conservation structures occur. Their results (Figure 1.3) have shown that in most regions conservation structures exist only on croplands. However, in central Tigray, eastern Tigray, south Tigray, north Wello and south Wello, structures exist on cropland, bushland, grassland, and degraded hills.

1.2 Problem statement and objectives

Several researchers have reported on the effectiveness of various SWC practices at plot and small-scale watersheds (<100 km^2) in erosion control (Gebremichael et al. 2005; Nyssen et al. 2007; Taye et al. 2013), soil fertility restoration (Descheemaeker et al. 2006; Mekuria et al. 2007), runoff reduction (Haregeweyn et al. 2012; Nyssen et al. 2010; Sultan et al. 2018a,b; Taye et al. 2013), sediment yield reduction (Ebabu et al. 2018; Haregeweyn et al., 2006, 2008; Nyssen et al. 2009a), and changes in land use/land cover (LULC) as a result of vegetation regeneration (Alemayehu et al. 2009; Haregeweyn et al. 2012; Nyssen et al. 2008). Other studies have also reported on the economic aspects of SWC interventions (Herweg and Ludi 1999; Kassie et al. 2011; Nyssen et al. 2007). In spite of these facts, studies at medium- or large-scale watersheds

(>100 km^2) which investigate the effects of watershed management practices and associated changes in LULC on hydrological response and soil erosion, and which are of great interest to policy makers are rather scarce (e.g., Haregeweyn et al. 2016, 2017; Nyssen et al. 2008). As a result, policies, decisions, and planning and implementation of SWC measures have been based on very few case studies and general recommendations of national level studies like river basin master-plan development studies. Furthermore, implementation of SWC structures demands huge resources (finance, labor, materials and equipment), and the adoption and recommendations of upscaling the SWC interventions to larger spatial scales should be justified by empirically proven evidence (Anley et al. 2007; Amsalu and de Graaff 2007; Haregeweyn et al. 2016, 2017; Teshome et al. 2016). In order to fill this information gap and support the country's effort in combating land degradation, a study that assesses the effectiveness of watershed management practices and changes in LULC on hydrological response and soil erosion at medium- or large-scale watersheds is of paramount importance for sustainable regional environmental planning and management of soil and water resources. Therefore, the overall objective of this study was to improve our current understanding on the effects of watershed management practices and associated changes in LULC on hydrological response and soil erosion for a medium-sized watershed (area = 442 km^2) in a semiarid environment. The specific objectives of this study were to: (i) quantitatively estimate to what extent watershed management practices and climate factors affect streamflow response; (ii) assess watershed-scale changes in soil erosion as a result of the watershed management practices and changes in LULC; and (iii) quantitatively analyze morphometric parameters of the watershed to better understand the hydro-geologic and erosion characteristics of the watershed for improved planning, management, and decision making to ensure sustainable use of watershed resources.

1.3 Description of the study area

1.3.1 Location, topography and climate

The case study site, Agula watershed, covers a total area of 442 km^2 and is located between 13°32′44″ to 13°54′49″N latitude and 39°34′40″ to 39°47′42″E longitude in Eastern Tigray region, northern Ethiopia (Figure 1.4). The area drains east to west bordering the Agula rural town in the south to join Geba River which is tributary of the Tekeze River basin. Topographically, the area is characterized by highly dissected and rugged terrain. Based on topographic information extracted from the 30 m spatial resolution SRTM-DEM (http://earthexplorer.usgs.gov/), the elevation in the watershed ranges from 1980 meters above sea level (masl) in the valley to 2887 masl on the hills with a mean value of 2341 masl. The dominant geological formations are Limestone with Shale intercalations, Meta-volcanic, Agula Shale, and Sandstones (Adigrat and Enticho sandstone formations) (Gebreyohannes et al. 2013). Based on meteorological data (1992–2012) from Atsbi and Wukro stations, the mean annual rainfall is 593 mm of which about 85% of the rain falls during the wet season (June-September). The mean daily minimum and maximum temperature is 10°C and 26°C, respectively and annual average potential evapotranspiration (PET) is 1693 mm (Fenta et al. 2017b). The aridity index which is defined as the ratio between rainfall and PET is about 0.35, which based on Barrow (1992) corresponds to semiarid climate. The dominant tree species of the watershed are *Juniperus procera, Ficus vasta, Olea europaea* L. subsp. *cuspidata*, *Acacia saligna,* and *Eucalyptus species*; while the common shrub species are *Acacia etbaica, Dodonaea angustifolia, and Euclea schimperi* (Getachew 2007). The community in the watershed is dependent on subsistence agriculture; and the major crop types of the study area are barley (*Hordeum vulgare*), wheat (*Triticum aestivum*), teff (*Eragrostis teff*) and millet (*Eleusine coracana*).

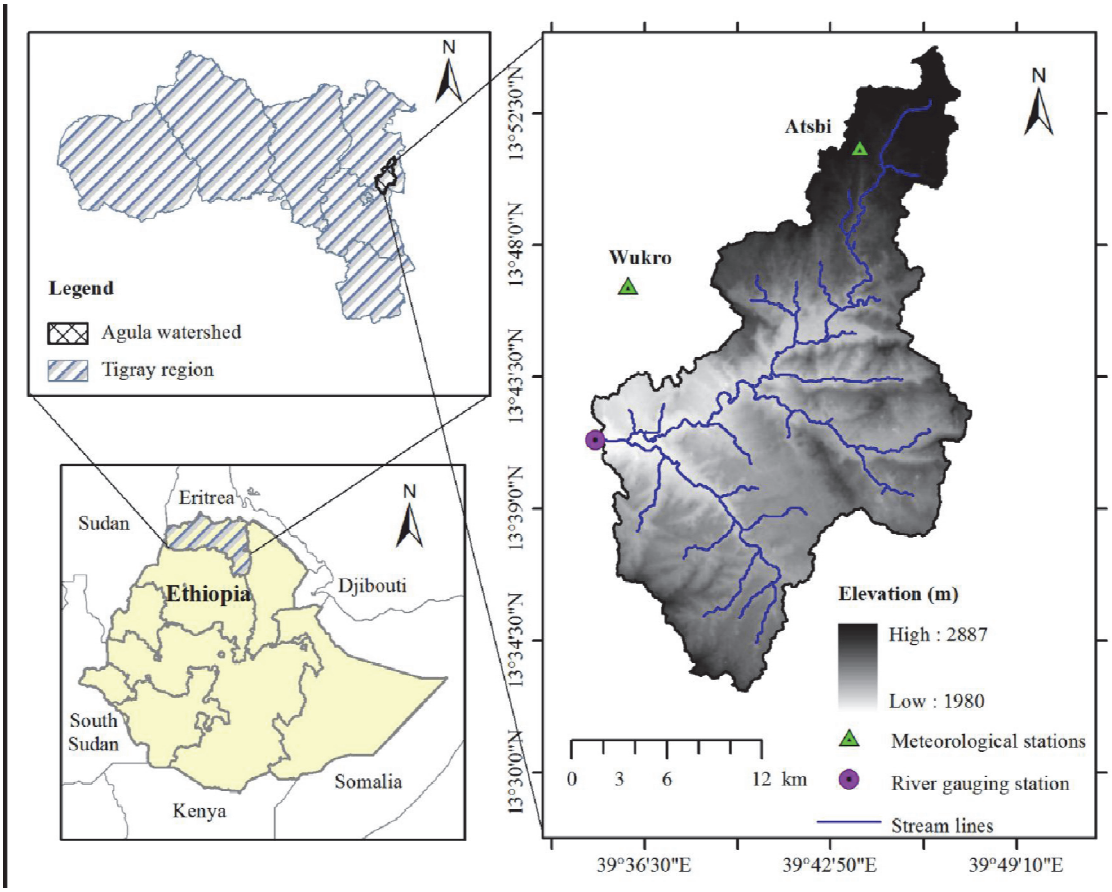

Figure 1.4 Location map of the study area: bottom left - Ethiopia and neighboring countries, top left - Tigray region in northern Ethiopia, right - Agula watershed with locations of gauging stations and major stream lines. The background provides elevation information extracted from the 30-m-resolution SRTM-DEM.

1.3.2 Watershed management practices in Agula watershed

In an effort to combat land degradation by soil erosion, implementation of watershed management practices started in Tigray region of northern Ethiopia in the 1970s. However, the earlier management interventions were largely unsuccessful because of top-down approach and negative attitudes of farmers; which was further exacerbated by a continuous civil war (from 1974 to 1991) in northern Ethiopia (Esser et al. 2002). During the civil war, more resource was

shifted from development to war effort which led to complete disregard for environmental restoration and continued land degradation with substantial damage to the physical environment in Ethiopia in general and Tigray region in particular (Lanckriet et al. 2015). However, after the downfall of the Derg regime in 1991, environmental rehabilitation has again become top agenda of the regional government and more coordinated and resolute efforts to remedy environmental degradation have been under way. The objectives of the watershed management practices were threefold: (i) to restore degraded areas, (ii) to secure water supply for agriculture and domestic uses, and (iii) to promote food security. In view of these objectives, Agula watershed was one of the target areas in the region where massive SWC measures have been implemented by the regional government and the local community in the form of free labor (40 free days per year from each household) with the support of World Vision, World Food Program (WFP) and Irish Aid. The components of the conservation practices include: construction of stone bunds and check dams and establishment of exclosures with or without enrichment plantation. The data on SWC measures implemented in Agula watershed since the late 1980s and until 2000 (Table 1.1) was summarized from the report of Getachew (2007).

Stone bunds

The stone bunds (Figure 1.5(a)–(c)) were constructed by building stone walls (0.3–1 m high) along the contour with large rocks, using small sized rock fragments as backfill. The backfill is topped with stone-rich soil or with small rock fragments, which serve to reduce overland flow and also act as a filter for sediment during major rainfall events (Nyssen et al. 2007). Combined with stone bunds, often additional trenches (Figure 1.5(c)) were dug behind the stone bunds, increasing their runoff and sediment trapping efficiencies. Until 1990, there were only small-scale conservation measures mainly construction of stone bunds (about 10% of the total) on

cultivated lands; whereas following the rise to power of the current Ethiopian government in 1991, large-scale watershed management practices were implemented and stone bunds with improved quality were constructed on cultivated lands, shrub lands and bare lands (Table 1.1, Figure 1.5(a)–(c)). Stone bunds have multiple effects such as to reduce slope length and to create small retention basins for runoff and sediment thereby reducing the volume and erosivity of overland flow, as well as to reduce slope gradient and form bench terraces in the long-term (Nyssen et al. 2007).

Table 1.1 Cumulative soil and water conservation measures in Agula watershed, summarized from Getachew (2007).

	Free labor	World Vision		WFP		Irish Aid		Plantation	
Year	Stone bunds (km)	Stone bunds (km)	Check dams (m)	Stone bunds (km)	Check dams (m)	Stone bunds (km)	Check dams (m)	Planted	Survived
1990	1543	845	200	90	0	0	0	4.9×10^6	3.1×10^6
1992	2278	1339	463	1560	2925	0	0	5.8×10^6	3.6×10^6
1995	3989	1603	463	4992	4008	8382	4400	8.8×10^6	5.7×10^6
1998	10931	1603	693	5026	5178	8539	5110	9.1×10^6	5.8×10^6
2000	11432	1603	693	5026	5178	8539	5110	9.1×10^6	5.8×10^6

Check dams

Check dams are 1–2 m high barriers constructed from gabion and/or dry masonry and placed across rivers and gullies (Figure 1.5(d)). Check dams reduce the effective slope of the channel, thereby reducing the velocity of flowing water, allowing sediment to settle and hence reducing channel erosion. As part of the integrated watershed management, about 14 km of check dams were constructed between 1990 and 2000 with the support of different non-governmental organizations (Table 1.1).

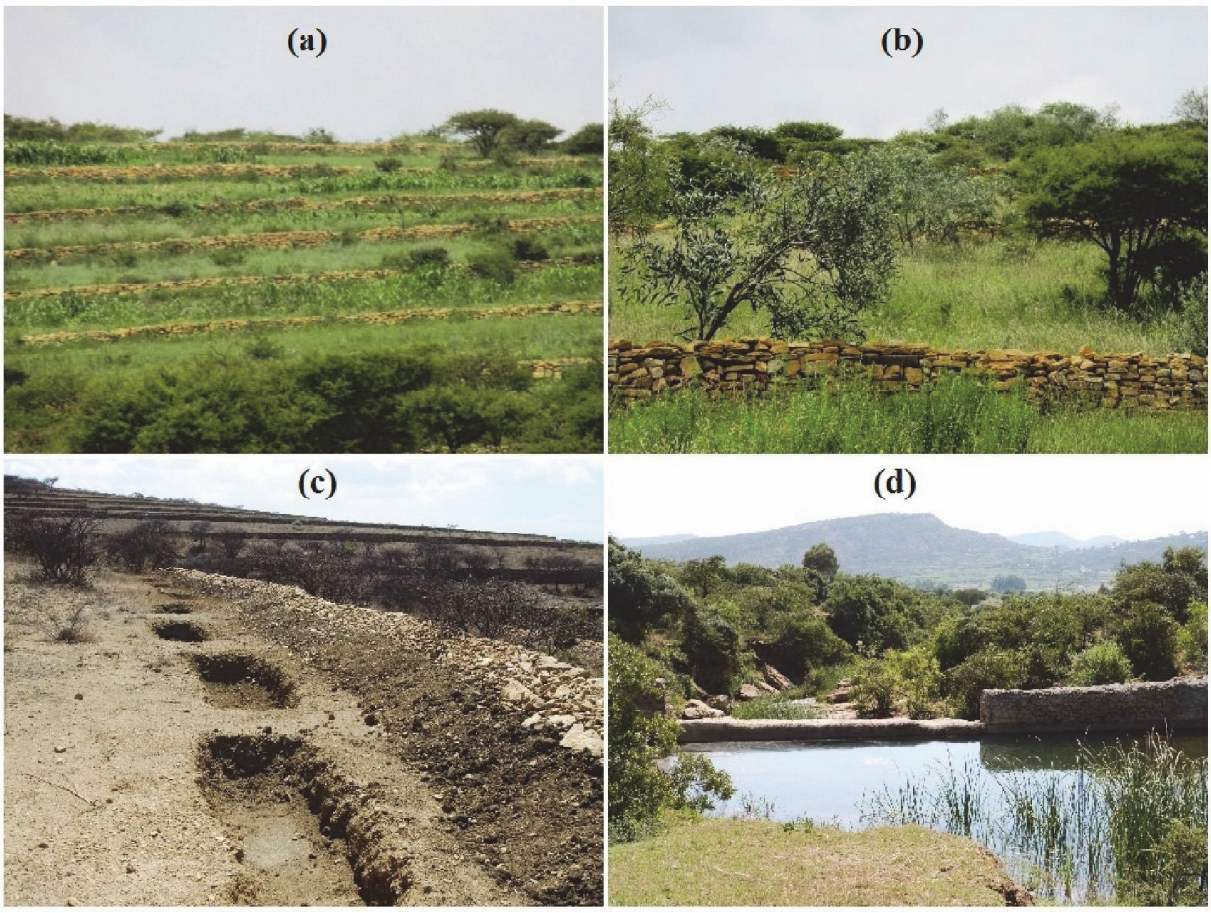

Figure 1.5 Watershed management practices: (a) stone bunds on cultivated lands, (b) stone bunds on shrub lands combined with enrichment plantation, (c) stone bunds combined with trenches on degraded bare lands and (d) check dam across river.

Exclosures

In addition to physical structures, the regional authorities have promoted rehabilitation of degraded lands through establishment of exclosures since 1991 (Mekuria et al. 2009). Exclosures are a type of land management by which areas are prohibited from human and livestock interference (Aerts et al. 2009); with the aim to improve environmental conditions and to enhance rehabilitation of steep slopes and degraded marginal lands. In Agula watershed, hill-slopes which include shrub lands and degraded bare lands (Figure 1.5(b),(c)) were set-aside as

exclosures since the mid 1990s so that the regeneration of the natural vegetation is enhanced. Exclosures are implemented using guards, not fences since fences are more expensive. After implementation, the recovery process in exclosures starts with a rapid increase in diversity and cover of grass, shrub and tree species and gradual development of afromontane forest (Mekuria and Veldkamp 2012). Furthermore, for improved restoration of hill-slopes, exclosures were often combined with construction of backfilled stone bunds and with or without enrichment plantations (forage grass and multi-use tress) (Figure 1.5(b),(c)). Exclosures have multiple benefits such as regeneration of natural vegetation (Mekuria et al. 2009; Mekuria and Veldkamp 2012), significantly reduces runoff (Descheemaeker et al. 2006; Girmay et al. 2009) and soil loss (Girmay et al. 2009; Mekuria et al. 2009; Nyssen et al. 2008).

1.4 Thesis outline

This thesis comprises five chapters. Chapter 1 presents the general introduction, which includes background information, the problem statement and research objectives, and description of the study area. As is well known, watershed management practices and changes in LULC can affect the hydrological regimes of watersheds. To discern any such effects, hydro-meteorological records of the watershed which were available for the past two decades were analyzed and results are reported in Chapter 2. Chapter 3 examines changes in watershed-scale soil erosion risk as a result of watershed management practices and LULC changes. Chapter 4 deals with quantitative analysis of morphometric parameters of the watershed to better understand the watershed characteristics for improved planning, management, and sustainable use of watershed resources. Chapter 5 presents the overall summary and significant findings of each study and the general conclusions of the thesis.

Chapter 2

Response of streamflow to climate variability and changes in human activities in the semiarid highlands of northern Ethiopia

This chapter is published as:

Fenta AA, Yasuda H, Shimizu K, Haregeweyn N. (2017). Response of streamflow to climate variability and changes in human activities in the semi-arid highlands of northern Ethiopia. Regional Environmental Change17: 1229–1240.

Abstract

Climate variability and human activities are two major drivers influencing changes in streamflow response of a watershed, and thus assessing their relative effect is essential for developing sustainable water resources planning and management strategies at watershed-scale. In this study, a runoff model driven by rainfall and potential evapotranspiration was established to estimate the effect of climate variability on the changes in annual streamflow of Agula watershed in northern Ethiopia. Significant decreasing trends were observed for annual and wet season streamflow between 1992 and 2012, while dry season streamflow showed an increasing trend. Analyses of seasonal and annual rainfall records showed no significant trends. The change-point test revealed that an abrupt change in annual streamflow occurred in 2000. In the period 2000–2012, the mean annual and wet season streamflow decreased by 36% and 49%, respectively compared with 1992–1999; while dry season streamflow increased by 57%. Climate variability was estimated to account for 22% of the total reduction in mean annual streamflow, whereas human activities (e.g., proper watershed management practices and associated changes in land use/land cover among other factors) were responsible for 78%; indicating that human activities were the major drivers of changes in the streamflow response. The results of this study point to the potential that reduced wet season flow and improved dry season water availability can be achieved by proper planning and implementation of appropriate watershed management practices.

Keywords: Climate variability; Watershed management; Trend analysis; Streamflow response; Semiarid; Ethiopia

2.1 Introduction

In arid and semiarid regions, where water is a scarce resource, changes in streamflow are significantly sensitive to external forces of change (Chen et al. 2012; Ma et al. 2008), and often have significant environmental and socioeconomic consequences. Climate and human activities are the major factors that largely determine the changes in streamflow (Quilbè et al. 2008). On the one hand, climate variables, especially rainfall and temperature influence streamflow (flow routing time, peak flows and volume) directly or indirectly (García-Ruiz et al. 2011; Legesse et al. 2003; Prowse et al. 2006; Zheng et al. 2009). On the other hand, human activities have direct (e.g., water use for agricultural and domestic purposes) and indirect (e.g., watershed management, land use/land cover (LULC) change) effects on streamflow (García-Ruiz et al. 2011; Legesse et al. 2003; Zhang et al. 2014). For example, different soil and water conservation (SWC) measures such as building of bunds, terraces and check dams and tree planting, result in noticeable changes in hydrological responses (Haregeweyn et al. 2012; Huang and Zhang 2004; Nyssen et al. 2010). Furthermore, human induced LULC change affects soil moisture content and infiltration capacity (Wahren et al. 2009), evapotranspiration (Zhang et al. 2001) and surface and subsurface flow regimes (Bellot et al. 2001), which in-turn influence streamflow response.

With increasing global water-related challenges, recent studies have focused on quantitative analysis of the effects of climate variability and human activities on the hydrologic response. Some studies used physical-based distributed models (e.g., Li et al. 2014; Ma et al. 2010) to simulate changes in streamflow with varying inputs. This approach is physically sound as it provides details of hydrological processes and responses to the changes in driving factors; however, physical-based models have high demand of input data (Beven 1989) and limitations in

model conceptualizations and parameter estimation (Brath et al. 2004). The commonly used approach is to establish relationships between long-term meteorological and hydrological data and use of statistical methods (e.g., Bewket and Sterk 2005; Chen et al. 2012; Ma et al. 2008; Zhang et al. 2014; Zheng et al. 2009) to identify the response of streamflow to external forces of change. These studies have proven statistical methods to be effective approaches to detect streamflow response to various drivers of change. Several of the reported studies have demonstrated that climate variability and human activities have varying effects on the streamflow response depending on the study region's topographic, meteorological, hydrological characteristics as well as land use and management practices, and as such require investigation at local-scale.

The dominant rain-fed agriculture sector in the semiarid highlands of Ethiopia is vulnerable to climate variability (El Kenawy et al. 2016; Bryan et al., 2009) and land degradation by water erosion (Taddese 2001). This in effect led to severe economic consequences such as declining agricultural production, distressing food shortages and reduced farm income (Sonneveld and Keyzer 2003). To reverse the situation, watershed management and water resources development schemes have been implemented in different parts of the country, especially in the past few decades (Esser et al. 2002; Haregeweyn et al. 2015). For instance, in the semiarid areas of Tigray region of northern Ethiopia, where the present study watershed is found, the regional government together with the local community and non-governmental organizations launched massive land restoration program. As a result, implementation of proper watershed management practices have been initiated; and the management practices include stone bunds with or without trenches on cultivated lands and on hill-slopes (Nyssen et al. 2007), check dams in gullies (Haregeweyn et al. 2012), and establishment of exclosures with or without enrichment plantation to restore

degraded hill-slopes (Mekuria et al. 2007; Yayneshet et al. 2009). In Ethiopia in general and in the northern regions of the country in particular, a number of impact studies on individual watershed management practices at plot-level and small-scale watersheds (< 100 km^2) reported considerable changes in LULC (e.g., Alemayehu et al. 2009; Haregeweyn et al. 2012) and alterations of hydrological response (e.g., Descheemaeker et al. 2006; Haregeweyn et al. 2012; Nyssen et al. 2010; Taye et al. 2013).

Despite large number of impact studies at plot-level and small-scale watersheds, comprehensive studies at medium to large-scale watersheds (>100 km^2) to evaluate the effects of climate variability and human activities (e.g., SWC practices and changes in LULC) on the changes in streamflow response are rather scarce. In Agula watershed, which covers about 442 km^2, resolute efforts to remedy environmental degradation through implementation of different watershed management practices have been under way by mobilizing the local community with provision of technical and material support from the government. Previous studies evaluated the effect of watershed management practices at subwatershed-scale (Alemayehu et al. 2009; Igbokwe and Adede 2001) and reported considerable changes in LULC that led to improved vegetation cover and groundwater availability. Nevertheless, to the authors' best knowledge, systematic quantitative estimation of the relative contributions of climatic variability and human activities to the changes in streamflow response of Agula watershed has not been reported. Understanding the response of streamflow to the major drivers of change has paramount importance especially for areas in arid and semiarid regions with limited water resources, to develop appropriate watershed management strategies and to ensure sustainable use of land and water resources. Therefore, the main objective of the present study was to understand to what extent climate variability and changes in human activities (mainly proper watershed management

practices and changes in LULC) in Agula watershed affect streamflow response. The specific objectives were: (i) to analyze trends and changes in streamflow and rainfall for the period 1992–2012, (ii) to assess the changes in LULC over the past two decades (1990–2012), and (iii) to quantitatively estimate the proportion of streamflow changes attributed to the influences of climatic variability and human activities.

2.2 Materials and methods

2.2.1 Data sources

Meteorological data of daily minimum and maximum temperature and rainfall obtained from Atsbi and Wukro stations of the National Meteorology Agency (NMA) of Ethiopia were used in this study. Streamflow data for Agula watershed for the period 1992–2012 was obtained from the Ministry of Water, Irrigation and Energy (MoWIE) of Ethiopia. Landsat-5 Thematic Mapper (TM) for the year 1990 and Landsat-7 Enhanced Thematic Mapper plus (ETM+) for the years 2000 and 2012 were used to produce the LULC maps for the respective years. The choice of the imaging dates was dictated by availability of cloud free images and results of the trend and change-point tests for the hydro-climatic series. In addition, the SRTM-DEM downloaded via http://earthexplorer.usgs.gov/ was used to delineate the boundary of the watershed and to describe the watershed topographic characteristics.

2.2.2 Trend and change-point analyses

Given the limited number of meteorological stations in and around the study watershed, the Thiessen polygon interpolation method was used to produce area-average meteorological records (Xu et al. 2013). Trends of streamflow and rainfall time-series were analyzed using the Mann-

Kendall (MK) test (Kendall 1975; Mann 1945). The MK test is a rank-based non-parametric method that has been widely applied for detecting monotonic trends in hydro-climatic series (e.g., Chen et al. 2012; Li et al. 2014; Ma et al. 2008; Zhang et al. 2014). The MK test was selected because of its robustness with respect to missing and tied values and non-normality which are common in hydro-climatic time-series and has the same power as its parametric competitors (Kahya and Kalayci 2004). For a time series X = $\{x_1, x_2, ..., x_n\}$ (n > 10), the MK test statistic Z is calculated as:

$$Z = \begin{cases} \dfrac{S-1}{\sqrt{\mathrm{Var}(S)}} & \text{if} \quad S > 0 \\ 0 & \text{if} \quad S = 0 \\ \dfrac{S+1}{\sqrt{\mathrm{Var}(S)}} & \text{if} \quad S < 0 \end{cases} \tag{2.1}$$

In which,

$$S = \sum_{i=1}^{n-1} \sum_{j=i+1}^{n} \mathrm{sgn}(x_j - x_i) \tag{2.2}$$

where, Var(S) is variance of S, sgn(θ) is equal to 1, 0, or −1 when θ is greater than, equal to, or less than 0, respectively. In a two-sided test for trend, the null hypothesis of no trend (H_o) should be accepted if $|z| \leq z_{\alpha/2}$ at α level of significance (in this study α = 0.05). A positive value of S indicates an increasing trend and a negative value indicates a decreasing trend.

To detect the approximate starting point of a trend in streamflow data series, the non-parametric Mann-Kendall-Sneyers (MKS) test (Kendall 1975; Mann 1945; Sneyers 1975) was applied. The test is a sequential version of the Mann-Kendall rank statistic proposed by Sneyers (1975). For a time series X = $\{x_1, x_2, ..., x_n\}$, the numbers m_i of elements x_j preceding x_i ($j < i$)

such that $x_j < x_i$ are computed, and under the null hypothesis (no trend), the test statistic can be calculated as:

$$S_k = \sum_{i=1}^{k} m_i \ (2 \le k \le n) \tag{2.3}$$

$$u(k) = \frac{S_k - E(S_k)}{\sqrt{\mathrm{var}(S_k)}} \tag{2.4}$$

where, $E(S_k)$ and $\mathrm{Var}(S_k)$ represent the mean and variance of S_k, respectively. The normalized variable statistic *u(k)* is the forward sequence, and the backward sequence *u*(k)* is calculated using the same equations but with a reversed series of data. The *u(k)* and *u*(k)* are plotted to locate the beginning of the change in trend of streamflow at the intersection between the curves. If the intersection occurs within the confidence interval ($\alpha = 0.05$), it indicates a change-point.

2.2.3 Image classification and LULC change detection

The Landsat images (path 168, row 51) were downloaded free of charge from the United States Geological Survey (USGS) via http://earthexplorer.usgs.gov/. TM image acquired on December 23, 1990 and ETM+ images acquired on February 05, 2000 and January 28, 2012 were used in this study. The image acquisition dates were selected to acquire cloud free images and for the dry season. A combined unsupervised/supervised image classification approach was used integrated with successive spatial analysis operations to classify the Landsat images. Supervised image classification was done using the Maximum Likelihood (ML) classifier algorithm. For classifiers like the ML, it is often recommended that a training sample size for each class should not be fewer than 10–30 times the number of bands (Van Niel et al. 2005). For classification of the 2012 Landsat image, a total of about 400 reference data points were

collected during field observation using global position system (GPS), of which three-fourth of the data points were used for classification and the remaining one-fourth were used for accuracy assessment. Classification of the 1990 and 2000 Landsat images was based on integration of unsupervised classification and visual signature editions (ERDAS 2006), supported by the spectral responses of features of the recent image that led to signature collection for supervised classification. The changes in LULC between 1990 and 2000, and 2000 and 2012 were analyzed using post-classification change detection by producing transition matrices (Table 2.3). Post-classification change detection was selected as it reduces possible effects of atmospheric variations and sensor differences between multi-temporal images (Lu et al. 2004).

2.2.4 Effect of climate variability on annual streamflow

The water balance equation for a watershed can be simplified as:

$$P = ET + Q + \Delta S \tag{2.5}$$

where, P is precipitation or rainfall, ET is evapotranspiration, Q is surface runoff measured as streamflow, and ΔS is change in watershed storage. Over a long period of time (i.e., 5–10 years or more), ΔS can be assumed as zero (Zhang et al. 2001). Since accurate field measurements are often difficult to acquire, evapotranspiration is usually estimated by potential evapotranspiration (PET). The PET represents the evaporative capacity of the atmosphere at a specific location and time which is primarily influenced by climatic parameters (Allen et al. 1998). Rainfall and PET are the dominant controlling variables of mean annual water balance (Budyko 1974); and hence, following Zhang et al. (2014), a non-linear runoff model driven by rainfall and PET was established to estimate the effect of climate variability on streamflow as:

$$Q = kP^{\alpha}\,\mathrm{PET}^{\beta} \tag{2.6}$$

where, Q is the annual streamflow, P is the annual rainfall, PET is the annual potential evapotranspiration; k, α and β are parameters calibrated for the baseline period, that is, when there was no or few human activities. The commonly used objective functions, regression coefficient and Nash-Sutcliffe efficiency were used to evaluate the credibility of the model (Moriasi et al. 2007). Several methods have been developed to calculate PET (Weiß and Menzel 2008); and selection of methods depends on data availability and precision required. Given the limited long-term meteorological data available for the study watershed, the temperature-based method developed by Hargreaves and Samani (1985) was applied to calculate PET. This method mainly reflected the effect of temperature on PET and is a widely used method recommended by FAO (Allen et al., 1998). The Hargreaves equation reads as:

$$\mathrm{PET} = 0.0023 \times Ra \times \left[\frac{T_{\max} + T_{\min}}{2} + 17.8 \right] \times \left(T_{\max} - T_{\min} \right)^{0.5} \qquad (2.7)$$

where, Ra is extraterrestrial radiation (in mm day^{-1}) estimated based on the approach suggested by Allen et al. (1998); $T_{\max}$ is mean maximum temperature in ^{o}C; and $T_{\min}$ is mean minimum temperature in ^{o}C.

2.2.5 Separating the effect of climate variability and human activities

Based on Zheng et al. (2009), for a given watershed, the streamflow can be modeled as a function of climate variables and human activities by:

$$Q = f(C,\ H) \qquad (2.8)$$

where, Q is streamflow, C and H represent climate factors and the integrated effects of human activities on streamflow, respectively. Following Eq. (2.8), the total change in observed

mean annual streamflow due to the combined effects of climate variability and human activities can be approximated as:

$$\Delta Q = f'_C \, \Delta C + f'_H \, \Delta H \tag{2.9}$$

where, ΔQ, ΔC and ΔH are changes in streamflow, climate, and human activities, respectively; with $f'C = \partial Q/\partial C$ and $f'H = \partial Q/\partial H$. Based on several studies (e.g., Chen et al. 2012; Zhang et al. 2014; Zheng et al. 2009) and as a first-order approximation, Eq. (2.9) can be expressed as:

$$\Delta Q = \Delta \overline{Q}_C + \Delta \overline{Q}_H = \overline{Q}_{\text{cp}}^{\text{obs}} - \overline{Q}_{\text{bp}}^{\text{obs}} \tag{2.10}$$

where, ΔQ is the change in observed mean annual streamflow before and after the change-point, $\Delta \overline{Q}_C$ and $\Delta \overline{Q}_H$ represent the change in observed mean annual streamflow due to climate variability and human activities, $\overline{Q}_{\text{cp}}^{\text{obs}}$ and $\overline{Q}_{\text{bp}}^{\text{obs}}$ indicate the observed mean annual streamflow in the change period and baseline period, respectively.

To compute the effect of climate variability on the changes in annual streamflow, first the non-linear runoff model (Eq. 6) was calibrated using the data of annual streamflow, rainfall and PET in the baseline period (1992–1999) and the parameters k, α and β were estimated. Then, the model was forced by rainfall and PET data of 2000–2012 to simulate annual streamflow in the change period that would occur if there were no significant human activities; this can therefore be regarded as the streamflow response to climate variation only (Zhang et al. 2014). Thus, the difference between the mean annual streamflow in the baseline period and simulated mean annual streamflow of the change period can be considered as representing the influence of climate variability on streamflow changes, with no underlying surface changes:

$$\Delta\overline{Q}_C = \overline{Q}_{\text{bp}}^{\text{obs}} - \overline{Q}_{\text{cp}}^{\text{simu}} \quad (2.11)$$

where, $\overline{Q}_{\text{cp}}^{\text{simu}}$ represents the simulated mean annual streamflow in the change period. The relative contributions of climate variability and human activities on the changes in streamflow, which are defined as μ_C and μ_H, respectively were quantitatively estimated by:

$$\mu_C = \frac{\Delta\overline{Q}_C}{\Delta Q} \times 100 \quad (2.12)$$

$$\mu_H = \frac{\Delta\overline{Q}_H}{\Delta Q} \times 100 \quad (2.13)$$

The methodological framework used for this study is summarized in Figure 2.1.

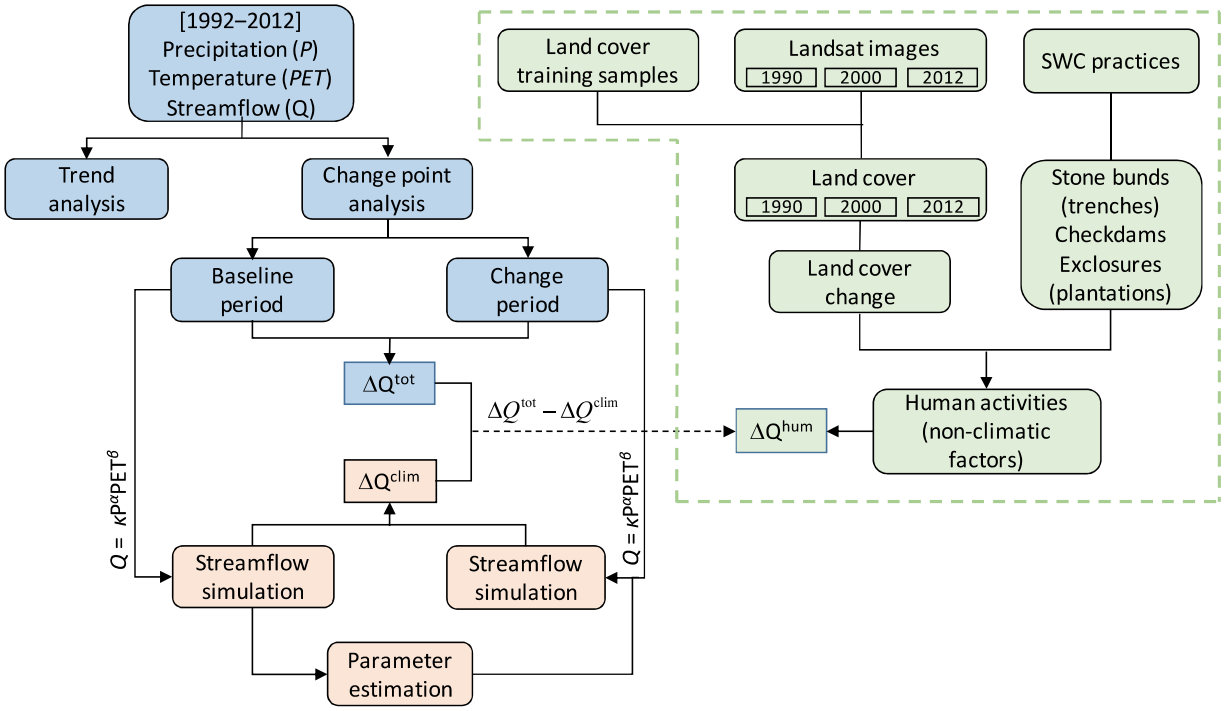

Figure 2.1 Methodological framework used to estimate the effect of climatic and non-climatic factors on changes of streamflow.

2.3 Results and discussion

2.3.1 Trend and change-point tests

The MK trend test ($p < 0.05$) was applied to annual, seasonal and monthly streamflow and rainfall records of the period 1992–2012 (Table 2.1). The annual and wet season streamflow exhibited decreasing trends that were statistically significant; by contrast statistically significant increasing trend was detected for the dry season streamflow. For the wet season months of July and August, streamflow showed significant decreasing trends, whereas for month of June decreasing but statistically insignificant trend was observed. Statistically significant increasing trends of streamflow were observed for November, December and January; while other dry season months showed increasing trends but test statistics were not significant. Trend test results of rainfall records on monthly, seasonal and annual bases revealed no statistically significant trends (Table 2.1). The results of the trend test of the rainfall records well agree with the findings of Hadgu et al. (2013) who reported that in Tigray region of northern Ethiopia, rainfall is highly variable with no significant trend for annual and seasonal totals. The decreasing trends of wet season and annual streamflow and increasing trend of dry season streamflow with no significant changes in rainfall implied that inter-annual rainfall pattern was not the major driver for the trend changes of streamflow observed in Agula watershed. Therefore, it is important to note that the observed trends of changes in streamflow could be attributed, among other factors, to modification of watershed responses through implementation of proper watershed management practices (Figure 1.5, Table 1.1) and associated changes in LULC (Figure 2.4, Table 2.3). For instance, the watershed management practices (Figure 1.5, Table 1.1) can influence hydrologic response thereby improving storage and recharge fluxes; whereas the increased in vegetation cover (shrub land and forest cover) (Figure 2.4, Table 2.3) is expected to enhance canopy

interception. These combined effects could lead to decreasing trends in wet season and annual streamflow while the dry season streamflow increased.

Table 2.1 Mann-Kendall trend test for monthly, seasonal and annual streamflow and rainfall data (* indicated statistically significant trends, *p*-value < 0.05).

	Streamflow		Rainfall	
Period	Z	*p*-value	Z	*p*-value
Annual	-2.33*	0.019	-0.82	0.415
Wet season	-3.06*	0.002	-0.82	0.415
Dry season	+3.11*	0.002	-0.03	0.976
January	+2.45*	0.014	+0.03	0.976
February	+1.08	0.280	-0.97	0.334
March	+1.51	0.131	+0.21	0.833
April	+1.90	0.057	+0.00	0.000
May	+0.88	0.381	-0.39	0.695
June	-1.24	0.216	-0.63	0.526
July	-2.45*	0.014	-0.27	0.786
August	-2.14*	0.032	-0.45	0.651
September	+0.03	0.976	-1.24	0.216
October	+0.21	0.833	+0.45	0.651
November	+2.08*	0.037	+0.15	0.880
December	+2.57*	0.010	-0.12	0.904

The change-point test result (Figure 2.2) showed that *u(t)* and *u*(t)* curves intersected around 2000 between the 5% significant level. This implied that around the year 2000, human activities started to considerably influence the streamflow response. Even though integrated watershed management practices in Agula watershed were started in early 1990s, the extent of implementation was very limited and construction of proper SWC measures was intensified after 1995 (Table 1.1). As such, the detection of the year 2000 as a change-point of annual streamflow corresponds to the period of intensification of proper watershed management practices such as construction of stone bunds with or without trenches and check dams and establishment of

exclosures, especially after 1995 (Table 1.1) as well as improved vegetation cover as reported in this study (Figure 2.4, Table 2.3) and by other previous studies (e.g., Alemayehu et al. 2009; Igbokwe and Adede 2001), which in effect can lead to reduction of direct runoff volume. It is worth noting that the result of change-point detection is in agreement with the SWC history in Agula watershed. Therefore, proper watershed management practices and changes in LULC, among other factors, can be considered as the main drivers of changes in streamflow of Agula watershed. Based on the result of the change-point test and to analyze the changes in streamflow regimes, the streamflow record was divided into two periods: a baseline period (1992–1999), representing streamflow with no or minimal influence of human activities; and a change period (2000–2012), representing streamflow under significant influence of human activities such as implementation of proper watershed management practices. In addition, since LULC change can have noticeable effects on streamflow, the change in LULC of Agula watershed was evaluated for the years 1990, 2000 and 2012.

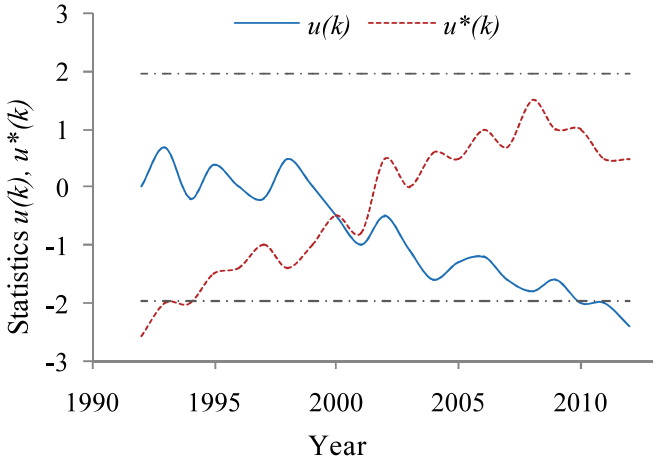

Figure 2.2 Mann–Kendall–Sneyers sequential trend test of annual streamflow with forward u(k) and backward u*(k) sequences. The horizontal dotted lines represent the critical value corresponding to the 5% significant level.

2.3.2 Changes in streamflow regimes

The mean annual rainfall and streamflow were 609 mm and 126 mm in the baseline period (1992–1999) and 583 mm and 80 mm in the change period (2000–2012) (Table 2.2). The total annual runoff coefficients were estimated to be 0.2 and 0.14 in the baseline and change periods, respectively; and the order of magnitude of the runoff coefficients are close to the results reported by Gebreyohannes et al. (2013) for the Geba watershed (0.18) of which Agula watershed is one of the major tributaries. The wet season rainfall and streamflow accounted for 85% and 88% of the annual rainfall and streamflow, respectively in the baseline period. However, in the change period the contribution of the wet season streamflow reduced to 70%; while the wet season rainfall was about 86% of the annual. Though the annual and wet season rainfall showed small reductions by about less than 5%, the observed reductions in the corresponding streamflow were considerably larger, 36% and 49%, respectively. Also, despite reduction of dry season rainfall by about 15% in the period 2000–2012, the dry season streamflow increased by about 57%. The inter-annual variability of rainfall and streamflow are shown by the coefficients of variation (CV), and in the baseline period, streamflow showed more variability than rainfall (Table 2.2). In the change period, CV values of rainfall almost remained unchanged; whereas CV values of annual and wet season flows significantly reduced; which showed a more uniform streamflow. Over all, the changes in streamflow regimes and variability without considerable change in rainfall indicated that other external drivers of change such as implementation of proper watershed management practices and associated changes in LULC may have considerably influenced streamflow response of Agula watershed.

Table 2.2 Rainfall and streamflow changes in the baseline (1992–1999) and change periods (2000–2012).

	1992–1999				2000–2012				Change (%)	
	$\overline{P}$ (mm)	CV	$\overline{Q}$ (mm)	CV	$\overline{P}$ (mm)	CV	$\overline{Q}$ (mm)	CV	$\overline{P}$	$\overline{Q}$
Annual	609	0.15	126	0.36	583	0.19	80	0.14	-4	-36
Wet season	517	0.16	111	0.39	505	0.18	56	0.15	-2	-49
Dry season	92	0.58	15	0.29	79	0.60	24	0.52	-15	57

Implementation of proper watershed management practices such as stone bunds on cultivated lands and on hill-slopes and check dams in gullies and rivers (Figure 1.5, Table 1.1) can increase storage and enhance subsequent groundwater recharge and hence influence the hydrologic response. In addition, in terms of LULC change, most pronounced was the dramatic decrease in bare land and increase in shrub land and forest cover (Figure 2.4, Table 2.3) as well as improved grass cover within shrubs (Figure 1.5(b)). The increase in vegetation cover observed in Agula watershed can enhance interception and recharge fluxes which in effect can result in reduction of wet season streamflow and increase in dry season streamflow, thus reducing water shortage in the dry season. As such, the decrease in annual and wet season streamflow and increase in dry season streamflow of Agula watershed can be attributed to factors such as proper watershed management practices and associated changes in LULC. The results of this study are in agreement with similar impact studies in Tigray region and elsewhere. In the same study region, Haregeweyn et al. (2012) and Nyssen et al. (2010) reported significant reductions of surface runoff by about 27% and 80%, respectively as a result of structural works such as stone bunds and check dams which in-turn enhance infiltration and subsequent groundwater recharge that improve dry season water availability. Another study in Tigray region of northern Ethiopia by

Taye et al. (2013) showed that stone bunds on cultivated lands can reduce runoff generation by about 30–60%. In the upper Agula watershed, Alemayehu et al. (2009) reported improved groundwater availability and wetland development in valley bottoms as a result of conservation efforts. In addition, in the middle and upper reaches of the watershed, geologic formations are dominantly sandstones (Adigrat and Enticho sandstone formations) (Gebreyohannes et al. 2013) which in combination with the SWC practices can enhance recharge fluxes (Nyssen et al. 2010), and in effect can lead to increase in dry season streamflow. Also, Igbokwe and Adede (2001) reported that increase in vegetation cover in eastern Tigray region of northern Ethiopia enhances groundwater recharge and hence improves dry season water availability. Descheemaeker et al. (2006) showed that establishment of exclosures in degraded highlands of Tigray region resulted in increase in vegetation cover that lead to significant reductions in runoff. A recent study by Haregeweyn et al. (2016) revealed that implementation of appropriate basin-wide SWC practices could reduce the total annual runoff yield of the upper Blue Nile basin by about 38%. A similar study by Huang and Zhang (2004) in the Loess Plateau of China showed that check dams and terraces significantly enhance soil water infiltration and prolong streamflow detention which in-turn reduces wet season streamflow but increase dry season streamflow.

2.3.3 Changes in LULC between 1990 and 2012

Based on the spectral responses of features and field observation of the study area, six LULC types (Figure 2.3) were identified and their descriptions are given below with some modification from Mayaux et al. (2004).

- Cultivated land - Land used for growing crops, including areas currently under crop and land under preparation.

- Grass land - Landscapes where grasses are the dominant vegetation forms.
- Shrub land - Areas covered with shrubs, bushes and small trees with little wood mixed with grasses. Shrub lands of the 1990 were degraded by human and livestock interference whereas after establishment of exclosures since the mid 1990s, shrub lands of 2000 and 2012 were non-degraded with improved vegetation cover.
- Forest - Land with high density of trees which include eucalyptus and coniferous or deciduous trees.
- Bare land - Areas with little or no vegetation cover consisting of exposed soil degraded due to soil erosion or misuses.
- Settlement - Built-up and residential areas mainly rural towns.

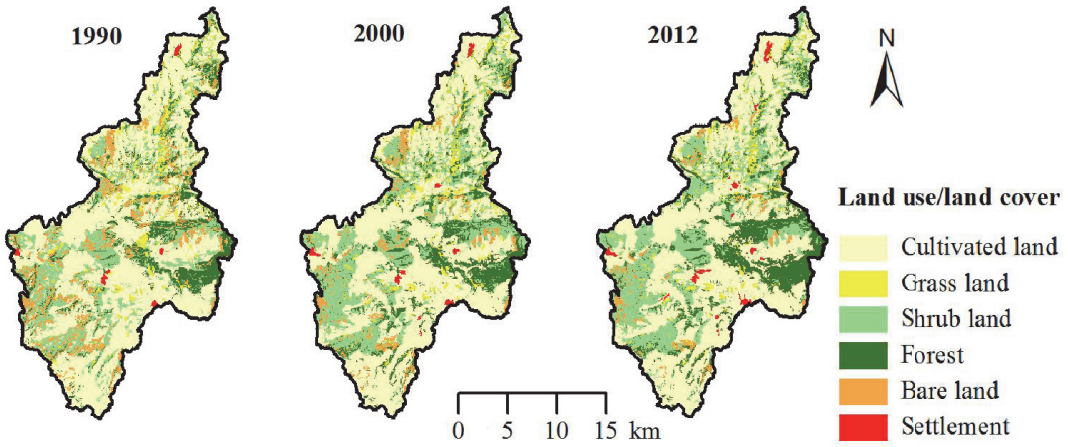

Figure 2.3 Land use/land cover maps of Agula watershed for the years 1990, 2000 and 2012.

The classified LULC maps (Figure 2.3) showed that cultivated land is the dominant LULC type which covered about 50% of the watershed between 1990 and 2012. Shrub land is the second dominant LULC type (20%) followed by forest cover and bare land each accounting for about 10% of the watershed in 1990. The grass land cover and settlement account for the least area coverage (about 5%) of the watershed during the study periods. Significant changes in

LULC were observed for shrub land and forest cover which increase by about 18 km^2 and 10 km^2 in the period 1990–2000; and then further increase by about 4 km^2 and 6 km^2, respectively during 2000–2012 (Figure 2.4). By contrast, bare land registered considerable reductions by about 23 km^2 and 13 km^2 in the periods 1990–2000 and 2000–2012, respectively.

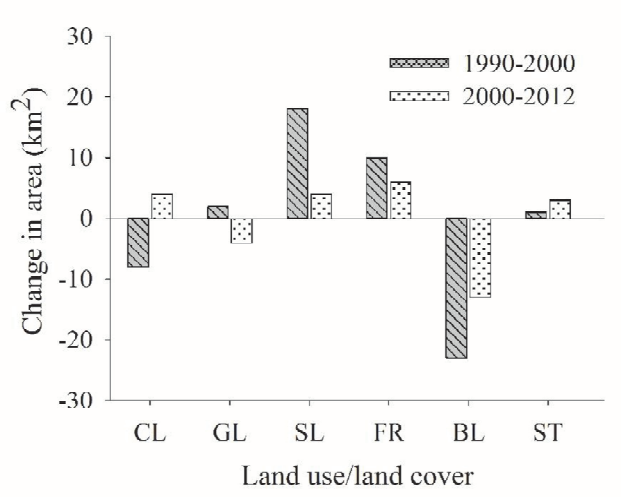

Figure 2.4 Changes in area (km^2) of land use/land cover in Agula watershed: *CL* cultivated land, *GL* grass land, *SL* shrub land, *FR* forest, *BL* bare land, *ST* settlement.

The increase in shrub land and forest cover can be attributed to proper watershed management practice such as establishment of exclosures combined with or without enrichment plantation (forage grass and multi-use tress) that enabled restoration of degraded areas of the watershed. In Tigray region of northern Ethiopia, previous studies (e.g., Mekuria et al. 2007; Yayneshet et al. 2009) reported conversions of degraded hill-slopes to shrub land and subsequent increase in forest cover in areas where exclosures are widely implemented. Furthermore, it is worth noting that considering the establishment of exclosures since the mid 1990s and as reported by Fenta et al. (2017b), shrub lands of the 1990 were degraded especially by overgrazing, whereas shrub lands of the 2000 and 2012 were non-degraded (with better grass

cover within shrubs, Figure 1.5(b)) as they were set-aside as exclosures. The LULC change results in this study are in agreement with the results of Alemayehu et al. (2009) and Belay et al. (2014) who reported increased restoration of degraded lands and improved vegetation cover for the eastern Tigray of northern Ethiopia wherein the present study watershed is found.

Table 2.3 Land use/land cover transition matrices (in km^2) from 1990 to 2000 and from 2000 to 2012 of Agula watershed in northern Ethiopia. *CL* cultivated land, *GL* grass land, *SL* shrub land, *FR* forest, *BL* bare land, *ST* settlement.

From initial state (1990)	To final state (2000)							
	CL	GL	SL	FR	BL	ST	Total 1990	Losses
CL	223	2	9	0	0	1	235	12
GL	3	17	0	0	0	0	20	3
SL	1	3	73	14	0	0	91	18
FR	0	0	4	46	0	0	50	4
BL	0	0	23	0	21	0	44	23
ST	0	0	0	0	0	2	2	0
Total 2000	227	22	109	60	21	3		
Gains	4	5	36	14	0	1		
Net change	-8	2	18	10	-23	1		
Net persistence	-0.04	0.12	0.25	0.22	-1.10	0.50		
From initial state (2000)	To final state (2012)							
	CL	GL	SL	FR	BL	ST	Total 2000	Losses
CL	221	2	3	0	0	1	227	6
GL	4	15	3	0	0	0	22	7
SL	2	0	97	10	0	0	109	12
FR	2	0	2	56	0	0	60	4
BL	2	1	8	0	8	2	21	13
ST	0	0	0	0	0	3	3	0
Total 2012	231	18	113	66	8	6		
Gains	10	3	16	10	0	3		
Net change	4	-4	4	6	-13	3		
Net persistence	0.02	-0.27	0.04	0.11	-1.63	1.00		

The LULC transition matrices (Table 2.3) showed that in the period 1990–2000, bare land experienced the highest loss of 23 km^2 which was converted to shrub land, which registered the highest gain, 36 km^2. During the same period, forest cover gained about 14 km^2 from shrub land. The net change was highest for bare land (decreased by 23 km^2) followed by shrub land (increased by 18 km^2). In the second period (2000–2012), shrub land registered the highest gain (16 km^2) primarily at the expense of bare land; and at the same time 10 km^2 of shrub land was converted to forest (Table 2.3). Based on the net persistence values, bare land showed more tendency to loss than persist or gain; whereas cultivated land showed more tendency to persist than to gain or to loss. The LULC change results in this study are in agreement with the results of Alemayehu et al. (2009) and Belay et al. (2014) who reported increased restoration of degraded lands and improved vegetation cover for the eastern Tigray of northern Ethiopia wherein the present study watershed is found. A similar study by Bewket (2002) indicated that community-based watershed management practices resulted in increase forest cover and shrub lands in the Chemoga watershed of northwestern Ethiopia. These studies demonstrated that watershed management practices implemented in different parts of Ethiopia are effective measures to restore areas severely affected by land degradation and resulted in considerable LULC changes.

2.3.4 Effects of climate variability and human activities on streamflow

Table 2.4 shows the changes of streamflow and climate variables in the baseline (1992–1999) and change (2000–2012) periods. The reduction in streamflow in the change period compared with the baseline period can be the result of both climate variability and human activities. The effect of climate variability on streamflow was estimated using the non-linear runoff model, Eq. (2.6). The parameters k, α and β in Eq. (2.6) were estimated using data of annual streamflow,

rainfall and PET for the baseline period and derived a runoff model, Eq. (2.14). The regression coefficient ($p < 0.05$) and Nash-Sutcliffe efficiency values were 0.86 and 0.83, respectively; which indicated that the annual streamflow calculated by Eq. (2.14) and the observed streamflow had the same basic trend, and the model had good efficiency.

$$Q = 0.024 P^{1.788} \mathrm{PET}^{-0.393} \tag{2.14}$$

To estimate the impact of climate variability on streamflow response, annual streamflow in the change period was simulated using Eq. (2.14) and data of annual rainfall and PET of the period 2000–2012. This provided the simulated annual streamflow for the period 2000–2012 that would occur if there were no significant human activities in the watershed. As a result, the simulated annual streamflow is impacted only by climatic variability. As described in the methods section, this approach assumed that for a given watershed the relationship between climatic variables (rainfall and PET) and streamflow remain unchanged unless watershed characteristics have been modified. As such, the difference between the mean annual streamflow in the baseline period $\left(\overline{Q}_{\mathrm{bp}}^{\mathrm{obs}}\right)$ and simulated mean annual streamflow of the change period $\left(\overline{Q}_{\mathrm{cp}}^{\mathrm{simu}}\right)$ represents the influence of climate variability on streamflow changes (Table 2.4). In addition, the quantity of the simulated mean annual streamflow in the change period was larger than the observed quantity (Table 2.4), indicating that the effect of streamflow reduction that resulted from human activities existed during this period. The contributions of climate variations and human activities on the decreasing annual streamflow were quantitatively estimated using Eqs. (2.8)–(2.13). During the change period, the effects of climate variability and human activities on streamflow showed a significant difference, with about 22% of the total reduction in mean annual streamflow caused by climate variations; whereas accounting for 78% of the

change, human activities were the major driving factors in changing the streamflow response (Table 2.4). Climate variability has been identified as a dominant driver of changes in streamflow in arid and semiarid regions (e.g., Chen et al. 2012; Ma et al. 2008); however, this study highlighted the significance of human activities in influencing the streamflow response.

Table 2.4 Contributions of climate variability and human activities on streamflow changes of Agula watershed.

Period	$\overline{P}$ (mm)	$\overline{PET}$ (mm)	$\overline{Q}^{obs}$ (mm)	$\overline{Q}^{simu}$ (mm)	μ_C (%)	μ_H (%)
1992-1999	609	1690	126	-	-	-
2000-2012	583	1700	80	116	22	78

The results showed that indirect effects of human activities such as implementation of proper watershed management practices and the changes in LULC were effective not only in terms of restoration of degraded lands but also positively influenced the streamflow response. Other direct impacts of human activities such as water abstractions for domestic and agricultural uses can also lead to changes of streamflow regimes. In recent years, in an effort to enhance food security, small-scale irrigation practices have increased in parts of Agula watershed; nonetheless, the amount of water used for irrigation by diverting the river water and use of hand-dug wells was not well documented; and hence, this study did not attempt to make quantitative estimations of the direct effects of human activities. Furthermore, it is important to note that, to make quantitative estimation of the contribution of climate variability and human activities to changes in streamflow, the two major factors are assumed be mutually independent variables. However, in fact, LULC change can be influenced by both human activities and climate variations; as such, the two factors are related to each other and are not readily separable. Also, the SWC measures,

LULC change, and other human activities might counteract each other and their effects on changes in streamflow are complicated. In addition, during calibration of the non-linear runoff model, a relatively good performance was observed; even so, the phenomenon of underestimation and overestimation may still exist, causing uncertainties in estimation of the climatic and human-induced effects on streamflow. Therefore, further observation, experiments and investigation should be conducted to improve the quantitative assessments, especially using physical-based distributed models to identify the physical mechanisms behind the changes. In the present study, however, the extent of conservation measures in Agula watershed are known, but the exact locations are not mapped; thus limiting the use of detailed physical based models to simulate the impact of SWC measures on the hydrologic response.

2.4 Conclusions

This study analyzed the changes in streamflow response as a result of climate variability and changes in human activities (mainly proper watershed management practices and changes in LULC) in Agula watershed of northern Ethiopia. The MK test results showed statistically significant decreasing trends for annual and wet season streamflow for the period 1992–2012, while an increasing trend was observed for dry season streamflow. Analyses of seasonal and annual rainfall records showed no significant trends. Based on the MKS test, an abrupt change-point in annual streamflow occurred around 2000; and hence the streamflow record was divided into two periods: a baseline period (1992–1999) and a change period (2000–2012). The mean annual and wet season streamflow decreased by about 36% and 49%, respectively during the change period compared to the baseline period; however, dry season streamflow increased by 57%. The results of this study point to the potential that reduced wet season flow and improved

dry season water availability can be achieved by proper planning and implementation of watershed management practices; and this potential is especially important for arid and semiarid areas where water is a scarce resource. The LULC change analysis showed improved shrub land and forest cover that led to restoration of about 36 km^2 bare land during the study period; which demonstrated the effectiveness of land restoration efforts undertaken in the past few decades. Model estimations revealed that climate variability accounted for 22% of the total reduction in mean annual streamflow; whereas the reduction due to human activities was about 78%. This study demonstrated that human activities primarily proper watershed management practices and associated changes in LULC, among other factors, play a more pronounced role in driving the changes in streamflow of Agula watershed. Quantifying the effects of climate variability and human activities on changes in streamflow response helps improve our understanding of the hydrological response in the watershed, but also is essential to develop appropriate watershed management strategies and ensure sustainable use of land and water resources.

Chapter 3

Dynamics of soil erosion as influenced by watershed management practices: A case study of the Agula watershed in the semiarid highlands of northern Ethiopia

This chapter is published as:

Fenta AA, Yasuda H, Shimizu K, Haregeweyn N, Negussie A. (2016). Dynamics of soil erosion as influenced by watershed management practices: A case study of the Agula watershed in the semiarid highlands of northern Ethiopia. Environmental Management 58: 889–905.

Abstract

Since the past two decades, watershed management practices such as construction of stone bunds and establishment of exclosures have been widely implemented in the semiarid highlands of northern Ethiopia to curb land degradation by soil erosion. This study assessed changes in soil erosion for the years 1990, 2000 and 2012 as a result of such watershed management practices in Agula watershed using the Revised Universal Soil Loss Equation (RUSLE). The RUSLE factors were computed in a geographic information system for 30×30 m raster layers using spatial data obtained from different sources. The results revealed significant reduction in soil loss rates by about 55% from about 28 to 12 t ha^{-1} yr^{-1} in 1990–2000 and an overall 64% reduction from 28 to 10 t ha^{-1} yr^{-1} in 1990–2012. This change in soil loss is attributed to improvement in surface cover and stone bund practices which resulted in the decrease in mean *C* and *P*-factors respectively by about 19% and 34% in 1990–2000 and an overall decrease in *C*-factor by 29% in 1990–2012. Considerable reductions in soil loss were observed from bare land (89%), followed by cultivated land (56%) and shrub land (49%). Furthermore, the reduction in soil loss was more pronounced in steeper slopes where very steep slope and steep slope classes experienced over 70% reduction. Validation of soil erosion estimations using field observed points showed an overall accuracy of 69%, which is fairly satisfactory. This study demonstrated the potential of watershed management efforts to bring remarkable restoration of degraded semiarid lands that could serve as a basis for sustainable planning of future developments of areas experiencing severe land degradation due to water erosion.

Keywords: Soil erosion; RUSLE model; Watershed management; Semiarid; Ethiopia

3.1 Introduction

Soil erosion is one of the biggest global challenges with its social, economic, and environmental effects (Pimentel 2006; Yang et al. 2003); and soil erosion by water is the most critical problem as it has several on-site and off-site effects. The severe on-site effects constitute loss of farmland (Nyssen et al. 2006), nutrient depletion (Haregeweyn et al. 2008), and soil quality degradation (Solomon et al. 2000). The off-site effects include siltation of downstream reservoirs (de Vente et al. 2008; Haregeweyn et al. 2006; Tamene et al. 2011) and lakes (Hrissanthou et al. 2010). In addition to its environmental effects, soil erosion has also economic consequences that led to distressing food shortages and reduced farm income (Sonneveld and Keyzer 2003). The economic challenges are more serious in developing and ecologically fragile areas of the world, where the subsistence farming population are unable to replace lost soils and nutrients (Ananda and Herath 2003). Given the multiple impacts of soil erosion, concern for the global environment has increased; however, soil erosion has accelerated in many parts of the world primarily driven by demographic and socio-economic factors (Yang et al. 2003).

In developing countries like Ethiopia, increased human and livestock population, cultivation on steep slopes, clearing of vegetation and overgrazing are the major drivers that accelerate soil erosion (Amsalu et al. 2007; Hurni 1993; Sonneveld and Keyzer 2003). El-Swaify and Hurni (1996) and Taddese (2001) reported that the Ethiopian highlands constitute one of the most degraded lands in Africa; and soil erosion considerably damaged the ecology in many parts of the highlands, some beyond recovery. Nation-wide soil erosion estimation by Hurni (1988) showed an annual gross soil loss of 1.5×10^{9} t; and the highest loss is from croplands (42 t ha^{-1} yr^{-1}). In Ethiopia, soil erosion has been a major problem for many years as it led to decreased

soil productivity (Berry 2003; Girmay et al. 2009) and severely affected the country's agriculture sector, which is the main stay for about 85% of the population. To reverse the situation, watershed management efforts have been undertaken through implementation of soil and water conservation (SWC) measures in different parts of the country, especially since the past two decades (Gebremedhin and Swinton 2003; Haregeweyn et al. 2015; Osman and Sauerborn 2001).

The soil erosion problem is more severe in the northern highlands of Ethiopia due to overgrazing, further exacerbated by high rainfall intensity and steep topography (Nyssen et al. 2005). As a result, in the past few decades massive land restoration programs have been initiated in the semiarid areas of northern Ethiopia especially in Tigray region, which aimed to rehabilitate degraded areas, to improve water availability and vegetation cover, and to enhance food security. The land restoration programs mainly focused on implementation of different SWC measures that include stone bunds with or without trenches on cultivated lands and on hill-slopes (Esser et al. 2002; Gebrernichael et al. 2005; Nyssen et al. 2007), check dams in gullies (Haregeweyn et al. 2012; Nyssen et al. 2004), and establishment of exclosures with or without enrichment plantations to restore degraded hill-slopes (Descheemaeker et al. 2006; Mekuria et al. 2009; Mekuria and Veldkamp 2012). Considering this, several impact studies have focused on effectiveness evaluation of the individual SWC measures at plot-scale (e.g., Descheemaeker et al. 2006; Gebrernichael et al. 2005; Girmay et al. 2009; Nyssen et al. 2007) and small-scale watersheds (<100 km^2) (e.g., Haregeweyn et al. 2012; Nyssen et al. 2009a); however, studies at medium or large-scale watersheds (>100 km^2) which are of great interest for land managers and policy-makers are rather scarce (e.g., Nyssen et al. 2008). This is partly due to the fact that estimation of soil erosion at watershed-scale is often difficult owing to the complex interaction of factors, such as climate, land use and land cover (LULC), soil, topography, and human activities.

In addition, up-scaling plot-scale erosion studies to larger spatial domains is commonly constrained by limited number of samples in complex environments (Lu et al. 2004).

However, recent advances in remote sensing with improved spatial accuracy and geographic information systems (GIS) facilitate derivation of input variables and computation of soil erosion at larger spatial domains. This character, coupled with the increased computing power of computers, allows assessment of watershed-scale soil erosion dynamics with reasonable cost and better accuracy (Wang et al. 2003). Quantitative information on soil erosion at watershed-scale helps guide conservation and development plans for sustainable use and management of watershed resources (e.g., Bewket and Teferi 2009; Chatterjee et al. 2014; Farhan et al. 2013; Haregeweyn et al. 2012; Meshesha et al. 2012). In this study, the Revised Universal Soil Loss Equation (RUSLE) model was applied in a GIS environment to assess the dynamics of soil erosion as influenced by watershed management practices in the semiarid highlands of northern Ethiopia, taking Agula watershed as a case study site. A recent study (Fenta et al. 2017b) as well as other previous watershed management related impact studies in Agula watershed (e.g., Alemayehu et al. 2009; Igbokwe and Adede 2001) reported considerable changes in LULC and improved vegetation cover that led to changes in watershed runoff responses (Fenta et al. 2017b). However, watershed-scale changes in soil erosion as a result of the watershed management practices and associated changes in LULC were not evaluated so far. Hence, this study was initiated (i) to assess the temporal and spatial dynamics of annual soil erosion rates between 1990 and 2012, (ii) to identify the factors controlling this dynamics with particular emphasis on watershed management practices, and (iii) to assess the soil erosion vis-à-vis LULC and topographic factor (slope).

3.2 Materials and methods

3.2.1 Assessment of the spatiotemporal changes in the rate of annual soil erosion

Various classes of soil erosion models ranging from simple empirical models such as the USLE (Wischmeier and Smith 1978) and its revised version RUSLE (Renard et al. 1991) to process-based models such as EUROSEM (Morgan et al. 1998) and WEPP (Nearing et al. 1989) have been developed to assess soil erosion at different spatio-temporal scales. Process-based models require representation of the physical processes responsible for erosion (Jetten et al. 2003) and hence are data intensive. Such models enable understanding of soil erosion at detailed spatio-temporal scales; however, the return in increased accuracy of soil erosion prediction is limited (Jetten et al. 2003; Tiwari et al. 2000). Despite the development of a range of process-based models, empirical models are the most commonly used to predict soil erosion because of their minimal data requirements and ease of application; and among the empirical models, the RUSLE is most commonly used. The RUSLE model was initially developed to estimate soil loss by sheet and rill erosion at small hill-slope and plot-scale, but also applied for use at watershed- and regional-scales (e.g., Bewket and Teferi 2009; Erdogan et al. 2007; Haregeweyn et al. 2012; Meshesha et al. 2012). Moreover, several parameters of the RUSLE model have been modified to Ethiopian conditions by Hurni (1985) (Table 2); other studies also adapted the RUSLE model and calibrated some of the input factors for Ethiopian settings (e.g., Gebremichael et al. 2005; Haregeweyn et al. 2013; Nyssen et al. 2009a).

In this study, the RUSLE model parameters adapted to the Ethiopian conditions (Gebremichael et al. 2005; Haregeweyn et al. 2013; Hurni 1985; Nyssen et al. 2009a) were used to assess the dynamics of soil erosion for three selected periods: 1990, 2000 and 2012. The study

periods were selected to assess the changes in soil erosion before and after implementation of large-scale watershed management practices in the study area (Table 1.1). Furthermore, the model has also been successfully applied for similar studies in different parts of Ethiopia (e.g., Bewket and Teferi 2009; Haregeweyn et al. 2012; Meshesha et al. 2012; Nyssen et al. 2008). Despite the fact that the RUSLE is an empirical model, its compatibility for use with remote sensing data and GIS tools is a merit as it enables soil erosion estimation at different space-time scales. However, the model has limitations as it provides long-term averages of soil erosion without estimating deposition, sediment yield, and channel/gully erosion and land slide (Renard et al. 1991). The RUSLE model estimates average annual soil erosion taking four major factors these are: climatological (rainfall erosivity), pedological (soil erodability), topographic (slope length and steepness) and anthropogenic (cropping and LULC and conservation support practices). Each of these factors are empirically standardized with the logic of lower values are less vulnerable and higher values refer to more vulnerability for erosion. The RUSLE model is given as:

$$A = R \times K \times LS \times C \times P \qquad (3.1)$$

where, A is the amount of soil erosion (t $ha^{-1}yr^{-1}$), R is the rainfall erosivity factor (J cm m^{-2} hr^{-1} yr^{-1}), K is the soil erodibility factor (t m^2 hr ha^{-1} J^{-1} cm^{-1}), LS is a slope length and steepness factor (dimensionless), C is a cover factor that accounts for the LULC class (dimensionless), and P is a conservation support practice factor (dimensionless).

When the RUSLE model is used in a GIS environment, each factor in Eq. 3.1 is described as a specific thematic layer and an overlay of these layers, through appropriate map algebra functions, allows computation of spatially distributed soil erosion at the watershed level. Spatial variations in watershed characteristics such as soil erodibility, surface cover, slope length and

steepness and rainfall erosivity can lead to variability in estimated soil erosion; therefore, the RUSLE model was used in raster-based GIS file format to assess soil erosion changes on a spatially explicit basis. Since the Landsat images and the SRTM-DEM used in this study have 30 m spatial resolution, all the data layers were set to a grid size of 30 m by 30 m and were re-projected to the Universal Transverse Mercator (UTM) map projection (zone 37N), Adindan datum and Ellipsoid - Clark 1880for computation of the soil erosion. Using Eq. 1, the RUSLE factor layers were multiplied together to estimate the average annual soil loss for the years 1990, 2000 and 2012 using the raster calculator functionality of the ArcGIS software. The temporal changes in the rate of soil erosion for the periods 1990–2000, 2000–2012 and 1990–2012 were analyzed by using the change statistics as:

$$\text{Change}\ (\%) = \left(\frac{A_{\text{final year}} - A_{\text{initial year}}}{A_{\text{initial year}}} \right) \times 100 \qquad (3.2)$$

where, A is the mean annual rate of soil loss (t $ha^{-1}yr^{-1}$). Positive percentage values suggest an increase whereas negative values imply a decrease in the rate of soil loss.

Based on the estimated annual soil loss rates and expert judgment, five erosion severity classes were identified: very slight (0–2 t ha^{-1} yr^{-1}), slight (2–10 t ha^{-1} yr^{-1}), moderate (10–20 t ha^{-1} yr^{-1}), severe (20–40 t ha^{-1} yr^{-1}) and very severe (> 40 t ha^{-1} yr^{-1}). This classification scheme also considered the tolerable soil erosion rate suggested by Hurni (1983b) for Ethiopia, which ranges from 2 to 18 t ha^{-1} yr^{-1}. Furthermore, the spatial variation of soil erosion in relation to different LULC types and slope ranges was assessed by using zonal statistics function of the spatial analyst tools in ArcGIS software. Slope map was generated from SRTM-DEM and reclassified into six slope categories: flat (0–3% slope), gentle (3–8% slope), sloping (8–15% slope), moderately steep (15–30% slope), steep (30–50% slope) and very steep (≥50% slope).

Such assessment enabled to identify the LULC types and slope categories that are most vulnerable for high soil erosion.

3.2.2 Computation of the RUSLE-factors

Rainfall erosivity (R)-factor

In the original USLE model (Wischmeier and Smith 1978), the rainfall erosivity (*R*)-factor was determined from total storm energy and maximum 30 minute rainfall intensity. However, there were no records of storm energy and rainfall intensity for Agula watershed. For areas where insufficient rainfall data is available, different empirical equations have been developed that estimate *R* values from mean rainfall. In this study, the empirical equation which was tested and adapted for the highlands of northern Ethiopia by Hurni (1985) was used to calculate the *R*-factor from mean annual rainfall. Meteorological data (1992–2012) for Atsbi and Wukro stations and mean annual 20 mm interval isohyets (line rainfall data) for the whole country were obtained from the National Meteorology Agency (NMA) of Ethiopia. Since the number of rainfall meteorological stations within and around the watershed was limited, rainfall grids were generated from interpolation of the national isohyets for better representation of rainfall variation across space. Simple comparison of the mean annual rainfall records from Atsbi and Wukro stations with the corresponding interpolated grid values showed that the rainfall data from the isohyets were close to the measurements from meteorological stations. Hence, the *R*-factor was calculated from the interpolated rainfall grids and extracted for the study watershed (Figure 3.1(a)). Several studies in different parts of Ethiopia used similar methods of determining *R*-factor from annual rainfall totals (e.g., Bewket and Teferi 2009; Haregeweyn et al. 2012; Meshesha et al. 2012). The *R*-factor was calculated as:

$$R = 0.562RF - 8.12 \quad (3.3)$$

where, RF is the mean annual rainfall in mm.

Table 3.1 The RUSLE factors adapted to Ethiopian conditions modified after Hurni (1985).

Annual rainfall (mm)	100	200	400	800	1,200	1,600	2,000	2,400
R: Rainfall erosivity								
Annual *R* factor	48	104	217	441	666	890	1,115	1,340
K: Soil erodibility								
Soil color	Black		Brown		Red		Yellow	
K factor	0.15		0.20		0.25		0.30	
L: Slope length								
Length (m)	5	10	20	40	80	160	240	320
L factor	0.5	0.7	1.0	1.4	1.9	2.7	3.2	3.8
S: Slope gradient								
Slope (%)	5	10	15	20	30	40	50	60
S factor	0.4	1.0	1.6	2.2	3.0	3.8	4.3	4.8
C: Land cover								
Dense forest			0.001		Dense grass			0.01
Other forest			0.01		Degraded grass			0.05
Badlands hard			0.05		Fallow hard			0.05
Badlands soft			0.40		Fallow ploughed			0.6
Sorghum, maize			0.10		Ethiopian *teff*			0.25
Cereals, pulses			0.15		Continuous fallow			1.00
Shrub land (degraded)[a]			0.05		Settlement[a]			0.01
Shrub land (non-degraded)[a]			0.03					
P: Management factor								
Ploughing up and down			1.00		Stone cover 40%			0.80
Strip cropping			0.80		Ploughing on contour			0.90
Applying mulch			0.60		Intercropping			0.80
Stone cover 80%			0.50		Dense intercropping			0.70
Stone bund-remains (crop land)[a]			0.70		Stone bund-moderate (non-crop land)[c]			0.60
Stone bund-moderate (crop land)[b]			0.32					

[a]Haregeweyn et al. (2013); [b]Gebremichael et al. (2005); [c]Nyssen et al. (2009a)

Soil erodibility (K)-factor

The soil erodibility (*K*)-factor is an empirical measure of the average long term susceptibility of soil to water erosion as determined by intrinsic soil properties; mainly soil texture, organic matter, soil structure and permeability of soil profile. The *K*-factor is rated on a scale from 0 to 1, with 0 indicating soils with the least susceptibility to erosion and 1 indicates soils, which are highly susceptible to soil erosion by water. The most commonly used method is the use of soil erodibility nomograph (Wischmeier and Smith 1978) to determine *K*-factor values from physical and biochemical soil properties. In this study, soil map (scale 1:50000) of Agula watershed was digitized from reports of Hunting Technical Services (HTS) (HTS 1976) and Tekeze River Basin Integrated Development Master Plan (MoWIE 1997). However, determining the physical and biochemical properties from a soil map is difficult. To overcome such data constraints, the experiment-based recommendations of Helldén (1987) and Hurni (1985) were adopted to use soil color which is a reflection of soil properties as a proxy to determine *K*-factor values (Figure 3.1(b)). The four major soil colors considered were black, brown, red and yellow, with corresponding *K*-factor values of 0.15, 0.2, 0.25 and 0.3, respectively (Table 3.1).

Topographic (L and S)-factors

The effect of topography on soil erosion is accounted for by the *LS*-factor, which combines the effects of slope length (*L*) and slope steepness (*S*)-factors. In general, as *L*-factor increases, total soil erosion and soil erosion per unit area increase due to the progressive accumulation of runoff in the down-slope direction; and as the *S*-factor increases, the velocity and erosivity of runoff increase (Wischmeier and Smith 1978). In the literature, several approaches are available for computing the *LS*-factor. The RUSLE model is sensitive to topographic factors, and hence it

is imperative to select the most appropriate formula especially when it is implemented in areas with steep-slopes. Given the mountainous topography of the study watershed, Eq. 3.4 which was proposed by Moore and Wilson (1992), was used to calculate the *LS*-factor (Figure 3.1(c)):

$$LS = \left(\frac{\beta\chi}{22.13}\right)^{0.4} \times \left(\frac{\sin(\theta)}{0.0896}\right)^{1.3} \tag{3.4}$$

where, β is flow accumulation which denotes the accumulated upslope contributing area for a given cell, χ is cell size (for this study 30 m), and θ is slope in degrees. The combined *LS*-factor was computed for the watershed by means of ArcGIS spatial analyst tools and ArcHydro tools extension using the SRTM-DEM. Based on Van Remortel et al. (2001), the assumption is that the 30 m spatial resolution DEM represents the natural micro-relief of the slopes being modeled. However, upon implementation two drawbacks were identified: first, the *LS*-factor showed exceptionally high values along rivers and streams that led to unrealistic erosion rates along these areas; second, in the flow accumulation layer, pixels without any upslope contributing areas (local maxima in height) showed a value of zero, and this resulted in an erosion estimate of zero, which does not represent the reality. Therefore, in the present study, adaptation of the flow accumulation layer was done to obtain realistic estimates of soil erosion. Since RUSLE is primarily suitable for estimating soil loss due to sheet and rill erosion processes, there is an upper bound on the accumulated upslope contributing area that should be used by defining a threshold for the flow accumulation layer. One possible way, proposed by Jain and Kothyari (2000), is to compare rivers and streams generated using a given threshold with observed rivers and streams manually digitized from topographic maps. In this study, the rivers and streams digitized from topographic maps (scale 1:50000) were well represented when stream definition threshold was set at 25 pixels of the flow accumulation layer. Hence, pixels representing rivers and streams

(flow accumulation ≥ 25) were excluded from the analysis. It should be noted that the threshold area is an average indicator and different physiographic regions may have different thresholds for defining rivers and streams. Furthermore, to account for erosion that occurred in pixels with local maxima in height and following Zhang et al. (2013), a value of 1 was added to the flow accumulation layer.

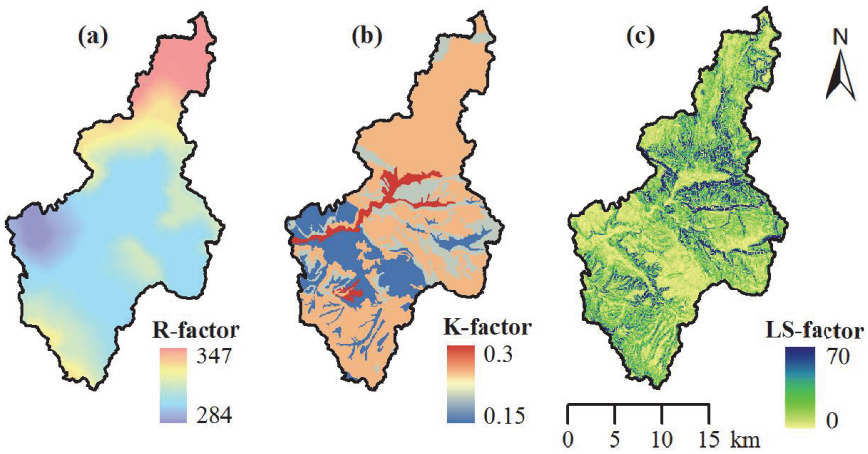

Figure 3.1 Spatial distribution of rainfall erosivity (a), soil erodibility (b), and slope steepness (c) factors of Agula watershed.

Cropping and land cover (C)-factor

The cropping and land cover (*C*)-factor reflects the effects of cropping system in agricultural lands or vegetation cover in plantation or forested areas on soil erosion rates (Renard et al. 1991). This wide range of factors is difficult and costly to measure and often vary considerably during the year. A good estimation of the *C*-factor can be derived from classification of remote sensing images. In this study, to determine the *C*-factor values, LULC maps of Agula watershed produced from Landsat TM and ETM+ images in our recent study (Fenta et al. 2017b) were used for the years 1990, 2000 and 2012. To produce the *C*-factor maps (Figure 3.2), the LULC maps

were reclassified and the *C*-factor values were assigned for different LULC types based on literature review of RUSLE factors adapted to Ethiopian conditions (Table 3.1).

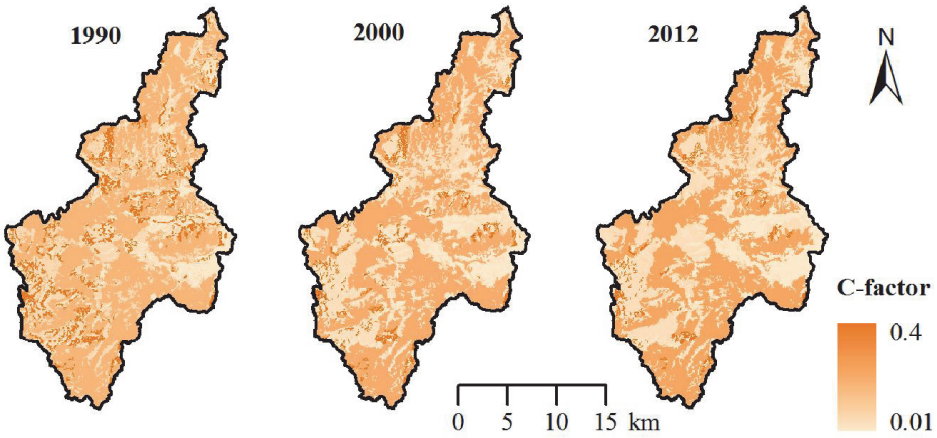

Figure 3.2 Spatial distribution map of *C*-factor values of Agula watershed.

In the case of cultivated lands, the *C*-factor values vary annually; however, the dominant crop types in the watershed remain the same. Hence, a value of 0.15 suggested for cereals and pulses by Hurni (1985) was used for all cultivated lands. In addition, considering the establishment of exclosures in the study area since the mid 1990s and as given on the descriptions of LULC types, shrub lands of the 1990 were degraded especially by overgrazing, whereas shrub lands of the 2000 and 2012 were kept as exclosures and considered as non-degraded with improved grass cover within shrubs. Thus, as suggested by Haregeweyn et al. (2013), *C*-factor values of 0.05 and 0.03 were assigned for shrub lands (degraded) of the 1990 and shrub lands (non-degraded) of the 2000 and 2012 LULC maps, respectively. Assigning different *C*-factor values for shrub lands based on the years is appropriate given the historical and political perspectives of environmental degradation and land rehabilitation activities in the region as well as the improved vegetation condition after 1991 as confirmed by field observation and results of previous studies conducted in the same study region (e.g., Mekuria et al. 2009; Nyssen et al. 2008).

Conservation practices (P)-factor

The conservation practices (*P*)-factor represents the ratio of soil loss with a specific conservation practice to the corresponding loss with up-and-down-slope tillage. As such, it reflects the effects of conservation measures to reduce the erosion potential of runoff by their influence on drainage patterns, runoff concentration, runoff velocity and hydraulic forces exerted by the runoff on the soil surface (Renard et al. 1991). The *P*-factor can be derived from change of DEM through examining change of *LS*-factor due to management practices. This, however, requires high spatial resolution DEMs with a fine vertical accuracy acquired before and after implementation of the SWC measures or a field survey on SWC structures. To date, a global high quality DEM available is the 1 arc second (30 m spatial resolution) SRTM-DEM which was acquired in February 2000. The SRTM-DEM has ±16 m absolute and ±6 m relative vertical accuracy (Rabus et al. 2003). The low vertical accuracy of the DEM relative to stone bund height (0.3–1 m high) and lack of multi-temporal DEMs constrained derivation of the *P*-factor from change of DEM. In addition, mapping individual SWC structures through field survey for large areas is difficult if not impossible and as a result the *P*-factor is often considered as the most uncertain of the RUSLE factors (Panagos et al. 2015). An alternative approach is to estimate the *P*-factor either from image classifications using remote sensing data or from experiment-based recommendations of previous studies. Recently, Hurni et al. (2015) attempted to map SWC structures of the Ethiopian highlands using automated model and high spatial resolution images (<1 m); however, the resulting maps were not satisfactory as crop and vegetation cover significantly impaired detection of conservation structures. In Agula watershed, SWC measures were implemented on specific LULC types and hence the *P*-factor maps (Figure 3.3) were produced by reclassification of the LULC maps considering the SWC history, expert judgment

on the status of the SWC structures from field observation, and experiment-based recommendations from literature.

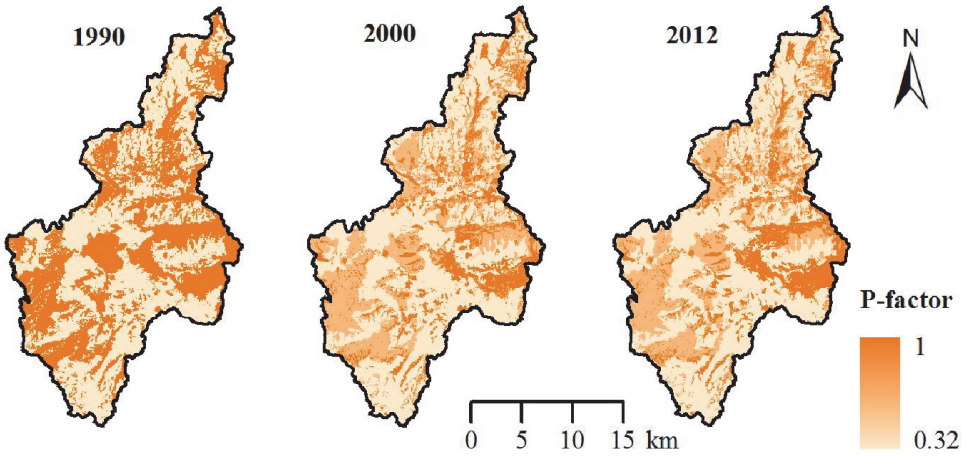

Figure 3.3 Spatial distribution map of *P*-factor values for Agula watershed.

Given that until 1990, there were only small-scale SWC measures such as construction of stone bunds on cultivated lands (Table 1, Getachew 2007), a *P*-factor value of 0.7 was assigned for cultivated lands of the1990 as suggested by previous studies (Haregeweyn el al. 2013; Nyssen et al. 2008). After 1991, large-scale SWC measures were implemented and stone bunds with improved quality were constructed on cultivated lands, shrub lands and bare lands (Table 1.1, Figure 1.5(a)–(c)). In the same study region, Gebremichael et al. (2005) reported that stone bunds of moderate quality installed on cultivated lands decrease erosion rates on average by 68%, corresponding to a *P*-factor value of 0.32. For stone bunds on non-crop lands, *P*-factor values vary from 0.4 to 0.8 depending on conditions and density of stone bunds (Nyssen et al. 2009a). Therefore, for the 2000 and 2012 LULC maps, *P*-factor value of 0.32 was assigned for cultivated lands (Gebremichael et al. 2005); whereas *P*-factor value of 0.6 was assigned for shrub and bare lands (Nyssen et al. 2009a). Based on Nyssen et al. (2007), the *P*-factor values may be

considered as medium-term values (up to 20 years) for stone bunds in the Ethiopian highlands. For other LULC types where no conservation measures were applied, a value of 1 was assigned.

3.2.3 Soil erosion model validation

Validation of the RUSLE model erosion estimations is important to ascertain the credibility of the model. However, lack of measured erosion data constrained the direct quantitative validation of the model estimations using the regular objective functions. Under such circumstances, the most common approaches of validating the results of model estimations are through comparison of erosion rates with reported measured values in the literature (Meshesha et al. 2012; Nyssen et al. 2008) or through qualitative erosion surveys by visual estimation of erosion status (Cohen et al. 2005; Jiang et al. 2012; Meshesha et al. 2012). For qualitative field erosion survey, the soil erosion status was defined based on the apparent soil erosion indicators such as the amount of vegetation, the presence of rills and small channels, whether the subsoil is exposed, thickness of topsoil and exposure of tree roots. During field survey, three erosion severity classes (slight, moderate, and severe erosion) were defined and their locations were recorded using global positioning system (GPS). Slight erosion represented areas with good vegetation cover and/or where the loss of topsoil was insignificant, whereas severe erosion referred to areas with very sparse grass cover, exposed subsoil, and visible rills/small channels. Moderate erosion class represented areas with erosion status between slight and severe classes. Similarly, the 2012 soil erosion map was reclassified into three classes of severity: slight (0–10 t $ha^{-1}yr^{-1}$), moderate (10–20 t $ha^{-1}yr^{-1}$), and severe (>20 t $ha^{-1}yr^{-1}$) erosion. Overlay analysis was performed between the field collected categorical data and the reclassified soil erosion severity map to generate a confusion matrix and compute overall accuracy. Such validation approach

follows similar procedure with image classification accuracy assessment described by Congalton (1991). The methodological framework used for this study is summarized in Figure 3.4.

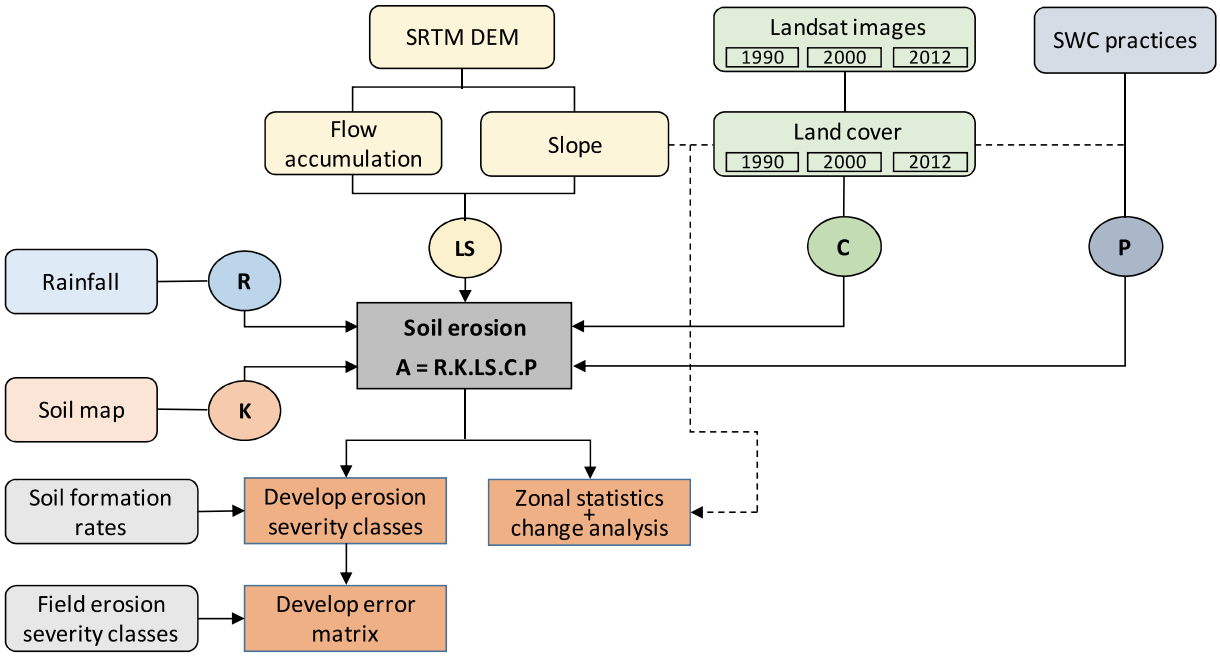

Figure 3.4 Methodological framework used to estimate the changes in soil erosion as a result of watershed management practices and changes in land use/land cover of Agula watershed.

3.3 Results and discussion

3.3.1 Temporal variability of soil erosion rates between 1990 and 2012

The annual soil loss rates for 1990, 2000, and 2012 were calculated based on the soil erosion maps (Figure 3.5). The mean specific soil loss rates were about 28, 12 and 10 t $ha^{-1}yr^{-1}$ for the years 1990, 2000 and 2012, respectively; while the corresponding absolute soil loss rates were 1220×10^3, 550×10^3 and 440×10^3 t yr^{-1}, respectively. Between 1990 and 2000, both the specific and absolute soil loss rates decreased considerably with annual rates of change of -1.5 t $ha^{-1}yr^{-1}$ and -67×10^3 t yr^{-1}, respectively; and for the whole study period (1990–2012), the respective

annual rates of change were -0.8 t $ha^{-1}yr^{-1}$ and -35×10^3 t yr^{-1}. The results also showed that between 1990 and 2000, the absolute soil loss rate by sheet and rill erosion decreased by about 55%; and an overall reduction by 64% was registered during 1990–2012. The overall reduction of soil loss from the watershed can be attributed to the combined effects of the extensive SWC measures implemented until 2000 (Table 1.1) and the associated changes in LULC that resulted in better surface cover conditions and improved vegetation cover through increased shrub land and forest cover (Figure 2.4). It is obvious that vegetation cover plays an important role for the protection of the soil surface from the beating action of raindrops (rain splash) and erosion by surface runoff. In addition, large scale implementation of stone bunds on cultivated lands and on hill-slopes played a considerable role to reduce the soil loss. The hill-slopes of the watershed were established as exclosures combined with or without enrichment plantations which also led to restoration of degraded lands and subsequent decrease in soil erosion. Analysis of the RUSLE reduction factors showed that the *C* and *P*-factors decreased respectively by about 19% and 34% in the period 1990–2000; and an overall decrease in the *C*-factor by about 29% in the period 1990–2012.

The results of this study are in agreement with reports of similar studies on the impact of SWC measures in Tigray region and elsewhere. For instance, in the Tigray highlands of northern Ethiopia, Haregeweyn et al. (2012) reported that integrated watershed management improves vegetation cover and reduce sheet and rill soil loss rates from all LULC classes by about 89% from 117 to 12.48 t $ha^{-1}yr^{-1}$ between 2004 and 2009. In another study, Nyssen et al. (2009a) demonstrated that integrated catchment management is an effective approach to combat land degradation thereby decreasing soil loss rate by 37% from 14·3 t $ha^{-1}yr^{-1}$ in 2000 to 9·0 t $ha^{-1}yr^{-1}$ in 2006. Similar study from this region based on a multi-scale assessment of environmental

rehabilitation for a time span of 30 years by Nyssen et al. (2008) showed that sheet and rill erosion rates have decreased by about 68% attributed to SWC practices and improved vegetation cover. Gebrernichael et al. (2005) also reported that stone bunds on crop lands reduce the annual soil loss by 68% (from 57 to 18 t $ha^{-1}yr^{-1}$). A study by Mekuria et al. (2009) on the effectiveness of exclosures to control soil erosion in northern Ethiopia reported that soil loss from exclosures decrease by 47% compared with soil loss from free grazing lands. In the central highlands of Ethiopia, Adimassu et al. (2014) investigated the effect of soil bunds on runoff and soil loss, and demonstrated that soil bunds reduce the average annual runoff and soil loss by 28% and 47%, respectively.

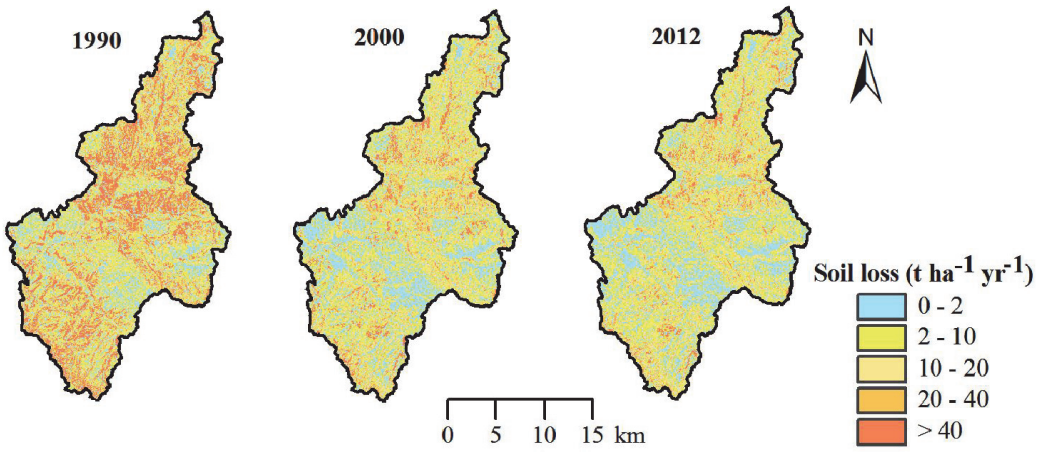

Figure 3.5 Soil loss maps of Agula watershed computed using RUSLE.

The result of erosion severity classes is presented in Table 3.2. Between 1990 and 2012, the areas of very slight and slight erosion categories each showed about 50% increment from 86 km^2 and 118 km^2 to 130 km^2 and 176 km^2, respectively. By contrast, the areas of severe and very severe erosion categories decreased from 72 km^2 and 88 km^2 in 1990 to 43 km^2 and 18 km^2 in 2012 which is a 40% and 80% reduction, respectively. However, the area of moderate erosion class showed only small changes. Based on Hurni (1983b) for Ethiopian condition, the minimum

and maximum tolerable soil loss rates are 2 and 18 t $ha^{-1}yr^{-1}$, respectively. Hence, it is worth noting that the very slight to moderate severity classes require less to medium priority, whereas the severe and very severe classes need high priority for soil conservation measures. In this regard, the results of this study also indicated that the SWC measures implemented in Agula watershed targeted primarily the areas experiencing the severe and very severe erosion and were effective in reducing the soil loss. However, it is important to note that for the recent year (2012), about 14% of the watershed experienced severe to very severe erosion with soil loss rate >20 t $ha^{-1}yr^{-1}$ which is higher than the maximum tolerable value. This implies that further planning and implementation of SWC measures on prioritized areas is required to reduce the soil erosion from the severe and very severe areas of the watershed.

Table 3.2 Erosion severity classes and area (km^2 and %) of each category.

Soil loss ($t\ ha^{-1}\ yr^{-1}$)	Erosion severity	1990		2000		2012	
		km^2	%	km^2	%	km^2	%
0–2	Very slight	86	19	124	28	130	29
2–10	Slight	118	27	169	38	176	40
10– 20	Moderate	78	18	76	17	75	17
20– 40	Severe	72	16	47	11	43	10
> 40	Very severe	88	20	26	6	18	4

3.3.2 Changes in soil erosion rates under different LULC types

Analysis based on zonal-statistics showed considerable reduction in soil loss (between 1990 and 2012) across the different LULC types (Table 3.3). Extreme soil erosion ($\geq$60 t $ha^{-1}yr^{-1}$) was observed in degraded bare lands of the watershed during 1990–2012; followed by cultivated land (about 24 t $ha^{-1}yr^{-1}$) in 1990 and grass land (about 18 t $ha^{-1}yr^{-1}$) in 2000 and 2012. The results showed that in 1990 about 80% of the total soil loss was generated from cultivated and degraded

bare lands combined. In 2000 and 2012 cultivated land had a lower specific soil loss rate (about 11 t $ha^{-1}yr^{-1}$) than grass land (about18 t $ha^{-1}yr^{-1}$) and bare land (>59 t $ha^{-1}yr^{-1}$); however, the total soil loss rate for cultivated land was much higher due to its larger coverage of the watershed (about 50%). Overall, between 1990 and 2012, significant reductions in absolute soil loss were observed for bare land (89%), cultivated land (56%) and shrub land (49%). The reduction in soil loss from different LULC types can be attributed to a combination of factors including decrease in *P*-factor as a result of construction of stone bunds (Figure 1.5(a)–(c)) and the decrease in *C*-factor, attributed to establishment of exclosures since the mid 1990s that resulted in improved vegetation cover (Figure 1.5(b)). Also, as a result of rehabilitation of degraded hill-slopes, considerable increase in shrub land cover was observed in the years 2000 and 2012 (Figure 2.4, Table 1.1); and this as well contributed for the reduction in soil loss. The order of magnitude of the estimated soil loss rates in this study are generally realistic compared with results from previous studies in the highlands of Ethiopia. For example, plot-scale study by Gebrernichael et al. (2005) in the Tigray highlands of northern Ethiopia, showed that soil loss rate from crop lands treated with stone bunds is about 18 t $ha^{-1}yr^{-1}$. In the same study region, Nyssen et al. (2009a) assessed the impact of SWC on catchment sediment budget and reported that soil loss from crop lands is about 9.9 t $ha^{-1}yr^{-1}$. Another study by Nyssen et al. (2009b), revealed that mean annual soil loss rate by sheet and rill erosion is about 3.5 t ha^{-1} in exclosures and forest and 17.4 t ha^{-1} in rangelands. Furthermore, some extreme soil loss rates (over 80 t $ha^{-1}yr^{-1}$) were reported in the north-western Ethiopian highlands where steep-lands are cultivated or overgrazed (e.g., Bewket and Teferi 2009; Herweg and Ludi 1999). At national level, Hurni (1993) estimated that soil loss by water erosion is the dominant driver of land degradation in the Ethiopian highlands, with annual soil erosion rates of 42 t ha^{-1} for croplands, and up to 300 t ha^{-1} in extreme cases.

Table 3.3 Changes in soil erosion rates under different land use/land cover types of Agula watershed. *CL* cultivated land, *GL* grass land, *SL* shrub land, *FR* forest, *BL* bare land, *ST* settlement.

LULC	Mean soil loss (t $ha^{-1}yr^{-1}$)			Total soil loss (10^3 t yr^{-1})			% of total soil loss		
type	1990	2000	2012	1990	2000	2012	1990	2000	2012
CL	23.7	10.8	10.7	558	245	248	46	45	56
GL	21.5	17.8	18.3	44	39	34	3	7	8
SL	16.1	7.5	6.6	149	82	75	12	15	17
FR	7.7	5.8	5.5	38	35	37	4	6	8
BL	98.3	69.4	59.4	435	146	49	35	27	11
ST	1.2	1.0	3	0	0	1	0	0	0

The change in soil erosion severity and LULC transition was also assessed by overlay operation of the soil erosion severity maps against the LULC maps in a GIS environment. The results of changes in soil erosion severity under different LULC for the reference years are shown in Figure 3.6. Most noticeable changes in the percentage of severe to very severe soil erosion categories were observed for cultivated land and shrub land. For instance, in 1990, about 40% of the cultivated land experienced severe to very severe erosion; while in 2012, the combined percentage reduced to about 20%. Similarly, for shrub land, in 1990 about 25% underwent severe to very severe erosion; however, in the year 2012, less than 10% of the shrub land had severe to very severe erosion. The changes in the distribution of erosion severity in the two LULC types can primarily be attributed to the implementation of SWC structures (stone bunds) and establishment of shrub lands as exclosures to rehabilitate the degraded areas of the watershed. Figure 8 also shows that more than 75% of bare land and about 35% of grass land experienced severe to very severe erosion during the entire study period. By contrast, forest cover was the least vulnerable LULC type with less than 10% of severe to very severe erosion categories; whereas settlement was only subject to very slight to slight erosion.

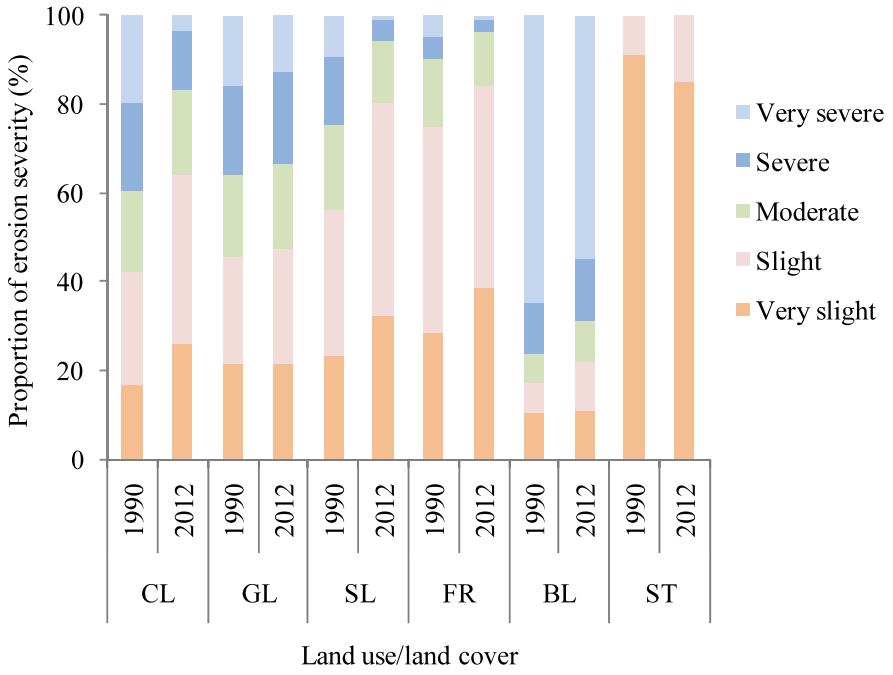

Figure 3.6 Changes in soil erosion severity under different land use/land cover types: *CL* cultivated land, *GL* grass land, *SL* shrub land, *FR* forest, *BL* bare land, *ST* settlement.

3.3.3 Changes in soil erosion rates under different slope ranges

Given slope is one of the major controlling factors that significantly influence rates of soil erosion, assessment of soil loss from different slope ranges was made. The slope categories of Agula watershed showed 5% flat (0–3% slope), 19% gentle (3–8% slope), 28% sloping (8–15% slope), 33% moderately steep (15–30% slope), 12% steep (30–50% slope) and 3% very steep (≥50% slope). In general, soil loss increases as the slope steepness increases in the watershed (Table 3.4). The steep and very steep slope classes together account for 15% of the total area; however, the contribution of this area to soil erosion was relatively high (more than 35% in 1990 and about 30% in 2000 and 2012). This demonstrates the significance of slope for soil erosion in Agula watershed, before and after implementation of extensive SWC measures. During the entire

study period, about 40% of the annual soil loss was from moderately steep slope category, followed by steep slope (more than 20%) and sloping land which contributed about 20% of the soil loss from Agula watershed (Table 5). The soil loss estimated from the flat lands was the lowest (1%) as compared to the other slope categories, and this shows that soil loss due to sheet and rill erosion can be counteracted by deposition within the flat landforms of the watershed. The result also showed that between 1990 and 2012, soil loss substantially decreased from all slope classes by about more than 60%; and the maximum reduction was observed from very steep slope (73%) followed by steep slope (70%) categories.

Table 3.4 Changes in soil erosion rates under different slope ranges.

Slope	Mean soil loss (t ha^{-1} yr^{-1})			Total soil loss (10^3 t yr^{-1})			% of total soil loss		
(%)	1990	2000	2012	1990	2000	2012	1990	2000	2012
0–3	8.8	4.4	3.7	16	8	7	1	1	1
3–8	10.9	5.4	4.6	95	47	40	8	9	9
8–15	17.2	8.6	7.1	213	107	88	17	19	20
15–30	30.5	15.8	12.3	475	231	180	38	42	40
30–50	62.4	22.6	18.7	331	120	99	27	22	22
> 50	83.3	25.3	22.5	117	35	32	9	6	7

3.3.4 Validation of erosion estimations

As discussed in the preceding sections (sections 3.3.1 and 3.3.2), the order of magnitude of soil erosion rates from different LULC types in this study were within the range of field measured soil erosion rates by several researchers (e.g., Gebrernichael et al. 2005; Herweg and Ludi 1999; Hurni 1993; Nyssen et al. 2009a,b). Furthermore, representative sample points collected from field survey for the three qualitative erosion severity classes (slight, moderate, and severe erosion) were also used for validation. As such, an error matrix (Table 3.5) was produced by superimposing or overlay analysis of the collected sample points on the reclassified

soil erosion map for validation. The summary statistics showed an overall accuracy of 69%; with highest accuracy of 72% for slight erosion category and lowest accuracy of 62% for moderate erosion category. The error matrix showed that there were high chances for areas with severe (7) and slight (6) erosion categories to be classified as moderate; which resulted in relatively low overall accuracy. Compared to the results of similar studies elsewhere that reported overall accuracies of 65% (Cohen et al. 2005) and 71% (Meshesha et al. 2012), the overall accuracy in the present study (69%) is fairly satisfactory. In general, the validation results indicated that the RUSLE model can reasonably indicate the soil loss distribution at the watershed scale. Even so, it is worth noting that model estimations are approximations of reality and therefore uncertainties with respect to the RUSLE factor maps are unavoidably present. Hence, equally important is to identify the constraints encountered in the soil erosion estimations for future improvements. The following section highlights the limitations of the input data used in the present study that should be taken into account in similar studies.

Table 3.5 Error matrix between actual erosion map and filed observation points.

	RUSLE severity class				
Field observation	Nil/slight	Moderate	Severe	Total	Accuracy (%)
Nil/slight	26	6	4	36	72
Moderate	5	13	3	21	62
Severe	3	7	23	33	70
			Overall accuracy		69

3.3.5 Limitations of erosion estimations

When applying erosion models such as RUSLE at regional or larger scale, a number of issues arise. First, the RUSLE model was initially developed at plot- or field-scale, and when it is applied over large areas the model output has to be interpreted carefully. Obviously, a model that

was designed to predict soil loss from agricultural plots may not produce accurate erosion estimates when applied at regional or large-scale watersheds on a grid of 30 m pixels or coarser. Second, uncertainties in the soil loss results obtained in this study could result from limitations in some of the input parameters used. The absence of storm energy and maximum 30 minute rainfall intensity data constrained a more accurate estimation of the *R* factor. Further, the assumption is that the 30 m spatial resolution DEM is good enough to represent the *LS*-factor; however, if the actual topography reflects slope breaks that are more or less frequent than the pixel size, any estimates of the *LS*-factor from the DEM can be expected to deviate accordingly. In addition, for large-scale watersheds it is usually difficult to measure the model's input data such as soil and cover management factors directly in the field; and as such the model input parameter values were assigned to mapping units on the soil and LULC maps based on suggestions on the literature. Nevertheless, this will yield parameter values that are less accurate than the results of field measurement. It is imperative to note that the RUSLE model layers can easily be updated when new data of higher spatial resolution become available which would enable improved assessment of changes in soil erosion. With all its limitations, the model results provide useful information on the general pattern of the relative differences in soil loss, rather than providing accurate absolute erosion rates. Furthermore, at regional and large-scale watersheds, usually no reliable data exist for validation of model estimates with actual soil losses, and hence the biggest challenge with erosion modeling is the difficulty of validating the estimates produced. In the present study, model validation was done by visual estimation of erosion status based on observed features; however, it is worth noting that such comparisons do not substitute for actual measurements.

3.4 Conclusions

In the past few decades, large-scale watershed management practices that include construction of stone bunds and check dams, and establishment of exclosures with or without enrichment plantations, have been extensively implemented in the semiarid highlands of northern Ethiopia, Agula watershed. This study evaluated the dynamics of soil erosion as a result of watershed management practices and associated changes in LULC over the period of 22 years (1990-2012) using RUSLE model in a GIS environment. The RUSLE application indicates that the average soil loss by sheet and rill erosion decreased by about 64% between 1990 and 2012. Soil loss reductions vary depending on LULC type and topography with considerable reductions (>50%) observed from bare and cultivated lands and from steep and very steep slope categories. Reductions in soil loss rates were due both to improved vegetation cover and to implementation of physical conservation structures that led to remarkable improvements in degraded land restoration. In the year 2012, about 14% of the watershed experienced soil loss rate in excess of 20 t ha^{-1} yr^{-1}, which signify the urgent need for further planning and implementation of SWC measures to reduce the soil erosion from areas experiencing severe and very severe erosion. Comparisons of erosion estimations with the results of previous studies in Ethiopia and based on ground-truthing using visual estimations of erosion status confirm that the RUSLE-based soil loss estimations are fairly satisfactory. This study demonstrates that the use of GIS-based RUSLE model and remote sensing data are effective approaches to assess changes in soil erosion brought about by watershed management practices and associated changes in LULC at watershed scale. The methods used in the present study can be applied in other regions to estimate soil loss and facilitate sustainable environmental management through appropriate conservation planning of areas experiencing severe land degradation due to water erosion.

Chapter 4

Quantitative analysis and implications of drainage morphometry of the Agula watershed in the semiarid northern Ethiopia

This chapter is published as:

Fenta AA, Yasuda H, Shimizu K, Haregeweyn N, Kifle W. (2017). Quantitative analysis and implications of drainage morphometry of the Agula watershed in the semiarid northern Ethiopia. Applied Water Science 7: 3825–3840.

Abstract

This study aimed at quantitative analysis of morphometric parameters of Agula watershed and its sub-watersheds using remote sensing data, geographic information system, and statistical methods. Morphometric parameters were evaluated from four perspectives: drainage network, watershed geometry, drainage texture, and relief characteristics. A 6th order river drains Agula watershed and the drainage network is mainly dendritic type. The mean bifurcation ratio (R_b) was 4.46 and at sub-watershed scale, high R_b values ($R_b > 5$) were observed which might be expected in regions of steeply sloping terrain. The longest flow path of Agula watershed is 48.5 km, with knickpoints along the main river which could be attributed to change of lithology and major faults which are common along the rift escarpments. The watershed has elongated shape suggesting low peak flows for longer duration and hence easier flood management. The drainage texture analysis revealed fine drainage which implies the dominance of impermeable soft rock with low resistance against erosion. High relief and steep slopes dominate, by which rough landforms (hills, breaks, and low mountains) make up 76% of the watershed. The S-shaped hypsometric curve with hypsometric integral of 0.4 suggests that Agula watershed is in equilibrium or mature stage of geomorphic evolution. At sub-watershed scale, the derived morphometric parameters were grouped into three clusters (low, moderate, and high) and considerable spatial variability was observed. The results of this study provide information on drainage morphometry that can help better understand the watershed characteristics and serve as a basis for improved planning, management, and decision making to ensure sustainable use of watershed resources.

Keywords: Morphometric analysis; Watershed characteristics; Remote sensing; Geographic information system; Semiarid; Ethiopia

4.1 Introduction

Morphometric analysis is an important aspect of characterization of watersheds. It involves computation of quantitative attributes of the landscape related to linear, aerial and relief aspects from elevation surface and drainage networks within a watershed. Over the past several decades, morphometric analysis to evaluate watersheds and to describe the characteristics of surface drainage networks with reference to land and water management has been a major emphasis in geomorphology. Pioneer studies by Horton (1932, 1945) demonstrated the significance of quantitative morphometric analysis to better understand the hydrologic and geomorphic properties of watersheds. Since then, several methods of watershed morphometry were further developed (e.g., Miller 1953; Strahler 1954, 1957, 1964; Schumm 1956; Melton 1957; Faniran 1968) that enabled morphometric characterization at watershed scale to extract pertinent information on the formation and development of land surface processes.

Morphometric analysis represents a relatively simple approach to describe the hydro-geological behavior, landform processes, soil physical properties and erosion characteristics; and hence provides a holistic insight into the hydrologic behavior of watersheds (Strahler 1964). The hydrological response of watersheds is interrelated with their physiographic characteristics, such as size, shape, slope, drainage density, and length of the streams (Gregory and Walling 1973). Recent studies demonstrated that quantitative morphometric analysis has several practical applications that include: land surface form characterization (Reddy et al. 2004; Thomas et al. 2012; Magesh et al. 2013; Kaliraj et al. 2014; Banerjee et al. 2015), watershed prioritization for soil and water conservation (Gajbhiye et al. 2014; Meshram and Sharma 2015), environmental assessment (Magesh et al. 2011; Al-Rowaily et al. 2012; Rai et al. 2014; Babu et al. 2016), and

evaluation and management of watershed resources (Pandey et al. 2004). Furthermore, comparison of the quantitative morphometric parameters helps understand the geomorphological effects on the spatial variation of hydrological functions (Romshoo et al. 2012; Sreedevi et al. 2013). Understanding drainage morphometry is also a prerequisite for runoff modeling, geotechnical investigation, identification of water recharge sites and groundwater prospect mapping (Sreedevi et al. 2005; Fenta et al. 2015; Roy and Sahu 2016). As such, morphometric analysis is an important procedure for quantitative description of the drainage system; thus enabling improved understanding and better characterization of watersheds.

Earlier studies successfully applied conventional methods of morphometric characterization based on map measurements or field surveys (e.g., Horton 1932, 1945; Strahler 1952, 1954, 1957, 1964); however, it has been recognized that such methods of generating information especially for large watersheds are expensive, time consuming, labor intensive and tedious. Recently, increasing availability of remote sensing datasets with improved spatial accuracy, advances in computational power and GIS, enable evaluation of morphometric parameters with ease and better accuracy (Grohmann 2004). On the one hand, remote sensing enables acquisition of synoptic data of large inaccessible areas and is very useful in analyzing drainage morphometry. On the other hand, GIS provides a powerful tool and a flexible environment and as such the information extraction techniques are less time consuming than ground surveys for morphometric characterization through manipulation and analysis of spatial data. Integrating remote sensing data and GIS tools, therefore, allow automated computation of morphometric parameters and have been successfully employed by several researchers (e.g., Magesh et al. 2011; Thomas et al. 2012; Kaliraj et al. 2014; Banerjee et al. 2015; Roy and Sahu 2016) for generating updated and reliable information to characterize watershed physiographic attributes.

Significant advances in remote sensing technology have led to availability of higher quality DEMs. For instance, availability of SRTM and Advanced Space-borne Thermal Emission and Reflection Radiometer (ASTER) DEMs free of charge via http://earthexplorer.usgs.gov/ has provided new potentials in watershed scale quantitative morphometric analysis. In the past decade, several studies used SRTM (90 m resolution) and/or ASTER (30 m resolution) DEMs in a GIS environment to derive morphometric characteristics of watersheds with different geological and hydrological settings (e.g., Romshoo et al. 2012; Thomas et al. 2012; Gajbhiye et al. 2014). These studies demonstrated that SRTM and ASTER-DEMs provide reliable datasets with global coverage that enabled evaluation of morphometric properties and various relief features. A recent comparative study by Thomas et al. (2014) showed that topographic attributes extracted from the space-borne (SRTM and ASTER) DEMs are in agreement with those derived from topographic maps. Their study also revealed that despite the coarser resolution (i.e., 90 m), SRTM-DEM shows relatively higher vertical accuracy and better spatial relationship of topographic attributes than the finer resolution (i.e., 30 m) ASTER-DEM when compared with topographic maps.

Turcotte et al. (2001) demonstrated that morphometric analysis solely based on automated DEM-based approaches, have limitations in representing the actual drainage structure of a watershed; and ways to recondition DEMs for improved performance have been suggested (e.g., Hellweger 1996; Soille et al. 2003). Studies by Turcotte et al. (2001) and Callow et al. (2007) showed that DEM reconditioning using stream networks digitized from topographic maps greatly improves replication of stream positions and reduces error introduction in the form of spurious parallel streams. Therefore, in the present study, a more rational approach of morphometric analysis has been employed by using SRTM-DEM with relatively fine spatial resolution (i.e., 30

m) and natural stream networks digitized from topographic maps (scale 1:50000). The natural stream networks were used to recondition the DEM prior to the computation of flow direction and flow accumulation grids. The objective of this study was to derive morphometric parameters related to drainage network, watershed geometry, drainage texture, and relief characteristics of Agula watershed and infer their implications by integrating remote sensing data, GIS tools and statistical methods. In general, watershed management practices and water resources development schemes are often implemented without proper assessment of the watershed characteristics. Such a study, therefore, provides pertinent information for an enhanced perceptive of the hydro-geologic and erosion characteristics of watersheds. Given the wide range of applications of derived morphometric parameters, this study presents selected parameters for a better understanding of watershed characteristics and can serve as a basis for improved planning, management and decision making to ensure sustainable use of watershed resources.

4.2 Materials and methods

4.2.1 Data sources

Topographic maps (scale 1:50000) for year 1997 were obtained from the National Mapping Agency (NMA) of Ethiopia. The study area was covered by four topographic maps with index: 1339-B1, 1339-B2, 1339-B3 and 1339-B4. The scanned topographic maps were geometrically rectified and geo-referenced to the UTM map projection (Zone 37N), Adindan datum and Spheroid - Clarke 1880 by taking the printed corner coordinates. The rectified topographic maps were then mosaicked to form a single topographic map from which stream networks were digitized and used to recondition the SRTM-DEM. SRTM generated the most complete digital topographic database for the Earth using two antenna pairs operating in C- and X-bands to

acquire interferometric radar data (Rabus et al. 2003). SRTM data with global coverage is readily available at 30 arc-seconds (~1 km), 3 arc-seconds (~90 m) and 1 arc second (~30 m) resolutions via http://earthexplorer.usgs.gov/. In the present study, the 1 arc second data of tile N13E39 was downloaded and re-projected to a similar projection and datum with that of the topographic maps for further use. Several studies (e.g., Rabus et al. 2003; Slater et al. 2006; Farr et al. 2007; Yang et al. 2011) provide more elaborated details of SRTM datasets including issues such as data processing, accuracy, errors, and applications.

4.2.2 Methodology

Watershed boundary delineation

ArcHydro tools extension of the ArcGIS software was used for watershed delineation which is automated and more consistent compared with a manual approach. The procedure used for watershed delineation in ArcHydro involved sequence of steps accessed through the toolbar menus. The first of these was the reconditioning of the SRTM-DEM data to reconcile with the digitized stream network from topographic maps using the AGREE method. AGREE is a surface reconditioning system for DEMs and enables to adjust the surface elevation of the DEM to be consistent with digitized stream networks. This helps increase the degree of agreement between stream networks delineated from the DEM and the input vector stream networks (Hellweger 1996). The next step was to fill the sinks (artifact features from DEM) and remove local depressions to assure flow continuity for proper determination of flow direction and flow accumulation grids. The D8 algorithm (O'Callaghan and Mark 1984) was used to determine flow direction of a grid cell based on elevations in a 3×3 window around it. The direction of each grid cell was determined by one of its eight surrounding grid cells with steepest descent. Based on

cumulative number of the upstream cells draining to each cell in the flow accumulation grid, stream networks for each of the watersheds were generated. In the present study, the rivers and streams digitized from topographic maps (scale 1:50000) were well represented/captured when stream definition threshold was set at 25 pixels of the flow accumulation layer. It should be noted, however, that the threshold area is an average indicator and different physiographic regions may have different thresholds for defining rivers and streams. Then, boundaries of Agula watershed and its sub-watersheds (Figure 4.1) were delineated using point delineation functionality of the ArcHydro tools.

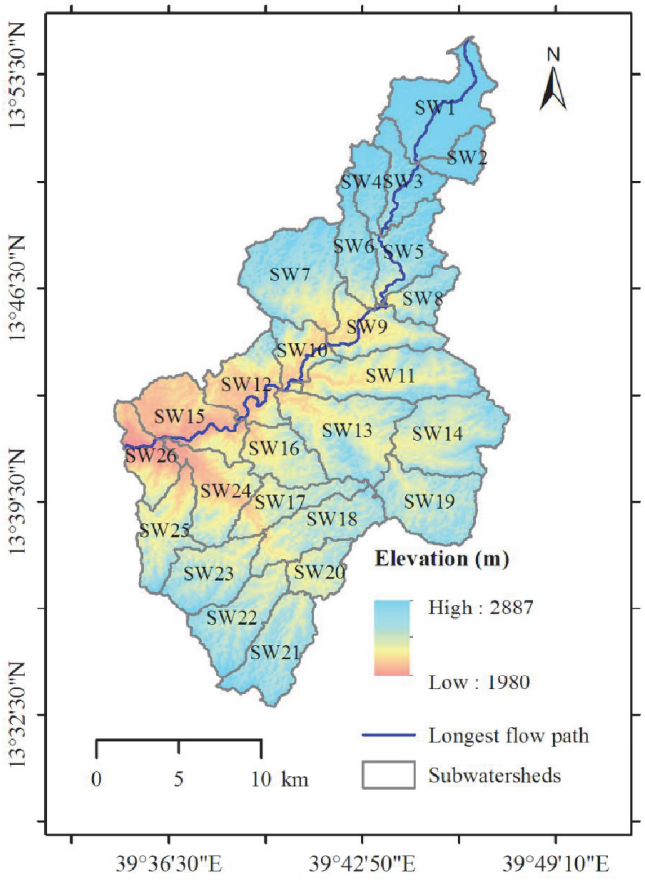

Figure 4.1 Sub-watersheds of Agula watershed and the longest flow path. The background provides elevation information extracted from the 30-m-resolution SRTM-DEM.

Morphometric analysis

A number of morphometric parameters which signify the watershed characteristics were computed in a GIS environment. In this study, Agula watershed was discretized into twenty-six sub-watersheds which include streams of at least three different orders following the work of Biswas et al. (2014). Areas of the sub-watersheds along with their perimeter, elevation information, basin length, and number and length of stream networks were extracted for further analysis. In addition, the longest flow path (from outlet point to the water divide line) and its longitudinal profile were also derived from SRTM-DEM with the ArcHydro tools and 3D-analyst extension. A smoothing process (smooth 3D line) was carried out to remove kinks from the longitudinal profile. The derived morphometric parameters were evaluated from four different aspects: drainage network, watershed geometry, drainage texture, and relief characteristics (Table 1). Overall, twenty-seven morphometric parameters were computed for Agula watershed and for each of the sub-watersheds. The computations of morphometric parameters were based on mathematical equations (Table 4.1), and the values of some of the watershed characteristics required for computing morphometric parameters are shown in Table 4.2. Furthermore, landforms of Agula watershed were topographically modeled from combinations of slope class and local relief produced from SRTM-DEM following the procedures suggested by Sayre et al. (2009). This approach of generating landforms from DEM is on the basis of applying a moving neighborhood analysis window and a land surface classification method modified from Hammond (1964). In this study, slope was generated using 3D analyst tools and classified as gently sloping or not gently sloping by using a slope threshold of 8%. Local relief was calculated using neighborhood analysis of the spatial analyst tools in a 3×3 moving window. Local relief was then divided into five classes with ranges: 0–≤15 m, >15–

≤30 m, >30–≤90 m, >90–≤150 m, and >150 m. Slope classes and relief classes were subsequently combined to produce eight land surface form classes (flat plains, smooth plains, irregular plains, escarpments, low hills, hills, breaks/foothills, and low mountains).

Table 4.1 Methods employed and corresponding computed values for morphometric parameters of Agula watershed.

S.No.	Morphometric parameters	Methods	References	Value
		Drainage network		
1	Stream order (U)	Hierarchical rank	Strahler (1964)	6
2	Stream number (N_u)	$N_u = N_1+N_2+...+N_n$	Horton (1945)	2235
3	Stream length (L_u) (km)	$Lu = L_1+L_2+...+L_n$	Horton (1945)	1150
4	Mean stream length (L_m) (km)	$L_m = L_u/N_u$	Strahler (1964)	0.51
5	Stream length ratio (R_L)	$R_L = L_{mu}/L_{mu-1}$	Horton (1945)	2.39
6	Bifurcation ratio (R_b)	$R_b = N_u/N_{u+1}$	Horton (1945)	4.46
7	Rho coefficient (ρ)	$\rho = R_L/R_b$	Horton (1945)	0.65
		Watershed geometry		
8	Basin length (L_b) (km)	–	Horton (1932)	41.76
9	Basin area (A) (km^2)	–	–	442
10	Basin perimeter (P) (km)	–	–	190.36
11	Form factor (F_f)	$F_f = A/L_b^2$	Horton (1932)	0.25
12	Elongation ratio (R_e)	$R_e = (2/L_b)\times(A/\pi)^{0.5}$	Schumm (1956)	0.57
13	Circularity ratio (R_c)	$R_c = 4\pi A/P^2$	Miller (1953)	0.15
14	Compactness coefficient (C_c)	$C_c = P/2(\pi A)^{0.5}$	Gravelius (1941)	2.55
		Drainage texture analysis		
15	Stream frequency (F_s)	$F_s = N_u/A$	Horton (1945)	5.05
16	Drainage texture (D_t)	$Dt = N_u/P$	Horton (1945)	11.74
17	Drainage density (D_d)	$D_d = L_u/A$	Horton (1932)	2.60
18	Drainage intensity (D_i)	$D_i = F_s/D_d$	Faniran (1968)	1.94
19	Infiltration number (I_f)	$I_f = F_s\times D_d$	Faniran (1968)	13.15
20	Length of overland flow (L_o)	$L_o = 1/(2D_d)$	Horton (1945)	0.19
21	Constant of channel maintenance (C)	$C = 1/D_d$	Schumm (1956)	0.38
		Relief characteristics		
22	Height of basin outlet (Z_{min}) (m)	–	–	1980
23	Maximum height of basin (Z_{max}) (m)	–	–	2887
24	Total basin relief (H) (m)	$H = Z_{max} - Z_{min}$	Strahler (1952)	907
25	Relief ratio (R_h)	$R_h = H/L_b$	Schumm (1956)	0.02
26	Relative relief (R_{hp})	$Rhp = H\times100/P$	Melton (1957)	0.48
27	Ruggedness number (R_n)	$R_n = H\times D_d$	Strahler (1954)	2.36
28	Dissection index (D_{is})	$D_{is} = H/Z_{max}$	Gravelius (1941)	0.31

Hypsometric analysis was also carried out to develop relationship between horizontal cross-sectional drainage area and elevation. This involved generating Hypsometric Curve (HC) which provides quantitative means for characterizing the topographic structure of a watershed. To generate the HC, the watershed is assumed to have vertical sides rising from a horizontal plane passing through the watershed outlet and under the entire watershed. According to Strahler (1952), the HC is a plot of the continuous function relating relative elevation to relative area. The relative elevation (h/H) is calculated as the ratio of height of a given contour above the base plane (h) to the maximum basin elevation from the outlet (H); whereas the relative area (a/A) is calculated as a ratio of the area above a particular contour (a) to the total area of the watershed (A). Thus, the HC describes the relative proportion of the watershed area that lies above a given height relative to the total relief of the watershed. In this study, following the procedures suggested by Davis (2010), the HC was produced from the SRTM-DEM by creating a binned histogram (100 classes of equal interval) with the reclassify tool; then area and elevation values were normalized by total area and total relief of the watershed. Strahler (1952) noted that differences in the shape of the HC for a particular landform provide a measure of the erosion state or geomorphic age of a watershed. Hence, hypsometric analysis has been widely used in past and recent researches dealing with erosional topography (e.g., Willgoose and Hancock 1998; Bishop et al. 2002; Singh et al. 2008; Thomas et al. 2012).

According to Harlin (1978), the HC can be considered as a cumulative probability distribution function of elevations; and in this approach, the HC is represented by a continuous polynomial function with the form:

$$f(x) = a_0 + a_1 x + a_2 x^2 + \ldots + a_n x^n \qquad (4.1)$$

where, $f(x)$ is a polynomial function fitted to the HC by regression and a_0, a_1, a_2, … a_n are the coefficients. For the entire watershed, the area under the HC also called the Hypsometric Integral (HI), which represents the relative fraction of landmass that remains above the base plane, was calculated by the integration of $f(x)$ between the limits of the unit square. Following Harlin (1978), the result of this integration can be solved as:

$$\mathrm{HI} = \iint_R \mathrm{d}x\mathrm{d}y = \int_0^1 f(x)\mathrm{d}x = \sum_{k=0}^{5} \frac{a_k}{k+1} \tag{4.2}$$

In addition to the exact integration approach, there are several approximation methods available for computing HI; one of which is the elevation-relief ratio method suggested by Pike and Wilson (1971) is less cumbersome and faster method used to calculate HI for the sub-watersheds of Agula. The statistical moments for the distribution of the HC and its density function (first derivative of the curve) were derived to characterize the planimetric and topographic structure of the watershed. Harlin (1978) defined the statistical moments as: skewness of the HC (hypsometric skewness, SK), kurtosis of the HC (hypsometric kurtosis, KUR), skewness of the hypsometric density function (density skewness, DSK) and kurtosis of the hypsometric density function (density kurtosis, DKUR). The first moment of $f(x)$ about the x-axis (μ_1) for the unit square which represents the x-mean can be defined as:

$$\mu_1 = \frac{1}{\mathrm{HI}} \int_0^1 xf(x)\mathrm{d}x = \frac{1}{\mathrm{HI}} \sum_{k=0}^{5} \frac{a_k}{k+2} \tag{4.3}$$

In the same way, the i^{th} moment of $f(x)$ about the x-mean can be expressed as:

$$\mu_i = \frac{1}{\mathrm{HI}} \int_0^1 (x - \mu'_1)^i f(x)\mathrm{d}x \tag{4.4}$$

The second moment (μ_2) of $f(x)$ about the x-mean is known as the variance, and can be solved as a summation expression by following a similar development as in Eqs. (2) and (3). The third (μ_3) and fourth (μ_4) moments about the x-mean are termed as the SK and KUR of the distribution function, respectively. Based on Harlin (1978), the SK and KUR are dimensionless coefficients defined as:

$$\text{SK} = \frac{\mu_3}{\sqrt{\mu_2}^3} \text{ and } \text{KUR} = \frac{\mu_4}{\sqrt{\mu_2}^4} \tag{4.5}$$

By following the same reasoning as for $f(x)$, the moments and coefficients of density function (first derivative of the curve) were derived to obtain the DSK and DKUR. When applied to the probability distribution function of the HC, the statistical moments can be interpreted in terms of erosion and watershed slope. As such, based on Harlin (1978), the SK indicates the amount of headward erosion in the upper reach of a watershed; DSK represents slope change; a large value of KUR indicates erosion on both upper and lower reaches of a watershed, and DKUR represents midbasin slope. These statistical moments can be used to describe and characterize the shape of the hypsometric curve and, hence, to quantify changes in the morphology of the watershed.

Table 4.2 Stream order-wise distribution of number of streams, stream length, mean stream length, stream length ratio and bifurcation ratio of Agula watershed.

Stream order (U)	Number of streams (N_u)	Stream length (L_u)	Mean stream length (L_m)	Stream length ratio (R_L)	Bifurcation ratio (R_b)
1	1662	545	0.33	-	3.75
2	443	299	0.67	2.06	4.34
3	102	155	1.52	2.25	4.43
4	23	78	3.39	2.23	5.75
5	4	53	13.25	3.91	4.00
6	1	20	20.00	1.51	-

Cluster analysis of morphometric parameters

Given the large number of sub-watersheds and morphometric parameters, hierarchical clustering was used to group the sub-watersheds into three major categories (that represent low, moderate, and high values) according to the four morphometric aspects. In this method, the sub-watersheds are grouped into successively larger clusters based on distance or similarities between data points. As such, hierarchical clustering produces dendrograms by which the sub-watersheds are grouped and presented as a tree-like hierarchical diagram. Euclidean distance was used for measuring similarity between pairs of sub-watersheds, and Ward method was chosen as a clustering technique, which is based on mutually exclusive subsets of the data set and is most appropriate for quantitative variables (Ward 1963). Furthermore, to understand how the different morphometric parameters interact and influence each other, a correlation matrix was produced. Some of the morphometric parameters were excluded as they depend totally on some other parameters which are already included (e.g., constant of channel maintenance is the inverse of drainage density and was therefore excluded).

4.3 Results and discussion

Quantitative description of drainage network, watershed geometry, drainage texture, and relief characteristics has been carried out for Agula watershed and its sub-watersheds using the methods described in Table 4.1. In the following sections, the various morphometric parameters and their implications are discussed for the entire watershed and the sub-watersheds based on the derived cluster groups (Figure 4.2).

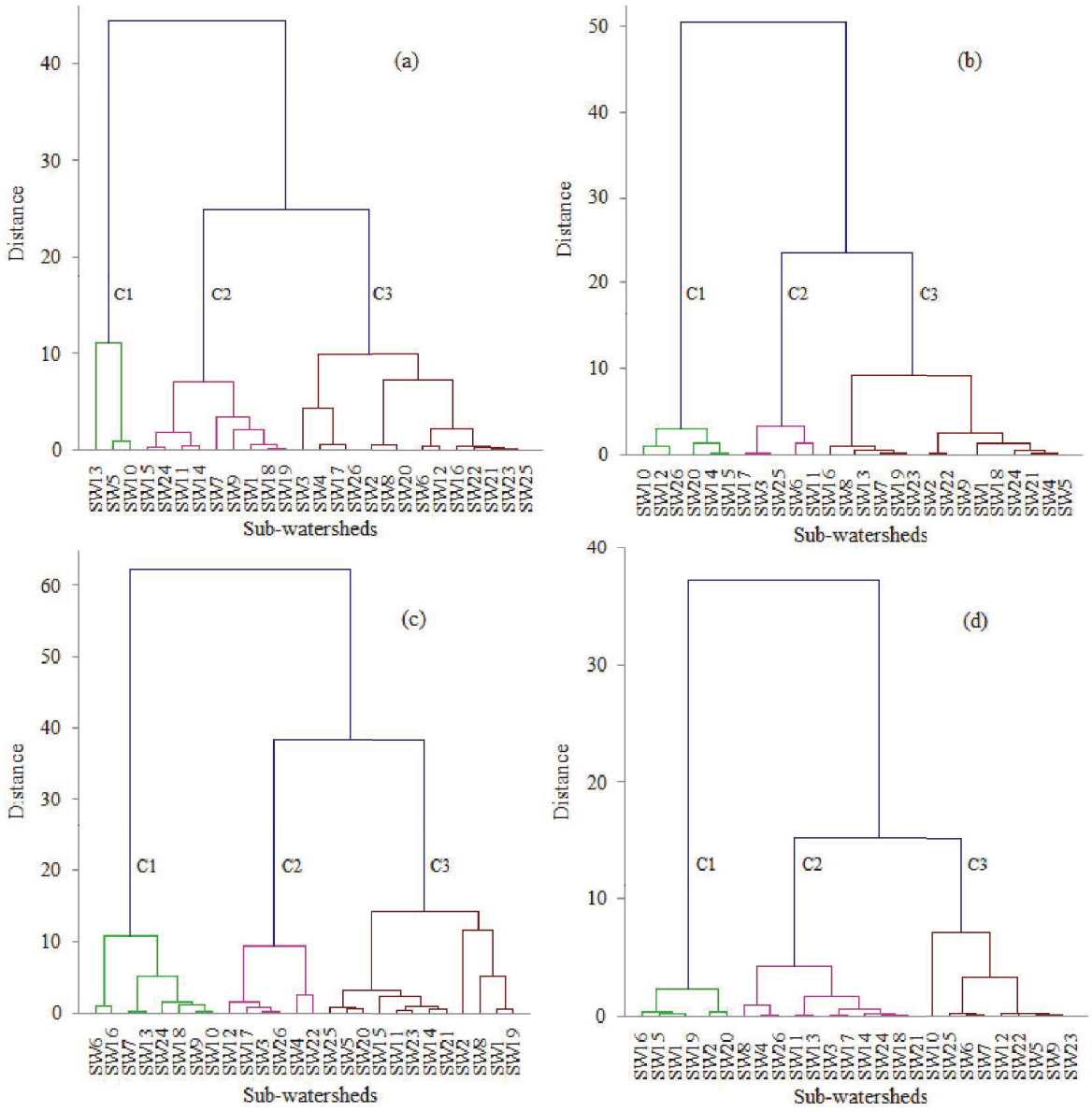

Figure 4.2 Dendrograms showing groups having similar properties related to: (a) drainage network, (b) watershed geometry, (c) drainage texture analysis, and (d) relief characteristics.

4.3.1 Drainage network

The network of drainage channels and tributaries forms a particular drainage pattern as determined by local topography and subsurface geology (lithology and structures). Drainage

channels develop where surface runoff is enhanced and Earth materials provide the least resistance to erosion. Hence, the drainage pattern of a watershed helps understand the topographic and structural/lithologic controls on the water flow. As shown in Figure 4.3, the drainage pattern of Agula watershed can be described as dominantly dendritic; however, in some sub-watersheds trellis and parallel patterns also co-exist. Dendritic drainage patterns form where the underlying rock structure does not strongly control the position of stream channels. Hence, dendritic patterns tend to develop in areas where the river channel follows the slope of the terrain and the subsurface geology has a roughly equal resistance to weathering (Ritter 1995; Twidale 2004). Further, the preferred direction of alignment of streams reflected fracture/lineament control on drainage network. Stream ordering of a drainage network represents a measure of the extent of stream branching within a watershed. As such, designation of stream order is the first step in morphometric characterization of watersheds; and in the present study, the stream ordering was done based on hierarchical ranking method proposed by Strahler (1964). The first order stream has no tributaries; the second order has only first order as tributaries, similarly third order streams has first and second order streams as its tributaries and so on. The order wise stream numbers and stream length of Agula watershed is given in Table 4.2. A 6^{th} order river drains Agula watershed with four 5^{th} order stream tributaries; namely Adi Felesti in the northeast, Adi Siano in the northwest, Era in the east and Mezerbei in the southeast.

The 1^{st} order streams accounted for about 74% of the total number of streams; and based on Macka (2003), such a high proportion of 1^{st} order streams indicates the structural weakness present in the watershed dominantly in the form of fractures/lineaments. The total length of stream segments (L_u) was 1150 km (Table 4.2) of which the 1^{st} and 2^{nd} order streams constituted about 74%. Mean stream length (L_m) is a dimensional property revealing the characteristic size

of components of a drainage network and its contributing areas. The L_m of a given order was higher than that of the next lower order, but lower than the next higher order, indicating that the evolution of the watershed followed the laws of erosion acting on homogeneous geologic material with uniform weathering-erosion characteristics. Stream length ratio (R_L) considered as an important factor in relation to both drainage composition and geomorphic development of watersheds was also computed. Variation existed in R_L values between the streams of different order (Table 4.2); which according to Horton (1945) might be attributed to morphological changes in slope and relief. The bifurcation ratio (R_b) values ranged between 3.75 and 5.75 for the Agula watershed (Table 4.2); with mean R_b value of 4.46. The R_b was designated as an index of relief and dissection by Horton (1945); with higher values indicating mountainous or highly dissected watersheds.

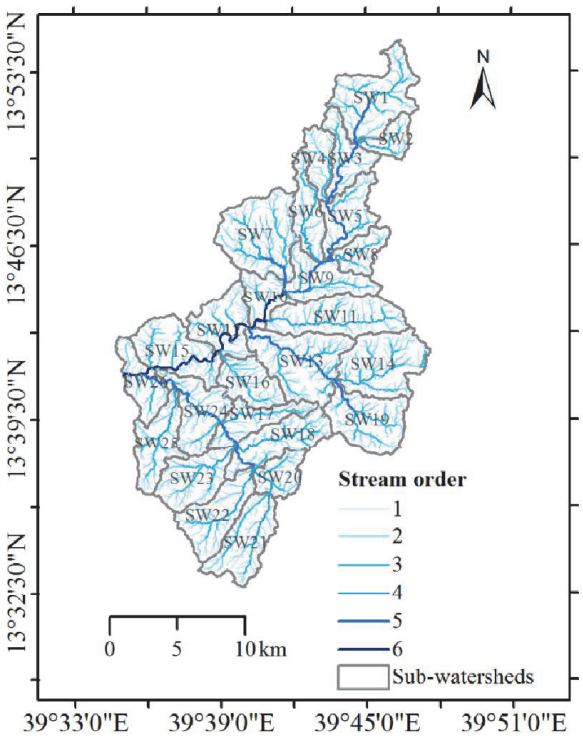

Figure 4.3 Stream orders of Agula watershed (ranked according to Strahler 1964).

Table 4.3 Results of morphometric parameters derived based on hierarchical cluster analysis method for the 26 sub-watersheds; the values represent the mean of each morphometric parameter within each cluster. The full names of parameters are given in Table 4.1.

Drainage network						
Cluster ID	N_u	L_u	R_L	R_b	ρ	
C1	98.33	49.76	1.97	3.33	0.60	
C2	119.89	59.50	0.67	4.01	0.18	
C3	62.64	34.91	0.63	4.12	0.16	
Watershed geometry						
Cluster ID	F_f	R_e	R_c	C_c		
C1	0.48	0.78	0.29	1.88		
C2	0.18	0.48	0.21	2.24		
C3	0.28	0.60	0.27	1.95		
Drainage texture analysis						
Cluster ID	F_s	D_d	D_i	I_f	L_o	C
C1	5.32	2.82	1.89	14.96	0.18	0.36
C2	4.24	2.61	1.62	11.09	0.19	0.38
C3	5.19	2.53	2.06	13.12	0.20	0.40
Relief characteristics						
Cluster ID	R_h	R_{hp}	R_n	D_{is}	HI	
C1	0.04	1.01	0.65	0.10	0.53	
C2	0.05	1.39	1.04	0.15	0.45	
C3	0.07	1.74	1.33	0.19	0.34	

In this study, the obscure trends in R_b values between various stream orders confirmed the substantial influence of geology and relief on drainage branching. Relatively high R_b values in sub-watersheds belonging to cluster C3 (Figure 4.2(a), Table 4.3) suggested the significant influence of structural elements on the drainage network and presence of highly dissected sub-watersheds. By contrast, low R_b values of sub-watersheds under cluster C1 are the characteristics of structurally less disturbed watersheds with minimal distortion in drainage pattern. Based on Horton (1945), natural drainage systems are generally characterized by R_b values between 3.0 and 5.0; however, anomalous R_b values (e.g., $R_b < 3.0$ and $R_b > 5.0$) were reported in several

studies (e.g., Gajbhiye et al. 2014; Roy and Sahu 2016). These anomalous values were considered as indirect manifestations of substantial structural controls. In some sub-watersheds, abnormally high bifurcation ratios ($R_b > 5.0$) were observed which might be expected in regions of steeply sloping terrain where narrow strike valleys are confined between ridges. The rho coefficient (ρ) signifies the storage capacity of a watershed and determines the relationship between drainage density and physiographic development of the watershed. Sub-watersheds belonging to C1 (Figure 4.2(a), Table 4.3) having high value of ρ are subject to a greater risk of being eroded by excess discharge during flood.

The longest flow path of Agula watershed is about 48.5 km and its longitudinal profile is shown in Figure 4.4. The resultant longitudinal profile was continuous, with values at intervals of 30 m (or 42.42 m where the streamline moves diagonally) along the entire stream. The longitudinal profile (Figure 4.4) showed that in the upper reach of the river, the gradient was steep (0.018 m m^{-1} for L_1), but gradually flattened out as the river eroded towards its outlet (0.008 m m^{-1} for L_4). This indicated that in the upper course, the river has high gravitational energy and so is the energy to erode vertically; whereas, in the lower course, the river has less erosive power and hence deposits its load. It is worth noting that knickpoints (Figure 4.4 at A, B, and C) with steep reaches developed along the main river at some 44, 37, and 28 km, respectively from the watershed outlet. Such abrupt changes in slope of the longitudinal profile could be attributed to change of lithology along the main river (e.g., from Meta-volcanic to Meta-sediments) resulting in differential erosion as well as the presence of major faults which are common along the rift escarpments. If a river flows over two or more rock types, there is often a slope break at the contact, especially where the adjoining rocks have varying resistance to erosion. According to Hack (1973), when the rock type of a river bed changes from a resistant

rock to a less resistant one, the river erodes the less resistant rock faster producing a sudden change in the gradient of the river with the resistant rock being higher up than the less resistant rock; this creates a higher hydraulic head. Hence, as the river flows over the resistant rock, it falls onto the less resistant rock, eroding it and creating a greater height difference between the two rock types, producing the knickpoints. Also, Bishop et al. (2005) suggested that knickpoints can be the result of disequilibrium steepening in response to a relative fall in base level, where the base level of the river falls giving it some extra gravitational energy to erode vertically. Computation of the longest flow path and its longitudinal profile is also an important step in hydrologic modeling as it helps estimate the time of concentration in empirical models.

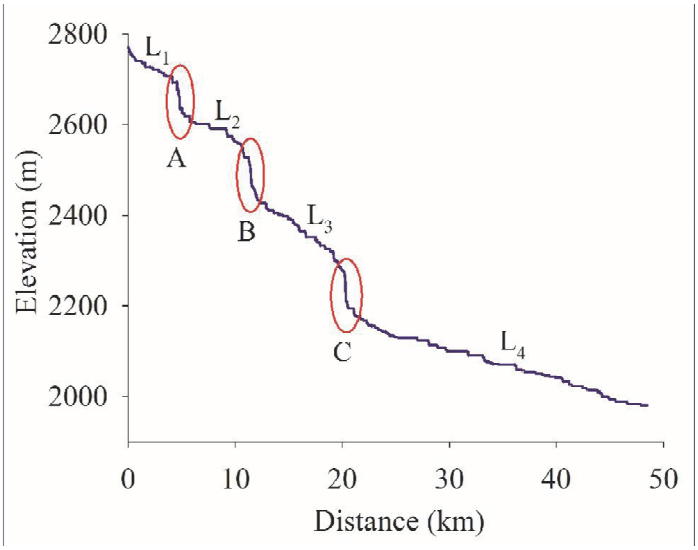

Figure 4.4 Longitudinal profile of Agula river extracted from SRTM-DEM: L_1, L_2, L_3, and L_4 are river segments with decreasing gradient and A, B, and C are knick-points along the river.

4.3.2 Watershed geometry

The shape of a watershed is controlled by geological structure, lithology, relief and climate; and varies from narrow elongated forms to circular or semicircular forms. The shape mainly

governs the rate at which water is supplied to the main channel. In the present study, four parameters namely: form factor (F_f), elongation ratio (R_e), circularity ratio (R_c), and compactness coefficient (C_c) were used for characterizing watershed shape, which is an important parameter from hydrological perspective. For Agula watershed, the F_f, R_e, R_c, and C_c values were 0.25, 0.57, 0.15 and 2.55, respectively (Table 4.1). Based on Schumm (1956), R_e values can be grouped into five categories, i.e., circular (0.9–1.0), oval (0.8–0.9), less elongated (0.7–0.8), elongated (0.5–0.7), and more elongated (<0.5). Horton (1932) also suggested that the smaller the value of F_f (<0.45), the more the basin will be elongated. For Agula watershed, low values of F_f, R_e, and R_c and high value of C_c implied that the watershed has elongated shape. For the sub-watersheds, the value ranges for the shape parameters were F_f (0.15–0.60), R_e (0.43–0.87), R_c (0.17–0.33), and C_c (1.75–2.43). Sub-watersheds that belong to cluster C2 (Figure 4.2(b)) have low F_f, R_e, and R_c values (Table 4.3); and by implication these sub-watersheds have elongated shape. According to Thomas et al. (2012), watersheds with elongated shape are characterized by flat hydrograph for longer duration with low slope of the rising and recession limbs. Furthermore, the low F_f, R_e, and R_c values of these sub-watersheds suggested a lower chance of occurrence of heavy rainfall covering the entire area, and hence lesser vulnerability to flash floods and as a result easier flood management than those of the circular basins (Pandey et al. 2004). Sub-watersheds in cluster C1 (Figure 4.2(b)) have more circular shape as suggested by moderately high F_f, R_e, and R_c values (Table 4.3). The more circular sub-watersheds have shorter lag time and higher peak flows of shorter duration compared to the elongated sub-watersheds (Thomas et al. 2012). As such, the more circular sub-watersheds are more efficient in the discharge of runoff than elongated sub-watersheds; but have a greater risk of flash floods as there will be a greater possibility that the entire area may contribute at the same time, and high susceptibility to erosion

and sediment load (Reddy et al. 2004). It is noteworthy, however, that the hydrologic response of watersheds is affected by several other factors, such as the rainfall event properties, soil type, LULC and slope. The correlation analysis revealed that the F_f, R_e, and R_c showed significant positive correlation to one another ($p < 0.05$); whereas a significant negative correlation was observed between C_c and the other shape parameters (Table 4.4). Moreover, the F_f, R_e, and R_c were negatively correlated with ruggedness number (R_n) and dissection index (D_{is}), but positive correlation was observed between C_c and the relief characteristics R_n and D_{is} (Table 4.4).

4.3.3 Drainage texture analysis

Drainage texture indicates the amount of landscape dissection by a channel network and includes parameters such as stream frequency (F_s), drainage texture (D_t), drainage density (D_d), infiltration number (I_f), length of overland flow (L_o), and constant of channel maintenance (C). These are important parameters as they are related to the dynamic nature of the network of streamlines and area of watersheds. These parameters largely reflect the inter-relationships among geomorphological elements like lithology, geological structure, topography, vegetation, hydrology and climate. As such, the drainage texture parameters can help predict watershed processes such as runoff and sediment yield as well as magnitude of dissection of terrain. The computed F_s, D_t, D_d, and I_f values of Agula watershed were 5.05, 11.74, 2.6 and 13.15 (Table 1) and these values are indicative of moderately dissected steep terrain. Based on Smith (1950), D_t has four categories: coarse ($D_t \leq 4$), moderate ($4 < D_t \leq 10$), fine ($D_t > 10$) and ultra-fine or badlands topography ($D_t > 15$). From such classification, the drainage of Agula watershed is categorized as fine drainage texture, which, in general, indicates that the watershed is dominated by low permeability soft rock with low resistance against erosion.

Table 4.4 Correlation matrix among selected morphometric parameters for the 26 sub-watersheds (* statistically significant correlations at $p < 0.05$). The full names of parameters are given in Table 4.1.

	R_b	F_f	R_e	R_c	C_c	F_s	D_t	D_d	D_i	I_f	L_o	R_h	R_n	D_{is}	HI	A
R_b	1.00															
F_f	-0.19	1.00														
R_e	-0.19	0.99*	1.00													
R_c	-0.15	0.57*	0.59*	1.00												
C_c	0.20	-0.56*	-0.58*	-0.99*	1.00											
F_s	-0.46*	0.14	0.16	0.04	-0.06	1.00										
D_t	-0.14	0.19	0.23	0.45*	-0.45*	0.57*	1.00									
D_d	0.05	0.13	0.13	-0.12	0.12	0.13	0.16	1.00								
D_i	-0.46*	0.07	0.08	0.10	-0.11	0.89*	0.45*	-0.34	1.00							
I_f	-0.37	0.18	0.20	-0.01	0.00	0.90*	0.56*	0.54*	0.61	1.00						
L_o	-0.08	-0.15	-0.14	0.13	-0.13	-0.13	-0.17	-0.99*	0.34	-0.53*	1.00					
R_h	-0.25	0.10	0.10	-0.19	0.17	0.08	-0.32	0.17	-0.01	0.14	-0.18	1.00				
R_n	-0.04	-0.48*	-0.48*	-0.41*	0.40*	0.09	0.12	0.41*	-0.11	0.26	-0.42*	0.53*	1.00			
D_{is}	-0.03	-0.46*	-0.46*	-0.38	0.37	0.13	0.14	0.33	-0.04	0.25	-0.34	0.54*	0.98*	1.00		
HI	-0.09	-0.21	-0.22	0.20	-0.20	0.00	-0.06	-0.01	0.03	-0.01	0.04	-0.25	-0.15	-0.24	1.00	
A	0.07	-0.02	0.01	0.23	-0.22	0.28	0.90*	0.15	0.18	0.31	-0.16	-0.40*	0.26	0.26	-0.16	1.00

Furthermore, fine drainage texture is favored in areas where basin relief is high and consequently the landscape is susceptible to erosion (Magesh et al. 2011). At sub-watershed level, the value ranges of F_s, D_d, and I_f were 3.49–6.30, 2.3–2.95, and 8.33–16.29, respectively. High values of F_s, D_d, and I_f were found in sub-watersheds under cluster C1; whereas sub-watersheds under cluster C2 registered relatively low values (Figure 4.2(c), Table 4.3). This indicates that sub-watersheds under cluster C1 are characterized by weak and impermeable subsurface material with sparse vegetation, high relief and steep slope landscape; which has high tendency to generate surface runoff. By contrast, watersheds under cluster C2 are likely to have highly resistant permeable subsurface material with good vegetation cover and low relief; which would result in more infiltration capacity and comparably could be good sites for ground water recharge.

In general, resistant surface materials and those with high infiltration capacities exhibit widely spaced streams, consequently yielding low F_s, D_d, and I_f. As surface permeability decreases, runoff is usually accentuated by the development of a greater number of more closely spaced channels, and thus F_s, D_d, and I_f tend to be higher. Horton (1945) demonstrated that high transmissibility (as evidenced by infiltration capacity) leads to low drainage density, high base flow and a resultant low magnitude peak flow. By contrast, an impermeable surface will generate high drainage density and efficiently carry away runoff; with high peak discharge but low base flow. However, Dingman (1978) noted that the relationship between D_d and flow may be overridden by other factor such as flood plain and channel storage; and in areas where saturated overland flow is the major source of runoff, D_d may not be related to the efficiency at which the watershed is drained. Further, D_d has also been used as an independent variable in the framing of L_o and C (Table 4.1); both have a reciprocal relationship with D_d. Hence, sub-watersheds with

high values of F_s, D_d, and I_f have corresponding low values of L_o and C, and vice versa (Table 4.3). The L_o is of great importance from hydrologic perspective as it indicates the distance which water must travel before reaching stream channels. It also bears a close relation to the hydrology of a watershed since the greater the L_o, the greater, in general, is the infiltration and the less the direct surface runoff (Horton, 1945). For Agula watershed, the computed L_o value was 0.19 (Table 4.1), which indicated the presence of short flow paths and steep ground slopes associated with more runoff. Thomas et al. (2012) also noted that relatively shorter L_o is characteristics of areas with steeper slopes and fine texture that lead to high surface runoff generation. For the sub-watersheds of Agula, the C value ranged between 0.34 and 0.43. High values of C for sub-watersheds of cluster C3 suggested strong control of lithology with a surface of high permeability; and by implication more area is required to produce surface flow. For sub-watersheds under cluster C1, low values of C indicated limited percolation/infiltration and hence more surface runoff (Sreedevi et al. 2013). The correlation analysis showed statistically significant ($p < 0.05$) positive correlations among the drainage texture parameters (Table 4.4).

4.3.4 Relief characteristics

Relief characteristics can help understand landforms of a watershed, drainage networks development, overland flow, and erosional properties of terrain. In the present study, relief ratio (R_h), relative relief (R_{hp}), ruggedness number (R_n), and dissection index (D_{is}) were used as these parameters reveal the runoff and erosion potential of a watershed. The total relief of Agula watershed is 907 m (Table 4.1). Such a high value indicated the high potential erosive energy of the watershed above a specified datum available to move water and sediment down the slope. The relief characteristic values of R_h (0.02), R_{hp} (0.48), R_n (2.36), and D_{is} (0.31) (Table 4.1),

indicated that Agula watershed is characterized by high relief, steep slopes and is moderately dissected. For the sub-watersheds, the R_h value ranged from 0.03–0.1 with low values in sub-watersheds under cluster C1 and high values in sub-watersheds under cluster C3 (Figure 4.2(d), Table 4.3). In a similar study, Kaliraj et al. (2014) attributed the low value of R_h mainly to resistant basement rocks and low degree of slope. Thomas et al. (2012) considered relatively high R_h values as indicative of comparatively steeply sloping terrain and consequently higher basin energy manifested as high intensity of erosion processes operating along the hillslopes as well as sediment transport capacity. As such, runoff is generally faster in sub-watershed with high R_h producing more peaked discharges and hence greater erosive power. For the sub-watersheds of Agula, the R_n and D_{is} values ranged from 0.41–1.63 and 0.07–0.22, respectively. Similar to the R_h, high values of R_n and D_{is} were found in sub-watersheds under cluster C3, whereas sub-watersheds under cluster C1 registered low R_n and D_{is} values (Figure 4.2(d), Table 4.3). The high R_n and D_{is} values indicated the presence of long and steep slopes and high degree of dissection which implied lower time of concentration of overland flow and possibilities of flash floods and high susceptibility to soil erosion than watersheds with low R_n and D_{is}. A study by Patton and Baker (1976) demonstrated that watersheds with high flash flood potential have greater R_n than low potential watersheds in several physiographic regions of the United States. Further, R_h, R_n, and D_{is} bear statistically significant ($p < 0.05$) positive correlations (Table 4.4).

In addition to the morphometric parameters related to relief characteristics, classification of terrain into various geomorphic classes (or landforms) was carried out. Following the approach of Sayre et al. (2009), five landform classes were generated for Agula watershed from combinations of local relief and slope (Figure 4.5). The relations among slope, relief, and landform class are depicted in Table 5. The smooth and irregular plains and low hills classes had

a very low occurrence and hence were combined with the flat plains and hills, respectively. Breaks/foothills and low mountains were the dominant landforms each accounting for about 35% of the watershed; and the low mountains dominated the central/middle parts of the watershed. Overall, three rough landforms, including hills, breaks, and low mountains make up 76% of the watershed; whereas flat plains and escarpments comprised 18% and 6% of the watershed, respectively (Table 4.5, Figure 4.5). Based on Wilcox et al. (2007), the rough landforms such as the hills, breaks, and low mountains are characterized by high runoff generation and minimal groundwater recharge. It is also obvious that physiographic and land surface forms strongly influence the distribution of terrestrial ecosystems, and landform is a key part of the ecosystem delineation process. As such, understanding landforms of a watershed helps predict the distribution, physical and chemical properties of soils, and type of LULC, and is a very essential input for comprehensive watershed planning and management.

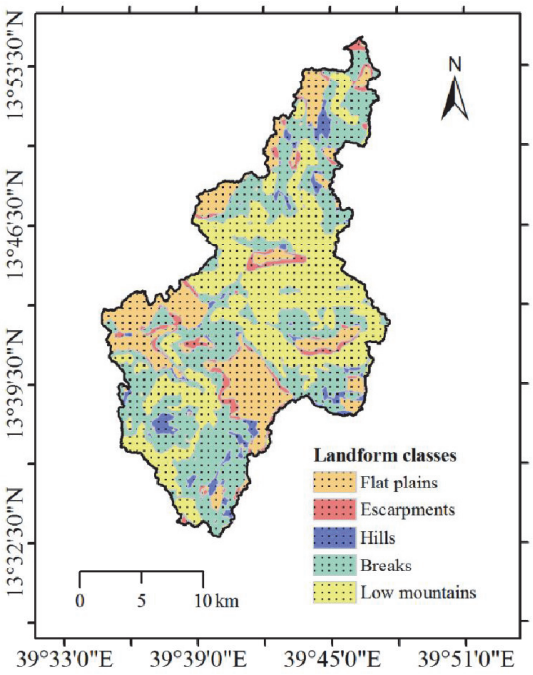

Figure 4.5 Landforms of Agula watershed derived from SRTM-DEM following the procedure of Sayre et al. (2009).

Table 4.5 Land surface form classes topographically modeled from combinations of slope class and local relief of Agula watershed following Sayre et al. (2009).

Slope class	Local relief (m)	Landform class	Area (km^2)	Area (%)
< 8%	≤15	Flat plains	81	18
	>15–≤30	Smooth plains	-	-
	>30–≤90	Irregular plains	-	-
	>90	Escarpments	25	6
≥ 8%	≤30	Low hills	-	-
	>30–≤90	Hills	20	5
	>90–≤150	Breaks/foothills	160	36
	>150	Low mountains	156	35

4.3.5 Hypsometric attributes

Identification of geomorphic stages and erosional surfaces of watersheds have been more suitably done by the analysis of area-altitude relationship in general and hypsometric analysis in particular. The HC of Agula watershed is S-shaped with HI value of 0.4 (Figure 4.6). The HC expresses the volume of rock mass in the watershed and the area below the curve represents the amount of material left after erosion. For Agula watershed, a 0.4 HI value indicated that about 40% of the original rock masses still exist in the watershed. The gradient of the HC was higher in its upper part (Figure 4.6), which indicated that the amount of material left after erosion is smaller (Harlin 1978; Luo 2000). Keller and Pinter (2002) related such higher gradient of the HC with maturity of a watershed, since it implied that lateral erosion must have been intensive in the river head. In addition, the HC was more concave upward in the upper portion of the curve (Figure 4.6), which according to Luo (2000), indicated more erosion in the upper reaches of the watershed. With reference to threshold limits recommended by Strahler (1952), HI ≥ 0.60 are typical of a youthful stage; 0.30 ≤ HI ≤ 0.60 are related to a maturity stage; and HI ≤ 0.30 are

indicative of a peneplain/old stage. Taking this classification scheme, Agula watershed is categorized as in the equilibrium or mature stage of geomorphic evolution. At sub-watershed scale, however, those under cluster C1 with relatively high values of HI (Table 4.3, Figure 4.2(d)) considered to be at youthful stage which are less dissected landscapes subject to erosion; whereas sub-watersheds with low HI values belonging to cluster C3 were at equilibrium or mature stage which are relatively stable, but still developing landforms. Willgoose and Hancock (1998) have a slightly different take on HI; and as such, watersheds with HI values >0.5 are relatively highland dominated by diffusive hillslope processes; whereas those having HI values <0.5 are considered dominated by fluvial erosion (channel processes play a larger role). The correlation matrix (Table 4.4) revealed negative correlation between HI and relief characteristics, but test statistics was not significant at $p < 0.05$. Similarly, Strahler (1952) also demonstrated that HI is inversely correlated with total relief, slope steepness, drainage density, and channel gradients; however, it is expected to correlate positively with rates of erosion.

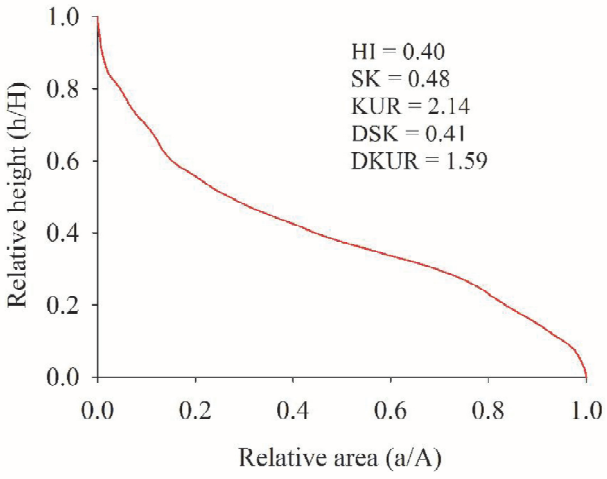

Figure 4.6 Hypsometric curve of Agula watershed and derived statistical attributes: *HI* hypsometric integral, *SK* hypsometric skewness, *KUR* hypsometric kurtosis, *DSK* density skewness, *DKUR* density kurtosis.

The HC was fitted to a fifth order polynomial function by regression using the least square fit (R^2 = 0.99) to get the coefficients a_0 = 0.95, a_1 = -3.58, a_2 = 11.46, a_3 = -20.80, a_4 = 18.72, and a_5 = -6.73. With these coefficients, it was possible to compute the statistical moments of the HC (SK and KUR) and its density function (DSK and DKUR) using Eqs. (4.2–4.5) defined by Harlin (1978). The derived statistical moments of the HC were SK (0.48), KUR (2.14), DSK (0.41), and DKUR (1.59). These derived hypsometric attributes are sensitive to subtle changes in overall watershed development as mass is removed by erosion over a long geological time period. According to Harlin (1978), the high value of SK for Agula watershed showed headward development of the main stream and its tributaries as these streams encroached the upper reaches of the watershed. DSK interprets the behavior of slope change in the watershed with positive (negative) values pointing to high erosion amounts in the upper (lower) regions of the watershed; hence the positive value of DSK was an indication of accelerated forms of erosion in the upper reaches and dominance of fluvial landforms (Luo 2000). The relatively high KUR value confirmed that erosional processes have occurred in both the upper and lower reaches of the watershed; whereas the platykurtic nature of the DKUR value was an indication that midbasin slope is moderate. Several studies (e.g., Luo 2000; Bertoldi et al. 2006; Vivoni et al. 2008) demonstrated that analysis of the HC and its statistical attributes are also useful metrics for inferring changes in watershed runoff response, which may result from landscape evolution.

4.4 Conclusions

In the present study, analysis of morphometric parameters was carried out from four aspects: drainage network, watershed geometry, drainage texture, and relief characteristics. A 6th order river drains Agula watershed and the drainage network is dominantly dendritic type. A mean

bifurcation ratio of R_b = 4.46 for the entire watershed is indicative of mountainous and moderately dissected terrain. However, at sub-watershed scale, high R_b values (R_b > 5) were observed which might be expected in regions of steeply sloping terrain. The longest flow path of Agula watershed is about 48.5 km, and the longitudinal profile showed changes in slope of the river bed with steep gradient (0.018 m m^{-1}) at the upper reach of the river which gradually flattened near its outlet (0.008 m m^{-1}). Knickpoints with abrupt changes in elevation also developed along the main river which could be attributed to change of lithology resulting in differential erosion as well as the presence of major faults which are common along the rift escarpments. Agula watershed has elongated shape; suggesting low peak flows for longer duration, lesser vulnerability to flash floods and easier flood management. The drainage texture parameters revealed that Agula watershed is characterized by fine drainage texture; implying that the watershed is dominated by impermeable soft rock with low resistance against erosion and sparse vegetation cover. Furthermore, high relief and steep slopes dominates, by which rough landforms including hills, breaks, and low mountains make up 76% of the watershed. The S-shaped hypsometric curve with hypsometric integral of 0.4 indicated that Agula watershed is in the equilibrium or mature stage of geomorphic evolution. At sub-watershed scale, the derived morphometric parameters from four perspectives (drainage network, watershed geometry, drainage texture, and relief characteristics) were further grouped into three clusters (that represented low, moderate, and high values) and considerable spatial variability was observed. Since, the watershed characteristics change owing to the spatial variations of the morphometric parameters, the inferred implications also differ accordingly. This study shows that remote sensing data and GIS techniques have become efficient tools to derive watershed-scale morphometic parameters which help better understand the status of landforms and their

processes relating to runoff generation and soil erosion risk. The results of this study provide information on drainage morphometry that can serve as a database of initial assessment for strategic planning, management and decision making that include watershed prioritization for soil and water conservation, assessment of surface and groundwater potential, soil erosion studies, flash flood hazard assessment, etc.

Chapter 5

General Conclusion

The results of MK test showed significant downward trends for annual and wet season streamflow; while dry season streamflow showed an upward trend during 1992–2012. For the same period, no significant trend was detected for seasonal and annual rainfall records. Based on the MKS test, an abrupt change-point in annual streamflow occurred around 2000. The detection of the year 2000 as a change-point of annual streamflow corresponds to the period of intensification of proper watershed management practices in Agula watershed. Based on the result of change-point test, the streamflow record was divided into two periods: a baseline period (1992–1999) and a change period (2000–2012). The mean annual streamflow decreased by about 36% during the change period compared to the baseline period; however, dry season streamflow increased by 57%. Model estimations revealed that climate variability accounted for 22% of the total reduction in mean annual streamflow; whereas the reduction due to human activities was about 78%. The results of study demonstrated that human activities primarily proper watershed management practices and associated changes in LULC play a more pronounced role in driving the changes in streamflow of Agula watershed. Other direct impacts of human activities such as water intake for domestic and agricultural uses can also lead to changes of streamflow regimes. Nevertheless, the amount of water used for irrigation by diverting the river water and use of hand-dug wells was not well documented; and hence, this study did not attempt to make quantitative estimations of the direct effects of human activities. In addition, the LULC change, SWC measures and other human activities might counteract each other and their effects on changes in streamflow are complicated, which invite further observation, experiments and investigation; especially using physical-based distributed models to identify the physical mechanisms behind the changes.

The RUSLE-based assessment of change in soil erosion revealed significant reduction in soil loss rates by about 55% from 28 to 12 t ha^{-1} yr^{-1} in 1990–2000 and an overall 64% reduction from 28 to 10 t ha^{-1} yr^{-1} in 1990–2012. Soil loss reductions vary depending on LULC type and topography with considerable reductions (>50 %) observed from bare and cultivated lands and from steep and very steep slope categories. Reductions in soil loss rates were due both to improved vegetation cover and to implementation of physical conservation structures that led to remarkable improvements in degraded land restoration. Comparisons of erosion estimations with the results of previous studies in Ethiopia and based on ground-truthing using visual estimations of erosion status confirm that the RUSLE-based soil loss estimations are fairly satisfactory. Even so, it is worth noting that model estimations are approximations of reality and therefore uncertainties with respect to the RUSLE factor maps are unavoidably present. Uncertainties in the soil loss results obtained in this study could result from limitations in some of the input parameters used and model estimations can be improved as better datasets are made available. With all its limitations, the model results provide useful information on the general pattern of the relative differences in soil loss, rather than providing accurate absolute erosion rates. This study demonstrates that the use of GIS-based RUSLE model and remote sensing data are effective approaches to assess changes in soil erosion brought about by watershed management practices and associated changes in LULC at watershed scale. Moreover, the methods used in the present study can be applied in other regions to estimate soil loss and facilitate sustainable environmental management through appropriate conservation planning of areas experiencing severe land degradation due to water erosion.

Analysis of sub-watershed scale morphometric parameters from four perspectives (drainage network, watershed geometry, drainage texture, and relief characteristics) revealed considerable

spatial variability. This suggests that the watershed characteristics and the inferred implications from the perspectives of runoff generation and soil erosion risk also differ accordingly. The S-shaped hypsometric curve with hypsometric integral of 0.4 indicated that Agula watershed is in the equilibrium or mature stage of geomorphic evolution with about 40% of the original rock masses still present in the watershed. This study demonstrates that remote sensing data and GIS techniques have become efficient tools to derive watershed-scale morphometic parameters which help better understand the status of landforms and their processes relating to runoff generation and soil erosion risk. The results of this study can help to prioritize high erosion risk areas for future planning of SWC practices.

References

Abtew W, Melesse AM (2014) The Nile River Basin. In: Mesele AM, Abtew W, Setegn S (Eds) Nile River basin: Ecohydrological challenges, climate change and hydropolitics, pp: 7–17, Springer-Verlag.

Adimassu Z, Mekonnen K, Yirga C, Kessler A (2014) Effect of soil bunds on runoff, soil and nutrient losses, and crop yield in the central highlands of Ethiopia. Land Degrad Dev 25(6): 554–564.

Aerts R, Nyssen J, Haile M (2009) On the difference between ‘‘exclosures’’ and ‘‘enclosures’’ in ecology and the environment. J Arid Environ 73(8): 762–763.

Alemayehu F, Taha N, Nyssen J, Girma A, Zenebe A, et al (2009) The impacts of watershed management on land use and land cover dynamics in Eastern Tigray (Ethiopia). Resour Conserv Recy 53(4): 192–198.

Allen RG, Pereira LS, Raes D, Smith M (1998) Crop evapotranspiration-guidelines for computing crop water requirements-FAO irrigation and drainage paper 56. FAO, Rome, Italy.

Al-Rowaily SL, El-Bana MI, Al-Dujain FA (2012) Changes in vegetation composition and diversity in relation to morphometry, soil and grazing on a hyper-arid watershed in the central Saudi Arabia. Catena 97: 41–49.

Amsalu A, de Graaff J (2007) Determinants of adoption and continued use of stone terraces for soil and water conservation in an Ethiopian highland watershed. Ecol Econ 61: 294–302.

Amsalu A, Stroosnijder L, de Graaff J (2007) Long-term dynamics in land resource use and the driving forces in the Beressa watershed, highlands of Ethiopia. J Environ Manage 83(4): 448–459.

Ananda J, Herath G (2003) Soil erosion in developing countries: a socio-economic appraisal. J Environ Manage 68(4): 343–353.

Anley Y, Bogale A, Haile-Gabriel A (2007) Adoption decision and use intensity of soil and water conservation measures by smallholder subsistence farmers in Dedo district, Western Ethiopia. Land Degrad Dev 18: 289–302.

Awlachew SB (2010) Irrigation potential in Ethiopia. International Water Management Institute, Addis Ababa, Ethiopia.

Babu K J, Sreekumar S, Aslam A (2016) Implication of drainage basin parameters of a tropical river basin of South India. Appl Water Sci 6: 67–75.

Banerjee A, Singh P, Pratap K (2015) Morphometric evaluation of Swarnrekha watershed, Madhya Pradesh, India: an integrated GIS-based approach. Appl Water Sci 7(4): 1807–1815.

Barrow CJ (1992) World atlas of desertification (United Nations Environment Programme). Land Degrad Dev 3(4): 249–249.

Bekele E (2003) Causes and consequences of environmental degradation in Ethiopia. In: Gedion A (Ed) Environment and environmental change in Ethiopia. Consultation Papers on Environment No. 1. Forum for Social Studies, Addis Ababa, pp: 24–31.

Belay KT, Van Rompaey A, Poesen J, Van Bruyssel S, Deckers J, et al (2014) Spatial analysis of land cover changes in eastern Tigray (Ethiopia) from 1965 to 2007: are there signs of a forest transition? Land Degrad Dev 26(7): 680–689.

Bellot J, Bonet A, Sanchez JR, Chirino E (2001) Likely effects of land use changes on the runoff and aquifer recharge in a semiarid landscape using a hydrological model. Landscape Urban Plan 55(1): 41–53.

Beltrando G, Camberlin P (1993) Interannual variability of rainfall in the eastern Horn of Africa and indicators of atmospheric circulations. Int J Climatol 13: 533–546.

Berhanu B, Seleshi Y, Melesse AM (2014) Surface water and groundwater resources of Ethiopia: Potentials and challenges of water resources development. In: Mesele AM, Abtew W, Setegn S (Eds) Nile River basin: Ecohydrological challenges, climate change and hydropolitics, pp: 97–117, Springer-Verlag.

Berry L (2003) *Land degradation in Ethiopia: Its extent and impact*. Washington DC: The World Bank.

Bertoldi G, Rigon R, Over TM (2006) Impact of watershed geomorphic characteristics on the energy and water budgets. J Hydrometeorol 7: 389–403.

Beven K (1989) Changing ideas in hydrology - the case of physically-based models. J Hydrol 105(1): 157–172.

Bewket W (2007) Soil and water conservation intervention with conventional technologies in north western highlands of Ethiopia: Acceptance and adoption by farmers. Land Use Policy 24: 404–416.

Bewket W, Sterk G (2005) Dynamics in land cover and its effect on stream flow in the Chemoga watershed, Blue Nile basin, Ethiopia. Hydrol Process 19(2): 445–458.

Bewket W, Teferi E (2009) Assessment of soil erosion hazard and prioritization for treatment at the watershed level: case study in the Chemoga watershed, Blue Nile basin, Ethiopia. Land Degrad Dev 20(6): 609–622.

Bishop MP, Shroder JF, Bonk R, Olsenholler J (2002) Geomorphic change in high mountains: a western Himalayan perspective. Glob Planet Change 32(4): 311–329.

Bishop P, Hoey TB, Jansen JD, Artza IL (2005) Knickpoint recession rate and catchment area: the case of uplifted rivers in eastern Scotland. Earth Surf Proc Land 30(6): 767–778.

Biswas A, Majumdar DD, Banerjee S (2014) Morphometry governs the dynamics of a drainage basin: analysis and implications. Geogr J. doi: 10.1155/2014/927176.

Brath A, Montanari A, Toth E (2004) Analysis of the effects of different scenarios of historical data availability on the calibration of a spatially-distributed hydrological model. J Hydrol 291(3): 232–253.

Bryan E, Deressa TT, Gbetibouo GA, Ringler C (2009) Adaptation to climate change in Ethiopia and South Africa: options and constraints. Environ Sci Policy 12(4): 413–426.

Budyko MI (1974) Climate and Life. Academic Press, San Diego CA.

Callow JN, Van Niel KP, Boggs GS (2007) How does modifying a DEM to reflect known hydrology affect subsequent terrain analysis. J Hydrol 332(1): 30–39.

Chatterjee S, Krishna AP, Sharma AP (2014) Geospatial assessment of soil erosion vulnerability at watershed level in some sections of the Upper Subarnarekha river basin, Jharkhand, India. Environ Earth Sci 71(1): 357–374.

Chen Z, Chen Y, Li B (2012) Quantifying the effects of climate variability and human activities on runoff for Kaidu River Basin in arid region of northwest China. Theor Appl Climatol 111(3): 537–545.

Cohen MJ, Shepherd KD, Walsh MG (2005) Empirical reformulation of the universal soil loss equation for erosion risk assessment in a tropical watershed. Geoderma 124 (3): 235–252.

Congalton RG (1991) A review of assessing the accuracy of classifications of remotely sensed data. Remote Sens Environ 37(1): 35–46.

Davis J (2010) Hypsometric Tools. http://arcscripts.esri.com/details.asp?dbid=16830. Accessed January 2016.

de Vente J, Poesen J, Verstraeten G, Van Rompaey A, Govers G (2008) Spatially distributed modelling of soil erosion and sediment yield at regional scales in Spain. Glob Planet Change 60(3): 393–415.

Descheemaeker K, Nyssen J, Poesen J, Raes D, Haile M, et al. (2006) Runoff on slopes with restoring vegetation: a case study from the Tigray highlands, Ethiopia. J Hydrol 331(1): 219–241

Dingman SL (1978) Drainage density and streamflow: a closer look. Water Resour Res 14(6): 1183–1187.

Ebabu K, Tsunekawa A, Haregeweyn N, Adgo E, Meshesha DT, et al (2018) Analyzing the variability of sediment yield: a case study from paired watersheds in the Upper Blue Nile basin, Ethiopia. Geomorphology 303: 446–455.

El Kenawy AM, McCabe MF, Vicente-Serrano, SM, López-Moreno JI, Robaa SM (2016) Changes in the frequency and severity of hydrological droughts over Ethiopia from 1960 to 2013. Cuadernos de Investigación Geográfica 42(1): 145–166.

El-Swaify SA, Hunri H (1996) Transboundary effects of soil erosion and conservation in the Nile basin. Land Husbandry 1(1/2): 5–21.

ERDAS (2006) ERDAS Field Guide. Leica Geosystems Geospatial Imaging, LCC. Norcross, GA, USA.

Erdogan EH, Erpul G, Bayramin İ (2007) Use of USLE/GIS methodology for predicting soil loss in a semiarid agricultural watershed. Environ Monit Assess 131(1-3): 153–161.

Esser K, Vågen TG, Tilahun Y, Haile M (2002) *Soil conservation in Tigray, Ethiopia*. Noragric Report No. 5. Agricultural University of Norway.

Faniran A (1968) The index of drainage intensity: a provisional new drainage factor. Aust J Sci 31(9): 326–330.

FAO (Food and Agriculture Organization) (2016) AQUASTAT Ethiopia: http://www.fao.org/nr/water/aquastat/countries_regions/ETH/, accessed February 22, 2018.

Farhan Y, Zregat D, Farhan I (2013) Spatial estimation of soil erosion risk using RUSLE approach, RS, and GIS techniques: a case study of Kufranja watershed, Northern Jordan. J Water Resource Prot 5(12): 1247–1261.

Farr TG, Rosen PA, Caro E, Crippen R, Duren R, et al. (2007) The Shuttle Radar Topography Mission. Rev Geophys 45(2): RG2004.

Fazzini M, Bisci C, Billi P (2015) The Climate of Ethiopia. In: Billi P (ed) Landscapes and Landforms of Ethiopia, pp. 65–87, Springer-Verlag.

Fenta AA, Kifle A, Gebreyohannes T, Hailu G (2015) Spatial analysis of groundwater potential using remote sensing and GIS-based multi-criteria evaluation in Raya Valley, northern Ethiopia. Hydrogeol J 23(1): 195–206.

Fenta AA, Yasuda H, Shimizu K, Haregeweyn N, Kawai T, et al (2017a). Spatial distribution and temporal trends of rainfall and erosivity in the Eastern Africa region. Hydrol Process 31(25): 4555–4567.

Fenta AA, Yasuda H, Shimizu K, Haregeweyn N (2017b) Response of streamflow to climate variability and changes in human activities in the semiarid highlands of northern Ethiopia. Reg Environ Change 17: 1229–1240.

Fenta AA, Yasuda H, Shimizu K, Haregeweyn N, Negussie A (2016) Dynamics of soil erosion as influenced by watershed management practices: a case study of the Agula watershed in the semiarid highlands of northern Ethiopia. Environ Manage 58(5): 889-905.

Gajbhiye S, Mishra SK, Pandey A (2014) Prioritizing erosion prone area through morphometric analysis: an RS and GIS perspective. Appl Water Sci 4(1): 51–61.

García-Ruiz JM, López-Moreno JI, Vicente-Serrano SM, Lasanta T, Beguería S (2011) Mediterranean water resources in a Global Change scenario. Earth-Sci Rev 105(3-4): 121–139.

Gebremedhin B, Swinton SM (2003) Investment in soil conservation in northern Ethiopia: the role of land tenure security and public programs. Agric Econ 29(1): 69–84.

Gebrernichael D, Nyssen J, Poesen J, Deckers J, Haile M et al (2005) Effectiveness of stone bunds in controlling soil erosion on cropland in the Tigray highlands, northern Ethiopia. Soil Use Manage 21(3): 287–297.

Gebreyohannes T, De Smedt F, Walraevens K, Gebresilassie S, Hussien A, et al (2013) Application of a spatially distributed water balance model for assessing surface water and groundwater resources in the Geba basin, Tigray, Ethiopia. J Hydrol 499: 110–123.

German L, Mansoor H, Getachew A, Mazengia W, Amede T, et al (2007) Participatory integrated watershed management: Evolution of concepts and methods in an ecoregional program of theeastern African highlands. Agri Syst 94(2): 189–204.

Getachew B (2007) Birki integrated watershed management study report. Tigray Bureau of Water Resources, Mekelle, Ethiopia.

Girmay G, Singh BR, Nyssen J, Borrosen T (2009) Runoff and sediment-associated nutrient losses under different land uses in Tigray, Northern Ethiopia. J Hydrol 376(1): 70–80.

Gravelius H (1941). Flusskunde, Goschen'sche Verlagshandlung. Berlin, Germany.

Gregory KJ, Walling DE (1973) Drainage basin form and process: a geomorphological approach. Willey, the University of Michigan.

Grohmann CH (2004) Morphometric analysis in geographic information systems: applications of free softwares. Comput Geosci 30: 1055–1067.

Hack JT (1973) Stream profile analysis and stream gradient index. J Res US Geol Survey 1(4): 421–429.

Hadgu G, Tesfaye K, Mamo G, Kassa B (2013) Trend and variability of rainfall in Tigray, northern Ethiopia: analysis of meteorological data and farmers' perception. J Agric Res 1(6): 088–100.

Hammond EH (1964) Analysis of properties in land form geography: an application to broad-scale land form mapping. Ann Assoc Am Geogr 54(1): 11–19.

Haregeweyn N, Berhe A, Tsunekawa A, Tsubo M, Meshesha DT (2012) Integrated watershed management as an effective approach to curb land degradation: a case study of the Enabered watershed in northern Ethiopia. Environ Manage 50(6): 1219–1233.

Haregeweyn N, Poesen J, Deckers J, Nyssen J, Haile M, Govers G (2008) Assessment and evaluation of sediment-bound nutrient export and associated costs from micro-dam catchments of Northern Ethiopia. Land Degrad Dev 19: 136–152.

Haregeweyn N, Poesen J, Nyssen J, De Wit J, Haile H, Govers G (2006) Reservoirs in Tigray: characteristics and sediment deposition problems. Land Degrad Dev 17(2): 211–230.

Haregeweyn N, Poesen J, Verstraeten G, Govers G, Vente J et al (2013) Assessing the performance of a spatially distributed soil erosion and sediment delivery model (WATEM/SEDEM) in Northern Ethiopia. Land Degrad Dev 24(2): 188–204.

Haregeweyn N, Tsunekawa A, Nyssen J, Poesen J, Tsubo M, et al (2015) Soil erosion and conservation in Ethiopia: a review. Prog Phys Geogr. 39(6): 750–774.

Haregeweyn N, Tsunekawa A, Poesen J, Tsubo M, Meshesha DT, et al (2017) Comprehensive assessment of soil erosion risk for better land use planning in river basins: Case study of the Upper Blue Nile River. Sci Total Environ 574: 95–108.

Haregeweyn N, Tsunekawa A, Tsubo M, Meshesha DT, Adgo E, et al (2016) Analyzing the hydrologic effects of region-wide land and water development interventions: a case study of the Upper Blue Nile basin. Reg Environ Change 16(4): 951–966.

Hargreaves GH, Samani ZA (1985) Reference crop evapotranspiration from temperature. Appl Eng Agric 1(2): 96–99.

Harlin JM (1978) Statistical moments of the hypsometric curve and its density function. Math Geol 10(1): 59–72.

Helldén U (1987) *An assessment of woody biomass, community forests, land use and soil erosion in Ethiopia*. Lund University Press.

Hellweger R (1996) AGREE – DEM surface reconditioning system. Center for Research in Water Resources, the University of Texas, Austin, TX.

Herweg K, Ludi E (1999) The performance of selected soil and water conservation measures-case studies from Ethiopia and Eritrea. Catena 36(1): 99–114.

Hijmans RJ, Cameron SE, Parra JL, Jones PG, Jarvis A (2005) The WorldClim interpolated global terrestrial climate surfaces, version 1.3. Available at http://biogeo.berkeley.edu/.

Horton RE (1932) Drainage basin characteristics. Trans Am Geophys Union 13(1): 350–361.

Horton RE (1945) Erosional development of streams and their drainage basins; hydrophysical approach to quantitative morphology. Geol Soc Am Bull 56(3): 275–370.

Hrissanthou V, Delimani P, Xeidakis G (2010) Estimate of sediment inflow into Vistonis Lake, Greece. Int J Sediment Res 25: 161–174.

Huang M, Zhang L (2004) Hydrological responses to conservation practices in a catchment of the Loess Plateau, China. Hydrol Process 18(10): 1885–1898.

Hunting Technical Service (HTS) (1976) *Tigray Rural Development Study*. HTS, Hemel Hempstead, UK.

Hurni H (1983a) *Ethiopian highland reclamation study. Soil formation rates in Ethiopia*. Working paper No. 2. Addis Ababa, Ethiopia.

Hurni H (1983a) Soil erosion and soil formation in agricultural ecosystems: Ethiopia and Northern Thailand. Mt Res Dev 3: 131–142

Hurni H (1985) *Soil Conservation Manual for Ethiopia: a field manual for conservation implementation*. Soil Conservation Research Project, Ministry of Agriculture, Addis Ababa.

Hurni H (1988) Degradation and conservation of the resources in the Ethiopian highlands. Mt Res Dev 8: 123–130.

Hurni H (1993). Land degradation, famine, and land resource scenarios in Ethiopia. In D. Pimentel (ed.), *World Soil Erosion and Conservation* (pp. 27–62). Cambridge University Press: Cambridge.

Hurni K, Zeleke G, Kassie M, Tegegne B, Kassawmar T et al (2015) *Soil degradation and sustainable land management in the rainfed agricultural areas of Ethiopia: An assessment of the economic implications*. Report for the Economics of Land Degradation Initiative.

Igbokwe KN, Adede J (2001) *Integrated watershed management in Eastern Tigray, Ethiopia*. Midterm impact evaluation report, Nairobi, Kenya.

Jain MK. Kothyari UC (2000) Estimation of soil erosion and sediment yield using GIS. Hydrol Sci J 45(5): 771–786.

Jetten V, Govers G, Hessel R (2003) Erosion models: quality of spatial predictions. Hydrol Process 17(5): 887–900.

Jiang Z, Su S, Jing C, Lin S, Fei X, et al (2012) Spatiotemporal dynamics of soil erosion risk for Anji County, China. Stoch Environ Res Risk Assess 26(6): 751–763.

Kahya E, Kalayci S (2004) Trend analysis of stream flow in Turkey. J Hydrol 289(1): 128–144.

Kaliraj S, Chandrasekar N, Magesh NS (2014) Morphometric analysis of the river Thamirabarani sub basin in Kanyakumari district, south west coast of Tamil Nadu, India, using remote sensing and GIS. Environ Earth Sci 73(11): 7375–7401.

Kassie M, Kohlin G, Bluffstone R, Holden S (2011) Are Soil Conservation Technologies "win-win"? A case Study of Anjeni in the North-Western Ethiopian Highlands. Nat Resour Forum 35: 89–99.

Keller EA, Pinter N (2002) Active tectonics: earthquakes, uplift, and landscape. Prentice Hall, New Jersey.

Kendall MG (1975) Rank correlation Methods. Charles Griffin, London.

Lanckriet S, Asfaha T, Frankl A, Zenebe A, Nyssen J (2016) Sediment in alluvial and lacustrine debris fans as an indicator for land degradation around Lake Ashenge (Ethiopia). Land Degrad Dev 27: 258–269.

Lanckriet S, Derudder B, Naudts J, Bauer H, Deckers J, et al. (2015) A political ecology perspective of land degradation in the north Ethiopian highlands. Land Degrad Develop 26: 521–530.

Legesse D, Vallet-Coulomb C, Gasse F (2003) Hydrological Response of a Catchment to Climate and Land Use Change in Tropical Africa: Case Study South Central Ethiopia. J Hydrol 275(1): 67–85.

Li B, Su H, Chen F, Li H, Zhang R, Tian J, Chen S, Yang Y, Rong Y (2014) Separation of the impact of climate change and human activity on streamflow in the upper and middle reaches of the Taoer River, northeastern China. Theor Appl Climatol 118: 271–283.

Lu D, Li G, Valladares GS, Batistella M (2004) Mapping soil erosion risk in Rondonia, Brazilian Amazonia: using RUSLE, remote sensing and GIS. Land Degrad Dev 15(5): 499–512.

Lu D, Mausel P, Brondi´Zio E, Moran E (2004) Change detection techniques. Int J Remote Sens 25(12): 2365–2407.

Luo W (2000) Quantifying groundwater sapping landforms with a hypsometric technique. J Geophys Res 105(1): 1685–1694.

Ma H, Yang D, Tan SK, Gao B, Hu Q (2010) Impact of climate variability and human activity on streamflow decrease in the Miyun Reservoir catchment. J Hydrol 389(3): 317–324.

Ma Z, Kang S, Zhang L, Tong L, Su X (2008) Analysis of impacts of climate variability and human activity on streamflow for a river basin in arid region of northwest China. J Hydrol 352(3): 239–249 .

Macka Z (2003) Structural control on drainage network orientation an example from the Loucka drainage basin, SE margin of the Bohemian Massif (S Moravia Czech Rep.). Landform Analysis 4: 109–117.

Magesh NS, Chandrasekar N, Soundranayagam J (2011) Morphometric evaluation of Papanasam and Manimuthar watersheds, parts of Western Ghats, Tirunelveli district, Tamil Nadu, India: a GIS approach. Environ Earth Sci 64(2): 373–381.

Magesh NS, Jitheshlal KV, Chandrasekar N, Jini KV (2013) Geographical information system-based morphometric analysis of Bharathapuzha river basin, Kerala, India. Appl Water Sci 3(2): 467–77.

Mann HB (1945) Nonparametric tests against trend. Econometrica 13: 245–259.

Mekuria W, Veldkamp E (2012) Restoration of native vegetation following exclosure establishment on communal grazing lands in Tigray, Ethiopia. Appl Veg Sci 15(1): 71–83.

Mekuria W, Veldkamp E, Haile M, Gebrehiwot K, Muys B, Nyssen J (2009) Effectiveness of exclosures to control soil erosion and local community perception on soil erosion in Tigray, Ethiopia. Afr J Agric Res 4: 365–377.

Mekuria W, Veldkamp E, Haile M, Nyssen J, Muys B, Gebrehiwot K (2007) Effectiveness of exclosures to restore degraded soils as a result of overgrazing in Tigray, Ethiopia. J Arid Environ 69(2): 270–284.

Melton M A (1957) An analysis of the relations among elements of climate, surface properties and geomorphology. Project NR 389-042, Tech Rep 11, Columbia University.

Meshesha DT, Tsunekawa A, Tsubo M, Haregeweyn N (2012) Dynamics and hotspots of soil erosion and management scenarios of the central Rift Valley of Ethiopia. Int J Sediment Res 27(1): 84–99.

Meshesha DT, Tsunekawa A, Tsubo M, Haregeweyn N, Adgo E (2014) Drop size distribution and kinetic energy load of rainfall events in the highlands of the Central Rift Valley, Ethiopia. Hydrol Sci J 59: 2203–2215.

Meshram SG, Sharma SK (2015) Prioritization of watershed through morphometric parameters: a PCA-based approach. Appl Water Sci 7(7): 1505–1519.

Miller VC (1953) A quantitative geomorphologic study of drainage basin characteristics in the Clinch mountain area, Virginia and Tennessee. Technical report 3, Columbia University, New York.

MoARD (Ministry of Agriculture and Rural Development) (2005) Community Based Participatory Watershed Development: A Guideline - Part 1. Addis Abeba, Ethiopia.

MoFED (Ministry of Finance and Economic Development) (2010) Draft Growth and Transformation Plan (GTP). Addis Ababa, Ethiopia.

Moore ID, Wilson JP (1992) Length-slope factors for the revised universal soil loss equation. Simplified method of estimation. Soil Water Conserv 47: 42–428.

Morgan RPC, Quinton JN, Smith RE, Govers G, Poesen J et al (1998) The European Soil Erosion Model (EUROSEM): a dynamic approach for predicting sediment transport from fields and small catchments. Earth Surf Process Landf 23(6): 527–544.

Moriasi DN, Arnold JG, Van Liew MW, Bingner RL, Harmel RD, et al (2007) Model evaluation guidelines for systematic quantification of accuracy in watershed simulations. T ASABE 50(3): 885–900.

MoWIE (Ministry of Water, Irrigation and Electricity of Ethiopia) (1997) *Tekeze River Basin Integrated Development Master Plan*. Addis Ababa, Ethiopia.

Nearing MA, Foster GR, Lane LJ, Finkner SC (1989) A process based soil erosion model for USDA-water erosion prediction project technology. Trans ASAE 32: 1587–1593.

Nyssen J, Clymans W, Descheemaeker K, Poesen J, Vandecasteele I, et al (2010) Impact of soil and water conservation measures on catchment hydrological response-a case in north Ethiopia. Hydrol Process 24(13): 1880–1895.

Nyssen J, Clymans W, Poesen J, Vandecasteele I, De Baets S, et al (2009a) How soil conservation affects the catchment sediment budget–a comprehensive study in the north Ethiopian highlands. Earth Surf Process Landf 34(9): 1216–1233.

Nyssen J, Poesen J, Descheemaeker K, Haregeweyn N, Haile M, et al (2008) Effects of region-wide soil and water conservation in semi-arid areas: the case of northern Ethiopia. Z Geomorph 52(3): 291–315.

Nyssen J, Poesen J, Gebremichael D, Vancampenhout K, D'aes M, et al (2007) Interdisciplinary on-site evaluation of stone bunds to control soil erosion on cropland in northern Ethiopia. Soil Tillage Res 94(1): 151–163.

Nyssen J, Poesen J, Haile M, Moeyersons J, Deckers J, et al (2009b) Effects of land use and land cover on sheet and rill erosion rates in the Tigray highlands, Ethiopia. Z Geomorph 53(2): 171–197.

Nyssen J, Poesen J, Veyret-Picot M, Moeyersons J, Haile M, et al (2006) Assessment of gully erosion rates through interviews and measurements: a case study from northern Ethiopia. Earth Surf Process Landf 31(2): 167–185.

Nyssen J, Vandenreyken H, Poesen J, Moeyersons J, Deckers J, et al (2005) Rainfall erosivity and variability in the northern Ethiopian highlands. J Hydrol 311(1): 172–187.

Nyssen J, Veyret-Picot M, Poesen J, Moeyersons J, Haile M, et al (2004) The effectiveness of loose rock check dams for gully control in Tigray, northern Ethiopia. Soil Use Manage 20(1): 55–64.

O'Callaghan JF, Mark DM (1984) The extraction of drainage networks from digital elevation data. Comput Vis Graph Image Process 28(3): 323–344.

Osman M, Sauerborn P (2001) Soil and water conservation in Ethiopia. J Soils Sediments 1(2): 117–123.

Panagos P, Borrelli P, Meusburgerb K, van der Zanden E, Poesen J, et al (2015) Modelling the effect of support practices (P-factor)on the reduction of soil erosion by water at European scale. Environ Sci Policy 51: 23–34.

Pandey A, Chowdary VM, Mal BC (2004) Morphological analysis and watershed management using geographical information system. J Hydro l27(3-4): 71–84.

Patton PC, Baker VR (1976) Morphometry and floods in small drainage basins subject to diverse hydrogeomorphic controls. Water Resour Res 12(5): 941–952.

Pike RJ, Wilson SE (1971) Elevation-relief ratio, hypsometric integral, and geomorphic area-altitude analysis. Geol Soc Am Bull 82(4): 1079–1084.

Pimentel D (2006). Soil erosion: a food and environmental threat. Environ Dev Sustain 8(1): 119–137.

Prowse TD, Beltaos S, Gardner JT, Gibson JJ, Granger RJ, et al (2006) Climate change, flow regulation and land-use effects on the hydrology of the Peace-Athabasca-Slave system; findings from the Northern Rivers ecosystem initiative. Environ Monit Assess 113(1-3): 167–197.

Quilbè R, Rousseau AN, Moquet JS, Savary S, Ricard S, et al (2008) Hydrological responses of a watershed to historical land use evolution and future land use scenarios under climate change conditions. Hydrol Earth Syst Sci 12(1): 101–110.

Rabus B, Eineder M, Roth A, Bamler R (2003) The Shuttle Radar Topography Mission: a new class of digital elevation models acquired by spaceborne radar. ISPRS J Photogramm Remote Sens 57(4): 241–262.

Rai PK, Mohan K, Mishra S, Ahmad A, Mishra VN (2014) A GIS-based approach in drainage morphometric analysis of Kanhar River Basin, India. Appl Water Sci 7(1): 217–232.

Reddy OGP, Maji AK, Gajbhiye SK (2004) Drainage morphometry and its influence on landform characteristics in a basaltic terrain, Central India-a remote sensing and GIS approach. Int J Appl Earth Obs Geoinformatics 6(1): 1–16.

Renard KG, Foster GR, Weesies GA, Porter JP (1991) RUSLE: revised universal soil loss equation. J Soil Water Conserv 46(1): 30–33.

Ritter DF, Kochel RC, Miller JR (1995) Process Geomorphology. Long Grove, Waveland Press.

Romshoo SA, Bhat SA, Rashid I (2012) Geoinformatics for assessing the morphometric control on hydrological response at watershed scale in the upper Indus basin. J Earth Syst Sci 121(3): 659–686.

Roy S, Sahu AS (2016) Effectiveness of basin morphometry, remote sensing and applied geosciences on groundwater recharge potential mapping: a comparative study within a small watershed. Front Earth Sci 10(2): 274–291.

Sayre R, Comer P, Warner H, Cress J (2009) A new map of standardized terrestrial ecosystems of the conterminous United States. USGS professional paper 1768.

Schumm SA (1956) Evaluation of drainage system and slopes in badlands at Perth Amboy, New Jersey. Geol Soc Am Bull 67(5): 597–646.

Shiferaw B, Holden S (1999) Soil Erosion and Smallholders' Conservation Decisions in the Highlands of Ethiopia. World Develop 27(4): 739–752.

Singh O, Sarangi A, Sharma MC (2008) Hypsometric integral estimation methods and its relevance on erosion status of north-western Lesser Himalayan watersheds. Water Resour Manag 22(11): 1545–1560.

Slater JA, Garvey G, Johnston C, Haase J, Heady B, et al. (2006) The SRTM "finishing" process and products. Photogramm Eng Remote Sens 72(3): 273–274.

Smith K (1950) Standards for grading textures of erosional topography. Am J Sci 248: 655–668.

Sneyers R (1975) Sur l'analyse statistique des s´eries d'observations. WMO Technical Note.

Soille P, Vogt J, Colombo R (2003) Carving and adaptive drainage enforcement of grid digital elevation models. Water Resour Res 39(12): 1366.

Solomon D, Lehmann J, Zech W (2000) Land use effects on soil organic matter properties of chromic Luvisols in semi-arid northern Tanzania: carbon, nitrogen, lignin and carbohydrates. Agric Ecosyst Environ 78(3): 203–213.

Sonneveld BGJS, Keyzer MA (2003) Land under pressure: soil conservation concerns and opportunities for Ethiopia. Land Degrad Dev 14(1): 5–23.

Sreedevi PD, Sreekanth PD, Khan HH, Ahmed S (2013) Drainage morphometry and its influence on hydrology in a semi-arid region: using SRTM data and GIS. Environ Earth Sci 70(2): 839–848.

Sreedevi PD, Subrahmanyam K, Ahmed S (2005) The significance of morphometric analysis for obtaining groundwater potential zones in a structurally controlled terrain. Environ Geol 47: 412–420.

Strahler AN (1952) Hypsometric area-altitude analysis of erosional topography. Geol Soc Am Bull 63(11): 1117–1142.

Strahler AN (1954) Quantitative geomorphology of erosional landscapes. 19th International Geologic Congress, section XIII, 341–354.

Strahler AN (1957) Quantitative analysis of watershed geomorphology. Trans Am Geophys Union 38(6): 913–920.

Strahler AN (1964) Quantitative geomorphology of drainage basins and channel networks. In Chow VT (ed) Handbook of Applied Hydrology. McGraw Hill Book Company, New York, 4–11.

Sultan D, Tsunekawa A, Haregeweyn N, Adgo E, Tsubo M, et al (2018a). Impact of soil and water conservation interventions on watershed runoff response in a tropical humid highland of Ethiopia. Environ Manage doi: 10.1007/s00267-018-1005-x.

Sultan D, Tsunekawa A, Haregeweyn N, Adgo E, Tsubo M, et al (2018b). Efficiency of soil and water conservation practices in different agro-ecological environments of Ethiopia's Upper Blue Nile basin. J Arid Land doi: 10.1007/s40333-018-0097-8.

Taddese G (2001) Land degradation: a challenge to Ethiopia. Environ Manage 27(6): 815–824.

Tamene L, Abegaz A, Aynekulu E, Woldearegay K, Vlek PL (2011) Estimating sediment yield risk of reservoirs in northern Ethiopia using expert knowledge and semi-quantitative approaches. Lakes Reservoirs Res Manage 16(4): 293–305.

Taye G, Poesen J, Wesemael BV, Vanmaercke M, Teka D, et al (2013) Effects of land use, slope gradient, and soil and water conservation structures on runoff and soil loss in semi-arid northern Ethiopia. Phys Geogr 34(3): 236–259.

Teshome A, de Graaff J, Kassie M (2016) Household level determinants of soil and water conservation adoption phases in the north-western Ethiopian highlands. Environ Manage 57: 620–636.

Thomas J, Joseph S, Thrivikramji K, Abe G, Kannan N (2012) Morphometrical analysis of two tropical mountain river basins of contrasting environmental settings, the southern western Ghats, India. Environ Earth Sci. 66(8): 2353–2366.

Thomas J, Joseph S, Thrivikramji KP, Arunkumar KS (2014) Sensitivity of digital elevation models: the scenario from two tropical mountain river basins of the western Ghats, India. Geoscience Frontiers 5(6): 893–909.

Tiwari AK, Risse LM, Nearing MA (2000) Evaluation of WEPP and its comparison with USLE and RUSLE. Trans ASAE 43(5): 1129–1135.

Trabucco, A., and Zomer, R.J. 2009. Global Potential Evapo-Transpiration (Global-PET) and Global Aridity Index (Global-Aridity) Geo-Database. CGIAR Consortium for Spatial Information. Available online from the CGIAR-CSI GeoPortal at: http://www.csi.cgiar.org.

Turcotte R, Fortin JP, Rousseau AN, Massicotte S, Villeneuve JP (2001) Determination of the drainage structure of a watershed using a digital elevation model and a digital river and lake network. J Hydrol 240(3): 225–242.

Twidale CR (2004) River patterns and their meaning. Earth-Sci Rev 67(3): 159–218.

UNESCO (United Nations Educational, Scientific, and Cultural Organization) (2004) National Water Development Report for Ethiopia (Final). Addis Ababa, Ethiopia.

Van Niel TG, McVicar TR, Datt B (2005) On the relationship between training sample size and data dimensionality: Monte Carlo analysis of broadband multi-temporal classification. Remote Sens Environ 98(4): 468–480.

Van Remortel RD, Hamilton ME, Hickey RJ (2001) Estimating the LS factor for RUSLE through iterative slope length processing of digital elevation data within Arclnfo grid. Cartography 30(1): 27–35.

Vivoni ER, Di Benedetto F, Grimaldi S, Eltahir EA (2008) Hypsometric control on surface and subsurface runoff. Water Resour Res 44(12).

Wahren A, Feger KH, Schwärzel K, Münch, A (2009) Land-use effects on flood generation–considering soil hydraulic measurements in modelling. Adv Geosci 21: 99–107.

Wang G, Gertner G, Fang S, Anderson AB (2003) Mapping multiple variables for predicting soil loss by geostatistical methods with TM images and a slope map. Photogramm Eng Rem S 69(8): 889–898.

Ward JH (1963) Hierarchical grouping to optimize an objective function. J Am Stat Assoc 58(301): 236–244.

Weiß M, Menzel L (2008) A global comparison of four potential evapotranspiration equations and their relevance to stream flow modelling in semi-arid environments. Adv Geosci 18: 15–23.

Wilcox BP, Wilding LP, Woodruff CM (2007) Soil and topographic controls on runoff generation from stepped landforms in the Edwards plateau of central Texas. Geophys Res Lett 34(24).

Willgoose G, Hancock G (1998) Revisiting the hypsometric curve as an indicator of form and process in transport-limited catchment. Earth Surf Proc Land 23: 611–623.

Wischmeier WH, Smith DD (1978) *Predicting rainfall erosion losses-A guide to conservation planning*. Agriculture Handbook No. 537. USDA, Washington DC.

Xu H, Xu CY, Chen H, Zhang Z, Li L (2013) Assessing the influence of rain gauge density and distribution on hydrological model performance in a humid region of China. J Hydrol 505: 1–12.

Yang D, Kanae S, Oki T, Koike T, Musiake K (2003) Global potential soil erosion with reference to land use and climate changes. Hydrol Process 17(14): 2913–2928.

Yang L, Meng X, Zhang X (2011) SRTM DEM and its application advances. Int J Remote Sens 32(14): 3875–3896.

Yayneshet T, Eik LO, Moe SR (2009) The effects of exclosures in restoring degraded semi-arid vegetation in communal grazing lands in northern Ethiopia. J Arid Environ 73(4): 542–549.

Zhang C, Zhang B, Li W, Liu M (2014) Response of streamflow to climate change and human activity in Xitiaoxi river basin in China. Hydrol Process 28(1): 43–50.

Zhang H, Yang Q, Li R, Liu Q, Moore D et al (2013). Extension of a GIS procedure for calculating the RUSLE equation LS factor. Comput Geosci 52: 177–188.

Zhang L, Dawes W, Walker G (2001) Response of mean annual evapotranspiration to vegetation changes at catchment scale. Water Resour Res 37(3): 701–708.

Zheng H, Zhang L, Zhu R, Liu C, Sato Y, Fukushima Y (2009) Responses of streamflow to climate and land surface change in the headwaters of the Yellow River Basin. Water Resour Res 45(7).

Summary

Land degradation by soil erosion is the most serious environmental threat in the Ethiopian highlands that led to substantial socio-economic and ecological problems. In response, the government of Ethiopia with the support of various non-governmental organizations has been promoting implementation of different soil and water conservation (SWC) measures to curb land degradation by soil erosion. Tigray region of northern Ethiopia is one of the drought-prone areas where resolute efforts have been under way to remedy environmental degradation through implementation of proper SWC practices, especially in the past two decades. The objectives of the watershed management practices were threefold: (i) to restore degraded areas, (ii) to secure water supply for agriculture and domestic uses, and (iii) to promote food security. In view of these objectives, Agula watershed was one of the target areas in the region where massive SWC measures have been implemented. The components of the SWC practices include: construction of stone bunds with or without trenches on cultivated lands and on hill-slopes, check dams across gullies and rivers, and establishment of exclosures with or without enrichment plantation.

Several previous studies have reported on the effectiveness of SWC practices at plot and small-scale watersheds (<100 km^2) in erosion control, runoff and sediment yield reduction, and changes in land use/land cover (LULC) as a result of vegetation regeneration. Despite the massive mobilization of resources for SWC, only very few studies have been done to analyze the impacts of SWC measures with respect to hydrological response, soil erosion and LULC change at medium- or large-scale watersheds (>100 km^2) which are of great interest to land managers and policy makers. The main objective of this study was therefore to estimate the changes in hydrological response and soil erosion for medium-sized watershed (area = 442 km^2) in the

semiarid highlands of northern Ethiopia and to link these changes to watershed management practices and associated changes in LULC. This research focused on three studies covering the following: (i) to quantitatively estimate to what extent watershed management practices and changes in LULC affect streamflow response; (ii) to assess watershed-scale changes in soil erosion as a result of the watershed management practices and LULC change; and (iii) to analyze morphometric parameters of the watershed to better understand the hydro-geologic and erosion characteristics of the watershed for improved planning, management, and decision making to ensure sustainable use of watershed resources. The studies are summarized as follows:

The first study evaluated changes in streamflow in response to climate variability and human activities such as watershed management practices and LULC change. The non-parametric Mann-Kendall (MK) and Mann-Kendall-Sneyers (MKS) tests were used to analyze trends and abrupt change-point of hydro-meteorological series for the period 1992-2012. The LULC change was assessed by classification of multi-temporal Landsat images of years 1990, 2000 and 2012 and post-classification change detection techniques. A runoff model, driven by rainfall and potential evapotranspiration was established to estimate the effect of climate variability on streamflow; then the effects of climate variability and human activities (watershed management practices and LULC change) on streamflow were separated. The MK test result showed significant downward trends for annual and wet season streamflow; while dry season streamflow showed an upward trend. For the same period, no significant trend was detected for seasonal and annual rainfall records. Based on the MKS test, an abrupt change-point in annual streamflow occurred around 2000; and hence the streamflow record was divided into two periods: a baseline period (1992–1999) and a change period (2000–2012). The mean annual and wet season streamflow decreased by about 36% and 49%, respectively during the change period compared

to the baseline period; however, dry season streamflow increased by 57%. The LULC change analysis showed improved shrub land and forest cover that led to restoration of about 36 km^2 of bare land. Model estimations revealed that climate variability accounted for 22% of the total reduction in mean annual streamflow; whereas the reduction due to human activities was about 78%. This study demonstrated that human activities primarily proper watershed management practices and associated changes in LULC play a more pronounced role in driving the changes in streamflow of Agula watershed.

The second study evaluated the changes in soil erosion for the years 1990, 2000 and 2012 as a result of watershed management practices and associated changes in LULC using the Revised Universal Soil Loss Equation (RUSLE). The RUSLE factors were computed using spatial data obtained from different sources in a geographic information system (GIS) environment for 30×30 m raster layers. The results revealed significant reduction in soil loss rates by about 55% from 28 to 12 t ha^{-1} yr^{-1} in 1990–2000 and an overall 64% reduction from 28 to 10 t ha^{-1} yr^{-1} in 1990–2012. This change in soil loss is attributed to improvement in surface cover and stone bund practices which resulted in the decrease in mean *C* and *P*-factors respectively by about 19% and 34% in 1990–2000 and an overall decrease in *C*-factor by 29% in 1990–2012. Between 1990 and 2012, the severe (20–40 t ha^{-1} yr^{-1}) and very severe (>40 t ha^{-1} yr^{-1}) erosion categories decreased by about 40% and 80%, respectively. During the same period, significant reductions in soil loss were observed for bare land (89%), cultivated land (56%) and shrub land (49%). Furthermore, the reduction in soil loss was more pronounced in steeper slopes where very steep slope and steep slope classes experienced over 70% reduction. However, it is important to note that for the recent year (2012) about 14% of the watershed experience soil erosion rate in excess of 20 t ha^{-1} yr^{-1}. This implies that further planning and implementation of SWC measures is required to

reduce the soil erosion from areas experiencing severe and very severe erosion. Validation of soil erosion estimations using field observed points showed an overall accuracy of 69%, which is fairly satisfactory. The SWC efforts undertaken in the past few decades have resulted in marked restoration of degraded semiarid lands that could serve as a basis for sustainable planning of future developments of areas experiencing severe land degradation due to water erosion.

The third study analyzed 28 morphometric parameters for 26 sub-watersheds of Agula watershed to characterize the watersheds' behavior in terms of runoff generation potential and soil erosion risk. Analysis of morphometric parameters was carried out from four perspectives: drainage network, watershed geometry, drainage texture, and relief characteristics. The longest flow path of Agula watershed was about 48.5 km; with changes in slope of the river bed from steep gradient (0.018 m m^{-1}) at the upper reach which gradually flattens near its outlet (0.008 m m^{-1}). Knickpoints with abrupt changes in elevation also developed along the main river which could be attributed to change of lithology resulting in differential erosion as well as the presence of major faults which are common along the rift escarpments. The drainage texture parameters revealed that Agula watershed was characterized by fine drainage texture; which implied that the watershed is dominated by impermeable soft rock with low resistance against erosion and sparse vegetation cover. Furthermore, high relief and steep slopes dominated; by which rough landforms, including hills, breaks, and low mountains made up 76% of the watershed. At sub-watershed scale, the derived morphometric parameters from four perspectives were further grouped into three clusters (that represented low, moderate, and high values); and considerable spatial variability was observed. The results of this study provide useful information to better understand the watersheds' characteristics and serve as a basis for improved planning, management, and decision making to ensure sustainable use of watersheds' resources.

学位論文概要

土地の劣化はエチオピア高原で最大の脅威であり、実質的な社会経済的・生態学的な問題を引き起こしている。そのため、エチオピア政府は NGO とともに、土壌侵食による土地劣化を抑制する水土保持(SWC)対策の実施を推進してきた。北エチオピアの Tigray 領域は、旱魃にさらされやすい地域の一つであり、そこでは特に過去 20 年間にわたり、適切な流域管理により環境劣化を是正するべく解決策が実施されてきている。

流域管理実施の目的は、1) 劣化地を復元する、2) 農業と生活用水の保証、3) 食糧保障の推進の３つがある。これらの目的から、Agula 流域は重点的水土保持対策が実施されてきた領域の目標地の一つである。保全実施の要素は、耕作地や傾斜地にある溝付き溝なしの石堤やガリや川沿いのチェックダムそして植生ありなしの囲い柵を含むものである。

いくつかの先行研究が実験区や小流域(<100 km^2)における侵食制御、流出流土の減少、土壌肥沃度保持そして土地利用、植生再生の結果としての被覆の変化について土保持実施の効果を報告している。水土保持資源の大規模な運用にもかかわらず、水土保持対策の土地管理者・政策策定者にとって多大なる関心事である中・大規模流域(>100 km^2)における水文学的効果、土地侵食、土地利用・被覆変化についての報告はごくわずかである。

本研究は、この情報ギャップを補完し、北エチオピア半乾燥高地にある Agula 流域(中規模流域： 442 km^2)における、水文応答と土地侵食について流域管理実践と土地利用・被覆(LULC) 変化の効果を解析することにより、土地劣化を克服する国家努力に貢献しようとするものである。

この研究は以下の３つの解析を重点とする：1)流域管理実施と LULC の変化がどのような範囲に河道の流量応答に影響を及ぼすかを定量的に推定すること； 2) 流域管理実施と LULC 変化の結果としての土壌侵食の流域スケールにおける変化の評価、3) 流域資源の持続的利用を確約する改善された計画策定・管理そして決定のための、水文地質と侵食特性のより一層の理解のための地形学的因子の解析。

本研究は以下のように要約される：

最初の研究は、流域管理と LULC 変化のような気候変動と人間活動に対応した河道流の変化を評価した。1992-2012 の期間について水文気象時系列のトレンドと急変点を解析するためにノンパラメトリック Mann-Kendall (MK)検定と Mann-Kendall-Sneyers (MKS)検定が用いられた。LULC 変化は 1990, 2000 そして 2012 年における多時点ランドサット画像の階数化と階数変化検出法により評価された。河道流量に対する気候変動の作用を評価するために、降雨と可能蒸発量による流出モデルが開発された。そして河道流量に対する気候変動と人間活動の効果（流域管理と LULC 変化）が分離された。MK 検定結果は明らかな年間、雨季河道流量の減少傾向を示していた。一方で、乾期の河道流量は増加傾向を示していた。同一期に、降雨の季節・年間記録には有意な傾向は見つからなかった。MKS 検定において、年間河道流量に 2000 年ごろ急変点が発生していた。そのため、河道流量記録は、基底期(1992-1999)と変化期(2000-2112)の 2 つの期間に分けられる。年平均そして雨季の河道流量は、基底期に比べて変化期にそれぞれ 36%、49%低下した。一方で、乾期の河道流量は 57%増加していた。LULC 変化解析は、

36Km^2 もの裸地の回復をもたらす低木と森林被覆の改善を示していた。モデルの推定では、年平均河道流量 22%の減少を引き起こす気候変動が明らかにされた。この点では人間活動による減少は 78%であった。本研究では、多くの要因の中で、人間活動が主導的な流域管理と LULC の統合的変化が、Agula 流域の河道流量の変化を促進するより大きな役割を果たすことを表したものである。

2 番目の研究は、流域管理実施と Revised Universal Soil Loss Equation (RUSLE)を用いての LULC における総合的変化の結果として 1990, 2000 及び 2012 年の土壌侵食の変化を評価した。結果は、1990-2000 に 28 から 12 $t\ ha^{-1}\ yr^{-1}$ と 55%もの土壌侵食の減少があり、1990–2012 には 28 から 10 $t\ ha^{-1}\ yr^{-1}$ と 64%もの土壌侵食の減少があったことを明らかとした。この土壌損失変化は、地被改善と石堤設置に起因するものであり、それは 1990‑2000 で C、P-ファクターのそれぞれ 19%と 34%ほどの平均減少、1990-2012 における C ファクターの全体的な 29%の総体的な減少の結果をもたらしている。1990-2012 年の間に、深刻な侵食(20–40 $t\ ha^{-1}\ yr^{-1}$)、極めて深刻な侵食(>40 $t\ ha^{-1}\ yr^{-1}$)は、それぞれ 40% , 80%減少していた。同時期に土壌流亡が裸地 (89%), 農耕地 (56%) そして低木地 (49%)で明らかに減少した。さらに、土壌流亡の減少は急斜面地でなお一層著しいものであり、急傾斜地と傾斜地では 70%の減少であった。しかし、近年(2012)流域の 14%ほどで土壌侵食は 20 $t\ ha^{-1}\ yr^{-1}$ を超えるものであったことを知っておくことは重要である。このことは、SWC 対策のさらなる計画そして実施にあって、深刻な侵食地そして極めて深刻な侵食地で土壌侵食を低減することが求められることを意味する。フィールド調査点を用いての土壌侵食評価の相対的精度は 69%を示しており、これはかなり満足できるものである。過去数十年間行われた流域管理は、劣化した半乾燥地の著しい回復をもたらしており、水食による極度の土地劣化にさらされている地域の将来の持続的な開発計画の基本となるものである。

3 番目の研究は、流出生起ポテンシャルと土壌侵食リスクにおいて、流域の状態を特徴づけるために、Agula 流域の 26 支流域に対して 28 の形状パラメターを解析した。形状パラメターの解析は、流路ネットワーク、流域地形、流路形成そして起伏形成の 4 つの観点による。

Agula 流域の最長流路はおよそ 48.5 km ; 河床勾配は上流端で急勾配(0.018 m m^{-1})から流出端近傍で平坦(0.008 m m^{-1})に変化する。主流路に沿って標高が大きく変化する急変点は主流路沿いの岩層の変化に帰するものであり、断層崖の存在と同様に偏侵食を引き起こす。Agula 流域は長時間に低いピーク流量を生じるような引き延ばされた形状をしているので洪水制御は容易である。排水構造定数は流域が微細な構成により特徴づけられていることを示していた。これは、侵食に対して抵抗性の低い不透水性の軟弱岩と疎らな植被により流域が支配され、激しい起伏と急こう配が支配的であることを示している。これは流域の 76%は急峻な地形、丘陵、断層、低山地により形成されていることによる。支流域のスケールでは、４つの観点から導かれた形状パラメターはさらに３つに分類され（低・中・高とあらわされる）、かなりの空間的変化が観察されたものであった。本研究の結果は、流域特性をよりよく理解する有益な情報を提供して、流域資源の持続的な利用を確実にするための計画・管理そして政策決定の質的向上のための根拠を与えるものである。

List of Publications

1. Fenta, A.A., Yasuda, H., Shimizu, K., Haregeweyn, N. and Negussie, A. Dynamics of Soil Erosion as Influenced by Watershed Management Practices: A Case Study of the Agula Watershed in the Semi-Arid Highlands of Northern Ethiopia. *Environmental Management 58: 889–905. DOI: 10.1007/s00267-016-0757-4*. This paper covers Chapter 3 in the thesis.

2. Fenta, A.A., Yasuda, H., Shimizu, K. and Haregeweyn, N. Response of streamflow to climate variability and changes in human activities in the semiarid highlands of northern Ethiopia. *Regional Environmental Change 17: 1229–1240. DOI: 10.1007/s10113-017-1103-y*. This paper covers Chapter 2 in the thesis.

3. Fenta, A.A., Yasuda, H., Shimizu, K., Haregeweyn, N. and Woldearegay, K. Quantitative analysis and implications of drainage morphometry of the Agula watershed in the semi-arid northern Ethiopia. *Applied Water Science 7: 3825–3840. DOI: 10.1007/s13201-017-0534-4*. This paper covers Chapter 4 in the thesis.